ERRATA

p. 4: Add the following note at the end:

Note: The ground state is often referred to as being the x^2-y^2. In the context of the molecular orbital theory as used in this thesis, the term "ground state" refers to the energetically highest occupied orbital in the Slater determinant.

p. 29 1.9: Replace Table 2 by Table 3

p. 31 1.5: Delete the whole line and replace it by the following:
are tabulated as well as some two-center integrals. For references see

p. 31 1.6: Replace Ref. 35 by Ref. 24.

p. 63 bottom: Replace Table 6 by Table 7

p. 103 1.5:Delete the word "nearest"

p. 104: The level at the middle of the first colum is yz, not xz.

p. 105 1.5: Replace Helmheltz by Helmholtz

T H E U N I V E R S I T Y O F M I C H I G A N

COLLEGE OF ENGINEERING
Department of Nuclear Engineering

Technical Report

MOLECULAR ORBITAL THEORY OF VANADIUM IN THE RUTILE STRUCTURE CRYSTALS SnO_2, TiO_2 AND GeO_2

Sophocles Karavelas
Chihiro Kikuchi

ORA Project 04381

under contract with:

NATIONAL AERONAUTICS AND SPACE ADMINISTRATION
GRANT NO. NSG-115-61
WASHINGTON, D.C.

administered through:

OFFICE OF RESEARCH ADMINISTRATION ANN ARBOR

July 1964

This report was also a dissertation submitted by the first author in partial fulfillment of the requirements for the degree of Doctor of Philosophy in The University of Michigan, 1964.

TABLE OF CONTENTS

Page

LIST OF TABLES

LIST OF FIGURES

Figure Page

Abstract

The purpose of this study is to investigate possible explanations of the observed ESR spectra in the rutile-type crystals of SnO_2, TiO_2, and GeO_2, with vanadium as an impurity. The observed electronic g tensors cannot be accounted for by the simple crystal field theory, and there is ambiguity in the energy level diagram. Molecular orbital theory is used in a semiempirical calculation with the linear combination of atomic orbitals approximation (LCAO).

The crystal region consisting of the vanadium ion and the six ligand oxygen ions is selected to be studied. The atomic orbitals to be used in the LCAO approximation are chosen. These are the nine vanadium 3d, 4s, 4p orbitals, and the twenty-four ligand oxygen 2s, 2p orbitals. It is argued that the hybridization of the oxygen orbitals is needed to account for the influence of the rest of the crystal, and these hybrid orbitals are constructed. Then it is shown how Group Theory can simplify the secular equation and formulate the selection rules.

The use of group theory requires the construction of LCAO transforming according to the irreducible representations (I.R.) of the D_{2h} group. These combinations are constructed by the method of projection operators.

The group overlap integrals are calculated, and the valence state ionization potentials (VSIP) of the oxygen and vanadium ions are estimated.

Then the reduced secular equations are solved using the VSIP as parameters. The best solutions are selected by using as a monitor either the vanadium charge or the g tensors. The results are compared and the need of a reduction in the original estimate of the π-electron VSIP is recognized. Also, it is concluded that charge self-consistency alone is not adequate in selecting the best solutions, but rather the detailed charge distribution among the orbitals must show self-consistency.

Finally, the following results are given:

(a) The ground state in all cases is of the form $-\alpha|z^2\rangle+\beta|x^2-y^2\rangle$ where $.10<\alpha<.20$ and $\beta\approx.99$.

(b) The pertinent to the g tensor levels are in order of increasing energy, the xy (filled), xz (filled), yz (filled), x^2-y^2 (ground state with one unpaired electron), yz (empty), xz (empty), and xy (empty).

(c) The small admixture of the $|z^2\rangle$ state in the ground state is relatively important in calculating Δg_{ii}.

(d) The ground state in (a) can explain the anisotropic part of the hyperfine tensors.

(e) All obtained results seem to agree with the recently observed ESR spectra of Mo^{5+} and W^{5+} in TiO_2.

CHAPTER I

INTRODUCTION

The purpose of this study is to investigate possible explanations of the observed ESR spectra in the rutile-type crystals of SnO_2, TiO_2, and GeO_2 with vanadium as an impurity.

Gerritsen and Lewis[1] were the first to study the paramagnetic spectrum of vanadium in TiO_2. They attributed the spectrum to a single 3d electron of tetravalent vanadium occupying a substitutional site in the crystal. The experimentally deduced g tensor ($g_x = 1.915$, $g_y = 1.913$, $g_z = 1.956$) had almost complete axial symmetry about the z-axis, and the application of the theory of Abragam and Pryce[2] was expected to give the splitting of the lower triplet, t_{2g}. However, calculation revealed inconsistencies, since the calculated splittings differed by a factor of two-and-a-half depending on whether $g_{\parallel} = g_z$ or $g_{\perp} = g_x \simeq g_y$ was used. They commented that perhaps the rhombic component of the crystalline field was responsible for making the theory inapplicable. An attempt by Réi[40] to account for the g and A tensors of V^{4+} in rutile by considering the rhombic component of the field and the covalent bonding proposed by Stevens[41] was not successful either. Later, Marley and MacAvoy[3] observed the ESR

spectrum of vanadium in SnO_2. Again the ESR spectrum was attributed to substitutional vanadium, but the g tensor showed nearly axial symmetry around the y axis; they tried to interpret this by the improbable assumption that the doublet e_g lies lower than the triplet t_{2g}. In 1963, Kasai[4] suggested that the rhombic part of the crystalline field has an important role in splitting the lower triplet t_{2g}. It was also argued that the $x^2 - y^2$ state would be the lowest due to the stabilizing effect of the two tin ions lying on the y-axis close to the vanadium ion. In 1964, From, Kikuchi and Dorain[5] investigated the large superhyperfine structure in SnO_2:V. They concurred that the ground state is $x^2 - y^2$ and that the next level is the state xz. The latter was arrived at by fitting the observed g values to the usual crystalline field formulas:

$$\Delta g_x = -\frac{2\lambda}{E_{yz}}, \quad \Delta g_y = -\frac{2\lambda}{E_{xz}}, \quad \Delta g_z = -\frac{8\lambda}{E_{xy}}$$

However, a point-charge-crystalline-field-type calculation showed (see Appendix G) that the levels are in the order $x^2 - y^2, xz, yz$, and xy. The same year, Siegel[6] observed the ESR spectrum of vanadium in tetragonal GeO_2 and obtained values comparable to that in TiO_2 and equally difficult to interpret.

Since SnO_2 is an important material in the production of conducting glasses, and GeO_2 exhibits both the crystalline and amorphous state related to glasses, the study of the electronic behavior of the

vanadium impurity may reveal important properties of conducting glasses. On the other hand, all three materials may have important quantum electronic properties. Theoretically, the interest is equally great because the spectra are due to a single unpaired electron, which can be thought of as the simplest case of magnetism.

The principal results reported in this thesis are:

(a) The ground state is of the form $-\alpha|z^2\rangle + \beta|x^2-y^2\rangle$ where $.10 < \alpha < .20$ and $\beta \approx .99$.

(b) The excited states are in the order of increasing energy:

$$|yz\rangle, |xz\rangle, |xy\rangle \quad \text{and} \quad |z^2\rangle$$

The first two states are inverted with respect to the prediction based on the simple crystalline field formulas.

(c) The observed g tensors and the anisotropic parts of the hyperfine tensors A can be explained.

(d) Results are applicable to the cases of Mo^{5+} and W^{5+} in rutile. (The electronic structures of V^{4+}, Mo^{5+}, and W^{5+} are similar, with a 3d, 4d, or 5d unpaired electron outside filled shells respectively.)

The general theory is given in Appendix A. Chapter II states the assumptions needed to make the calculation feasible. The difficult problem of how to restrict the calculation to a limited number of ions surrounding the impurity ion and still get reliable results is considered. Only the nearest neighbors are taken into account for the sp^2 hybridization of the valence electrons. Group theoretical methods are used to reduce the labor of solving the secular equation.

As described in Appendix A the secular determinant contains Coulomb integrals H_{ii} and group overlap integrals S_{ij}. The latter are calculated by using self-consistent field radial functions. However, the Coulomb integrals H_{ii} are taken as semiempirical parameters. This necessitates a trial and error method which is monitored by the self-consistency of the assumed and calculated vanadium charge. In addition, the g tensor is taken as monitor of the calculation.

Finally the results are discussed and conclusions are drawn.

CHAPTER II

RUTILE CRYSTAL STRUCTURE AND SYMMETRY

This chapter presents certain fundamental ideas essential for the development of the theory to be followed in dealing with the problem of vanadium in the rutile-type structures. First the rutile crystal structure is given and then the use of the symmetry properties is examined.

1. Crystal Structure

The crystallographic data of SnO_2, TiO_2 (rutile) and GeO_2 (tetragonal) crystals, all having the rutile structure, are given in Figure 1 and Table 1.

The macroscopic symmetry is tetragonal, but the metal sites have the orthorhombic symmetry D_{2h}, and the oxygen sites the orthorhombic symmetry C_{2v}. D_{2h} represents collectively the following symmetry elements: three two-fold axes perpendicular to each other, three mirror planes perpendicular to them respectively, a center of inversion, and the identity element. Figure 1 shows that for the central metal ion, each of the x-, y- and z-axes is a two-fold symmetry axis and the planes perpendicular to them are the mirror planes. Similarly, C_{2v} represents collectively a two-fold symmetry axis with two mirror

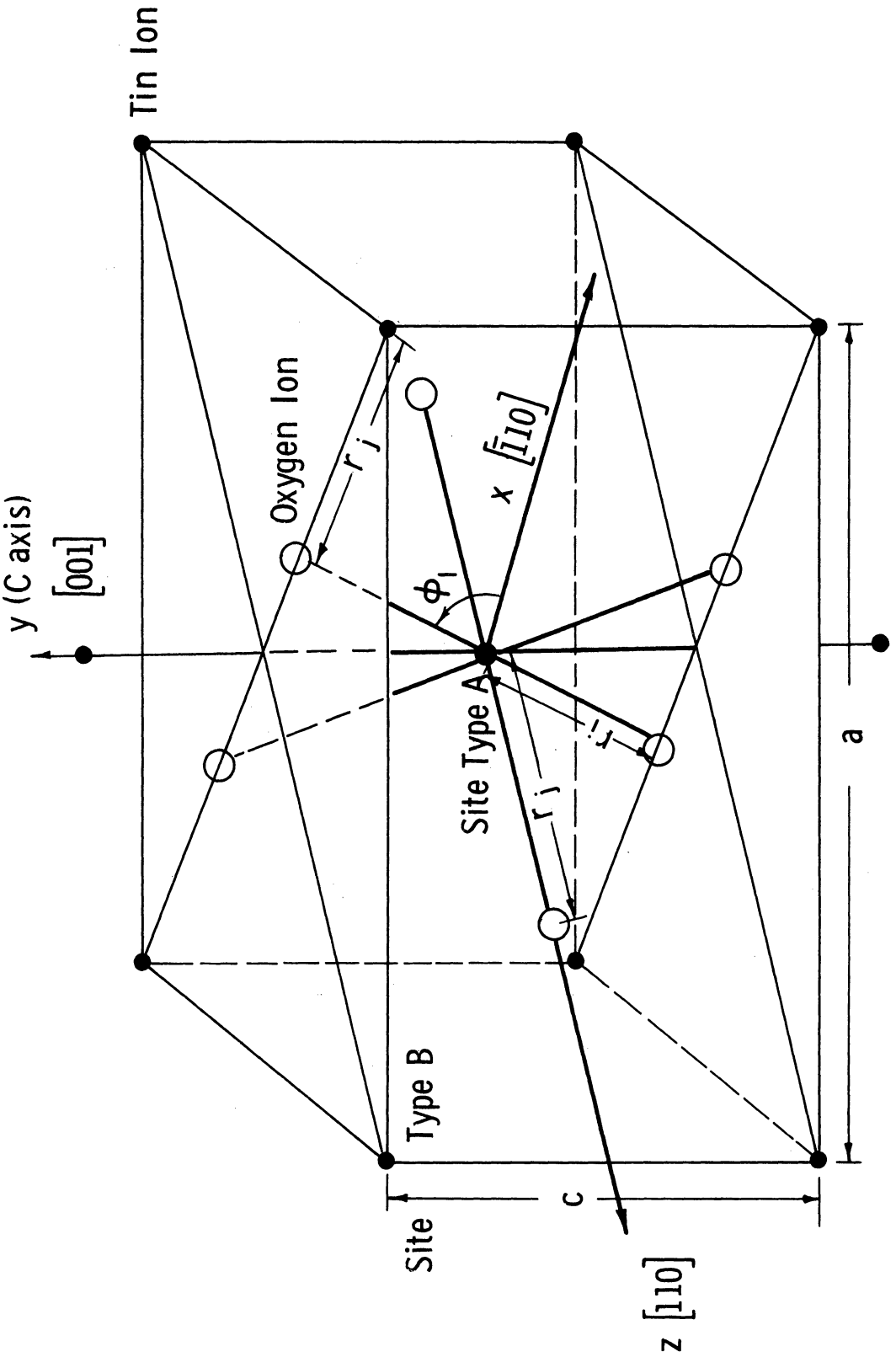

Fig. 1. Rutile-Type Crystal Structure

TABLE 1

CRYSTALLOGRAPHIC DATA OF SnO_2, TiO_2 AND GeO_2

	SnO_2	TiO_2	GeO_2
a(Å)	4.737	4.593	4.395
c (Å)	3.185	2.959	2.859
r(a. u.)	3.876	3.674	3.502
r(a. u.)	3.887	3.757	3.637
$\cos\varphi_1$	.63031	.64815	.63107
φ_1	51°	49°.5	50°.9

planes perpendicular to each other, both containing the axis. For example, the site of the oxygen ion #3 has a two-fold axis parallel to the x-axis, the diagonal plane xy as a mirror plane and the plane perpendicular to the y-axis and passing through the oxygen #3 site, as another mirror plane. The unit cell has two types of metal sites, A and B. All considerations will be referred to type A. The axes of type B are rotated 90° about the crystal c-axis with respect to type A site.

2. Additional Assumptions

Certain assumptions needed for a semiempirical molecular orbital calculation will be considered (see Appendix A for the general theory). It is assumed that the valence electrons move in orbitals Φ_v satisfying the Schrödinger equation

$$H_{eff}(\mu)\ \Phi_v(\mu) = E_v\ \Phi_v(\mu) \qquad (1)$$

where H_{eff} is the one-electron effective Hamiltonian. The H_{eff} is taken to be the same for all valence electrons, even when they occupy excited states. In addition, the linear combination of atomic orbitals (LCAO)

$$\phi_v = \sum_{i=1}^{n} c_i \varphi_i \tag{2}$$

is used to provide a trial function for solving Eq. (1). The selection of the n atomic orbitals φ_i to be used in Eq. (2) rests on intuition and experience, while the coefficients c_i as well as the energy eigenvalues are given by solving the secular equation,

$$\det|H_{ik} - E S_{ik}| = 0 \qquad k, i = 1, 2 \ldots n \tag{3}$$

where by definition

$$H_{ik} \equiv \langle \varphi_i | H_{eff} | \varphi_k \rangle \tag{4}$$

$$S_{ik} \equiv \langle \varphi_i | \varphi_k \rangle \tag{5}$$

The application of the above program to a crystal is hopelessly complicated by the great number of atomic orbitals needed in the expansion of Eq. (2). Therefore further assumptions are required to simplify the problem to a solvable one.

For this, a region of the crystal around the vanadium impurity is defined, as small as possible, where there is a high probability of finding a specific number of electrons. The problem is confined to this region and these electrons. Also, the interaction of the rest of the

crystal must be considered. The smallest region then will be that containing the vanadium ion and the six ligand oxygen ions. The electronic configuration of the oxygen atom is $[He]\,2s^2\,2p^4$, and that of vanadium atom $[A]\,3d^3\,4s^2$, where $[He]$ and $[A]$ represent the core of filled shells (see Appendix A) having the helium and argon configurations respectively. The set of nine vanadium 3d, 4s, 4p, and the twenty-four oxygen 2s, 2p, orbitals will be used as the trial solution for Eq. (1); i.e.,

$$\phi_v = \sum_{i=1}^{33} c_i \varphi_i \tag{6}$$

to solve the problem

$$H_{eff}\,\phi_v = E\,\phi_v \tag{7}$$

Equation (3) yields a 33x33 determinant. Group theory can be used to reduce this determinant to smaller 2x2 and 3x3 secular determinants. Then the calculation is simplified and the various states can be classified according to the irreducible representations (I.R.) of the symmetry group. This allows the formulation of new selection rules that replace the ones found in atomic spectroscopy. The lack of spherical symmetry in H_{eff} renders classification into s-, p-, d-, states, etc., impossible.

Another question must be considered: So far, the assumptions made do not allow for any interaction from the rest of the crystal. The vanadium ion and the six ligand oxygen ions are treated as a complex, i.e., as if they were isolated in space and were not part of an

extensive three dimensional structure. Complex-type calculations have been made by Wolfsberg and Helmholtz,[22] by Ballhausen and Gray,[23] and by Kuroda, Ito and Yamatera.[24] What is needed here is a modification to account for the extensive crystal structure.

To be more explicit, consider oxygen ion #5 of Figure 1 as an example. In the complex-type calculation all ions, except the central vanadium and the nearest six oxygen ions, are ignored so that only the bonding of oxygen #5 with the central vanadium is considered. The obvious bonding scheme is: (a) a hybrid orbital of the form $\sin\vartheta(2s)_5 + \cos\vartheta(2p_z)_5$ which is directed toward the central vanadium ion, resulting in a greater overlap $S(\vartheta)$ with the appropriate vanadium orbital than either one of the $(2s)_5$ and $(2p_z)_5$; (b) the orbital orthogonal to it $\cos\vartheta(2s)_5 - \sin\vartheta(2p_z)_5$ directed away from the vanadium ion and therefore nonbonding; and (c) the two orbitals $(2p_x)_5$ and $(2p_y)_5$ possibly involved in π - bonding. The angle ϑ is determined by the requirement that $F(\vartheta) = \frac{VSIP(\vartheta)}{S(\vartheta)}$ be a minimum (VSIP is discussed in Appendix H). This is done for example in ref. 23. In minimizing the fraction $F(\vartheta)$, a compromise is achieved between the tendency for greater overlapping by forming ligand hybrid orbitals and the promotion energy (see Appendix H) needed for the formation of these hybrid orbitals. However, if one considers the two metal ions, with which the oxygen ion #5 is to be bonded in addition to the vanadium ion, the bonding schemes just discussed is not appropriate since none of the considered orbitals is directed toward these two metal ions. Therefore a small total overlapping will result in a less stable situation.[25,26]

On the other hand, the sp^2 hybridization scheme, for which the $(2s)_5$ $(2p_z)_5$ and $(2p_y)_5$ orbitals form three hybrid orbitals directed toward the vanadium ion and the two metal ions, will result in a greater total overlap and therefore is more stable. The $(2p_x)_5$ is not hybridized with a possible involvement in π - bonding. Hybridization requires an increase in the promotion energy which is expected to be compensated[39] by better and more numerous bondings.

3. Oxygen sp^2 Hybrid Orbitals

The sp^2 hybridization assumption was made in an effort to account for the influence of the part of the crystal that is left outside of the region containing the vanadium ion and the six ligand oxygen ions. Now the problem of constructing these hybrid orbitals will be dealt with. These are linear combinations of the usual 2s, 2p functions of the same center, which are directed towards the neighboring metal ions, thus securing greater overlapping and therefore a larger binding energy.[25,26] Since the three metal ions lie in the same plane, as in Figure 2, only the 2s, $2p_x$ and $2p_y$ atomic orbitals can be used. Furthermore the orthogonality condition is imposed on these hybrids, so that they can form bonds with the metal ions independently of each other. Such normalized hybrid orbitals along the x direction and along the directions of metal ions 2 and 3 are, respectively:

$$\begin{aligned} &\sin\theta''(2s)+\cos\theta''(2p_x) \\ &\sin\theta'(2s)+\cos\theta'(2p_2) \\ &\sin\theta'(2s)+\cos\theta'(2p_3) \end{aligned} \qquad (8)$$

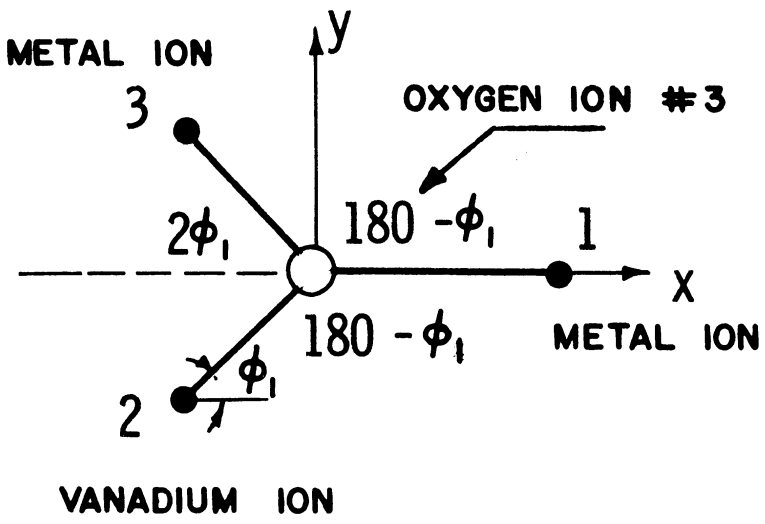

Fig. 2. Coordination of the Oxygen Ions in the Rutile-Type Structures

where $2p_2$ and $2p_3$ are the 2p orbitals having the directions of atom 2 and 3 respectively. The same mixing coefficients are used in the last two hybrids due to symmetry. Orthogonality between the first and second hybrids gives

$$\langle \sin\theta''(2s)+\cos\theta''(2p_x) \mid \sin\theta'(2s)+\cos\theta'(2p_2)\rangle = 0 \qquad (9)$$

$$\sin\theta''\sin\theta'+\cos\theta''\cos\theta'\cos\theta_{12} = 0 \qquad (10)$$

and between the second and third hybrids gives:

$$\sin^2\theta'+\cos^2\theta'\cos\theta_{23} = 0 \qquad (11)$$

From Eq. (10), (11), the known angles $\theta_{12} = 180-\varphi_1$ and $\theta_{23} = 2\varphi_1$, the mixing coefficients are calculated. Table 2 summarizes the results for the three crystals SnO_2, TiO_2, GeO_2. The hybrid orbitals are written as $\sigma = \sin\theta(2s)+\cos\theta(2p)$. The longer metal-oxygen bond is specified by θ'', and the shorter one by θ'.

TABLE 2

COEFFICIENTS OF THE OXYGEN HYBRID ORBITALS
$\sigma = \sin\theta(2s)+\cos\theta(2p)$

	SnO_2	TiO_2	GeO_2
$\sin\theta'$	.413	.371	.411
$\cos\theta'$	.911	.929	.912
$\sin\theta''$	.812	.851	.814
$\cos\theta''$	.584	.525	.582

The construction of the hybrid orbitals σ effects an additional simplification to the trial function ϕ_v in Eq. (6) and therefore to the secular determinant Eq. (3), which is reduced from 33x33 to 21x21. At each ligand oxygen ion, three σ orbitals replace one 2s and two 2p atomic orbitals so that the total number of functions in the expansion Eq. (6) remains thirty-three. However, of the hybrid σ orbitals only those directed toward the central vanadium ion will be considered in treating the selected region of the vanadium ion and the surrounding six oxygen ions. Obviously the other σ hybrid orbitals are involved in bonding with the neighboring metal ions. Therefore, referring to Figure 3, the following twelve ligand orbitals

$$\sigma_i = \sin\delta'(2s)_i + \cos\delta'(2p_z)_i\,, \quad (2p_y)_i\,, \quad i=1,2,3,4$$

$$\sigma_j = \sin\delta''(2s)_j + \cos\delta''(2p_z)_j\,, \quad (2p_x)_j\,, \quad j=5,6 \qquad (13)$$

and the nine vanadium orbitals 3d, 4s, 4p will be considered in the expansion Eq. (2). Thus

$$\phi_v = \sum_{i=1}^{21} c_i \varphi_i \qquad (14)$$

In Eq. (13) the numerical subscripts of the orbitals denote the oxygen ions to which they belong, and the coordinate subscripts refer to the ligand left-handed coordinate systems of Figure 3. The use of Eq. (4) as a trial function in solving Eq. (1) results in the 21x21 secular

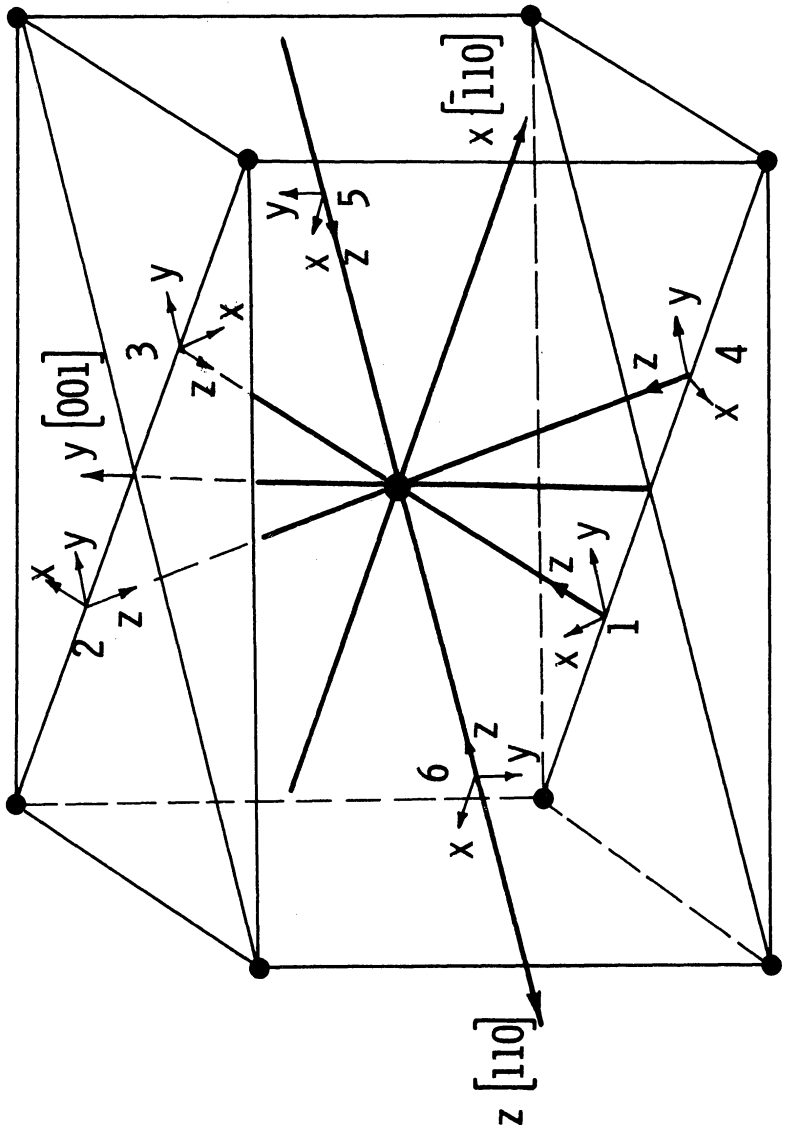

Fig. 3. Left-Handed Coordinate Systems Centered at the Oxygen Ligand Ions

determinantal equation:

$$\det | H_{ik} - E S_{ik} | = 0 \qquad i,k = 1, 2 \ldots 21 \qquad (15)$$

4. Reduction of the Secular Determinant by Group Theory and Selection Rules

This section will consider the use of group theory to reduce the secular determinant of Eq. (15) and to derive the selection rules. First a simplified argument will be presented based on the fact that the D_{2h} group is an Abelian group and then a general theorem of group theory will be stated.

(a) Reduction of the Secular Determinant.

The reduction of the secular determinant depends upon the following argument: The region under consideration is centered at a metal site of symmetry D_{2h}. The symmetry operators of this group leave the Hamiltonian H_{eff} invariant, i.e., they commute with it. Thus for every symmetry operator T of this group:

$$T H_{eff} = H_{eff} T \qquad (16)$$

Furthermore D_{2h} is an Abelian group (the symmetry operators commute among themselves). If several operators commute among themselves it is possible to choose basis functions which are simultaneous eigenfunctions of all the operators. Any two such functions are orthogonal if they differ in the eigenvalue of any one of the commuting operators. The character table of D_{2h} group (see Appendix C) shows that there are only eight different types of basis functions for the symmetry

operators. Note that the characters are the eigenvalues of the symmetry operators. This is generally true when one deals with one-dimensional I.R. Any basis function must transform according to one of the eight irreducible representations. For example the function xy belongs to the B (or N_{3g} or Γ_{2g}) irreducible representation.

In a matrix representation based on j simultaneous eigenfunctions of the symmetry operators of the D_{2h} group, Eq. (16) becomes

$$\sum_{\delta} T_{i\delta} H_{\delta k} = \sum_{\delta} H_{i\delta} T_{\delta k} \tag{17}$$

However, the T matrix is diagonal since eigenfunctions of the T operator are used. Therefore, Eq. (17) reduces to

$$T_{ii} H_{ik} = H_{ik} T_{kk} \tag{18}$$

or

$$(T_{ii} - T_{kk}) H_{ik} = 0 \tag{19}$$

Thus the off-diagonal matrix element H_{ik} is zero if the eigenfunctions i and k give different eigenvalues for the operator T. Since there is always a symmetry operator with different eigenvalues in two different I.R. (it is exactly this property that distinguishes the various I.R.s), all energy matrix elements H_{ik} are zero, if i and k refer to functions transforming according to different I.R. of the D_{2h} group. The same applies to the matrix S_{ik} in Eq. (15) because the whole argument can be repeated when the Hamiltonian operator is replaced by the unit operator.

Therefore, if instead of the 21 atomic orbitals φ_i in Eq. (14) combinations of them transforming according to the I.R. of the rhombic symmetry group are used, the secular determinant Eq. (15) will be reduced to a number of smaller determinants equal to the number of the different I.R.'s contained in the combinations of the φ_i's. The order of each one of these determinants will be equal to the number of φ_i's belonging to an irreducible representation.

(b) Selection Rules.

To formulate the selection rules one must find a way to determine if a matrix element of the form

$$M = \langle \psi_i^{(\lambda)} | \sigma_k^{(\mu)} | \psi_j^{(\nu)} \rangle \tag{20}$$

is identically zero or not. Let the functions $\psi_i^{(\lambda)}$, $\psi_j^{(\nu)}$ and the operator $\sigma_k^{(\mu)}$ transform according to the λ^{th}, ν^{th}, and μ^{th} I.R.'s respectively. Since the matrix element Eq. (20) is a number it should remain invariant under the application of all the symmetry operators of the D_{2h} group. The application of a symmetry operator to Eq. (20) results in multiplying each one of the $\psi_i^{(\lambda)}$, $\sigma_k^{(\mu)}$, and $\psi_j^{(\nu)}$ by the corresponding eigenvalue which is given in the character table in the Appendix C. Therefore the matrix element Eq. (20) is not zero only if the product of the characters (eigenvalues) which correspond to $\psi_i^{(\lambda)}$, $\sigma_k^{(\mu)}$, $\psi_j^{(\nu)}$ for every symmetry operation of the group is equal to unity.

(c) General Theorem of Group Theory.

In general, both the reduction of the secular equation and the selection rules are based on the following theorem of group theory:

The matrix element M_{ij} of Eq. (20) is nonzero only if the reduction of the direct product $D^{(\mu)} \otimes D^{(\nu)}$ contains the I.R. $D^{(\lambda)}$. For a proof see, for example, Heine.[20] When the operator $\sigma_k^{(\mu)}$ is the Hamiltonian H_{eff} or the unit operator, the I.R. $D^{(\mu)}$ is the identity I.R. Then the product $D^{(\mu)} \otimes D^{(\nu)}$ is merely $D^{(\nu)}$, and for a nonzero matrix element the I.R. $D^{(\lambda)}$ must be the same as $D^{(\nu)}$. Thus all off-diagonal matrix element H_{ij} and S_{ij} are zero for functions ψ_i and ψ_j belonging to different I.R.'s.

CHAPTER III

LINEAR COMBINATIONS OF ATOMIC ORBITALS (LCAO) TRANSFORMING ACCORDING TO THE I.R.'S OF THE D_{2h} GROUP

Chapter II-4 demonstrated that in order to simplify the secular determinant Eq. (3), combinations of atomic orbitals transforming according to the I.R. of the D_{2h} group are needed. The symmetry classification of the metal orbitals is as shown in the character table in Appendix C. For the ligand orbitals the method of projection operators is convenient in constructing the combinations which transform according to the I.R. In the case of one-dimensional representations the recipe is simply

$$\phi^{(\lambda)} = N \sum_{T} \chi^{(\lambda)^*}(T)\, T\varphi_i \qquad (21)$$

where φ_i is any member of the original set of orbitals, $\chi^{(\lambda)}(T)$ is the character of the transformation T for the irreducible representation λ, N is a normalization constant, and $\phi^{(\lambda)}$ is the orbital which transforms according to the λ th I.R. expressed as a linear combination of the φ_i's. Occasionally the function $\phi^{(\lambda)}$ is zero. This happens when the function φ_i already has symmetry properties incompatible with the irreducible representation λ, i.e., its projection on λ is zero.

The functions φ_i to be used in Eq. (21) are the twelve ligand orbitals in Eq. (13). For a sample application of Eq. (21) consider σ_1. The symmetry operators T applied to it give:

	E	C_2^z	C_2^y	C_2^x	I	σ_h^z	σ_v^y	σ_v^x
σ_1	σ_1	σ_3	σ_4	σ_2	σ_3	σ_1	σ_2	σ_4

(22)

Multiplying by the characters of the B I.R. and summing one gets:

$$\sigma_1+\sigma_3-\sigma_4-\sigma_2+\sigma_3+\sigma_1-\sigma_2-\sigma_4=2(\sigma_1-\sigma_2+\sigma_3-\sigma_4) \tag{23}$$

or after normalization

$$\Phi_2=\frac{\sigma_1-\sigma_2+\sigma_3-\sigma_4}{2} \tag{24}$$

The final twelve ligand combinations are listed in Table 3. The signs in front of these functions are chosen so that the majority of the overlap integrals with the metal orbitals is positive. This is done to facilitate programming for the IBM 7090 computer.

Table 3 contains also the metal orbitals given in Appendix C. The last column indicates the number of metal and ligand functions which transform according to each I.R. According to Chapter II-4, nonzero matrix elements H_{ik} and S_{ik} may occur only between functions of the same I.R. Therefore if the twenty-one functions of Table 2 are used in the expansion Eq. (14) instead of the functions Eq. (13), the secular determinant Eq. (15) splits into eight smaller ones. The dimension of these smaller determinants is exactly equal to the number

TABLE 3

LCAO TRANSFORMING ACCORDING TO THE IRREDUCIBLE REPRESENTATIONS OF THE D_{2h} GROUP

	D_{2h}	Metal Orbital	σ Ligand	π Ligand	No.
A	N_{ig}	$4S;\ 3d_{Z^2};\ 3d_{X^2-y^2}$	$\Phi_1=\frac{\sigma_1+\sigma_2+\sigma_3+\sigma_4}{2};\ \Phi_5=\frac{\sigma_5+\sigma_6}{\sqrt{2}}$		5
B	N_{3g}	$3dxy$	$\Phi_2=\frac{\sigma_1-\sigma_2+\sigma_3-\sigma_4}{2}$		2
C	N_{2g}	$3dxz$	——	$\chi_1=\frac{(P_y)_1+(P_y)_2-(P_y)_3-(P_y)_4}{2};\ \chi_5=\frac{(P_x)_5-(P_x)_6}{\sqrt{2}}$	3
D	N_{4g}	$3dyz$	——	$\chi_2=\frac{(P_y)_1-(P_y)_2-(P_y)_3+(P_y)_4}{2}$	2
	N_{1u}	——	——	$\chi_3=\frac{(P_y)_1-(P_y)_2+(P_y)_3-(P_y)_4}{2}$	1
E	N_{3u}	$4P_z$	$\Phi_6=\frac{\sigma_6-\sigma_5}{\sqrt{2}}$	$\chi_4=\frac{(P_y)_1+(P_y)_2+(P_y)_3+(P_y)_4}{2}$	3
Z	N_{2u}	$4P_y$	$\Phi_3=\frac{-\sigma_1+\sigma_2+\sigma_3-\sigma_4}{2}$	——	2
H	N_{4u}	$4P_x$	$\Phi_4=\frac{-\sigma_1-\sigma_2+\sigma_3+\sigma_4}{2}$	$\chi_6=-\frac{(P_x)_5+(P_x)_6}{\sqrt{2}}$	3

$\sigma_i = \sin\theta' S_i + \cos\theta' (P_Z)_i$, $i=1,2,3,4$; $\sigma_i = \sin\theta'' S_j + \cos\theta'' (P_Z)_j$, $j=5,6$

appearing in the last column of Table 3. Thus one gets eight secular equations of the form

$$\det \left| H_{ik} - E S_{ik} \right| = 0 \qquad (25)$$

where i, k refer to the five functions of the A I.R., to the two functions of the B I.R., etc. The eigenstates belonging to the different I.R. are denoted by A_1, A_2, A_3, A_4, A_5; B_1, B_2; C_1, C_2, C_3; . . . H_1, H_2, H_3. For example, a 5x5 determinant corresponds to the I.R. A (or N_{1g} or Γ_{1g}) with five eigenfunctions of the form

$$C_1 \left| 4s \right\rangle + C_2 \left| 3d_{z^2} \right\rangle + C_3 \left| 3d_{x^2-y^2} \right\rangle + C_4 \left| \Phi_1 \right\rangle + C_5 \left| \Phi_5 \right\rangle \qquad (26)$$

For a particular case, the five coefficients C_i and the five eigenstates A_i , obtained by solving the corresponding secular equation, are given in Table 7 of Chapter V-2.

CHAPTER IV

COMPONENTS OF THE SECULAR EQUATIONS

In order to solve the secular Eq. (25), the overlap integrals S_{ik} and the energy matrix elements H_{ik} as defined in Eqs. (4) and (5) must first be determined. The indices refer to the functions of Table 2 and not to the atomic orbitals. This chapter describes ways of obtaining the S_{ik}.

1. Group Overlap Integrals

When combinations of ligand functions transforming according to the various I.R.'s are used, the overlap integrals S_{ik} are called group overlap integrals because they involve more than one two-center overlap integrals. Their evaluation is straightforward but tedious. For example, consider the D I.R. for which there are the metal orbital $3d_{yz}$ and the ligand π-orbital χ_2, as shown in Table 3. The group overlap integral is given by

$$I = \int \chi_2^* (3d_{yz})\, d\tau \tag{27}$$

By substituting χ_2^* from Table 3:

$$I = \frac{1}{2}\left[\langle (p_y)_1 | 3d_{yz}\rangle - \langle (p_y)_2 | 3d_{yz}\rangle - \langle (p_y)_3 | 3d_{yz}\rangle + \langle (p_y)_4 | 3d_{yz}\rangle\right] \tag{28}$$

An integral like $\langle (p_y)_1 | 3d_{yz} \rangle$ is called a <u>two-center integral</u> because the function $(p_y)_1$ is centered at the oxygen ion #1, and the $3d_{yz}$ at the vanadium ion. Since there are many tabulations of two-centered integrals referred to a spheroidal coordinate system (see Figure 4) one must express the central metal orbital

$$3d_{yz} = R(r) \sin\Theta \cdot \sin\Phi \cos\Theta \tag{29}$$

in four different coordinate systems which have their z-axis pointing towards the ligand oxygen #1, #2, #3, and #4 respectively, and their $x-$, $y-$ axes parallel to the x , y axes of the left-handed systems at the individual ligand oxygen. Figure 3 shows that the above-mentioned transformation can be accomplished by substituting for $\cos\Theta$, $\sin\Theta \cdot \sin\Phi$ and $\sin\Theta \cdot \cos\Phi$ the expressions given in Table 4, where α and β are angles in the rotated coordinate systems, which play the role of Θ and Φ of the old system.

TABLE 4

TRANSFORMATION OF THE SPHERICAL HARMONICS

Ligand	$\cos\Theta$	$\sin\Theta \sin\Phi$	$\sin\Theta \cos\Phi$
1	$-\sin\alpha \sin\beta$	A - B	$-\Gamma - \Delta$
2	$-\sin\alpha \sin\beta$	A + B	$+\Gamma - \Delta$
3	$-\sin\alpha \sin\beta$	-A + B	$+\Gamma + \Delta$
4	$-\sin\alpha \sin\beta$	-A - B	$-\Gamma + \Delta$
5	$-\cos\alpha$	$\sin\alpha \sin\beta$	$-\sin\alpha \cos\beta$
6	$+\cos\alpha$	$-\sin\alpha \sin\beta$	$-\sin\alpha \cos\beta$

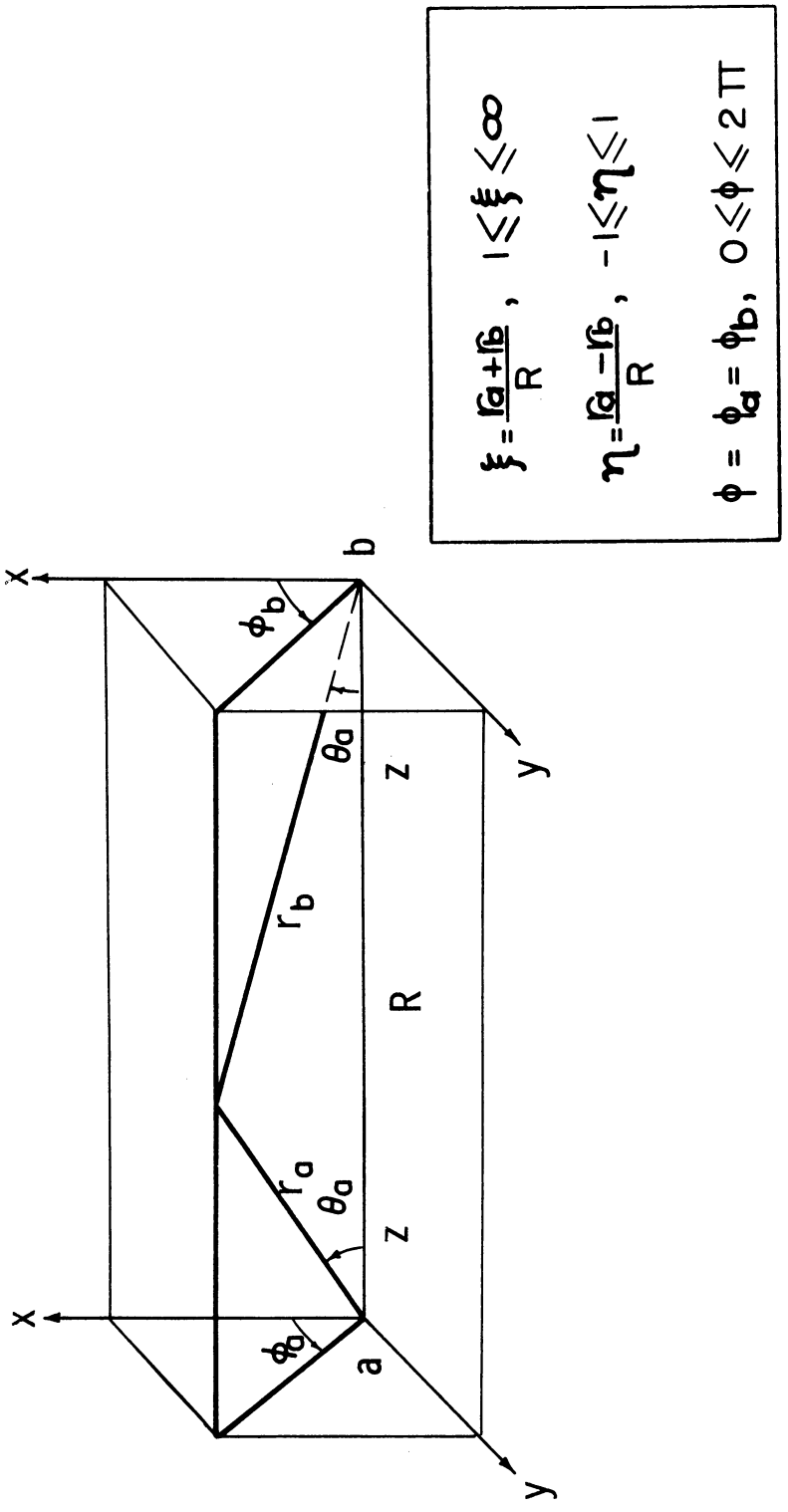

Fig. 4. Speroidal Coordinate System

where $A = \cos\varphi_\perp \cdot \sin\alpha\cos\beta$, $B = \sin\varphi_\perp \cdot \cos\alpha$, $\Gamma = \sin\varphi_\perp \cdot \sin\alpha \cdot \cos\beta$, $\Delta = \cos\varphi_\perp \cdot \cos\alpha$.

Therefore

$$
\begin{aligned}
I = \frac{1}{2}\Big[& \langle (p_y)_1 | R(r)(-\sin\alpha\sin\beta)(\cos\varphi_\perp \sin\alpha\cos\beta - \sin\varphi_\perp\cos\alpha) \rangle \\
& - \langle (p_y)_2 | R(r)(-\sin\alpha\sin\beta)(\cos\varphi_\perp \sin\alpha\cos\beta + \sin\varphi_\perp\cos\alpha) \rangle \\
& - \langle (p_y)_3 | R(r)(-\sin\alpha\sin\beta)(-\cos\varphi_\perp \sin\alpha\cos\beta + \sin\varphi_\perp\cos\alpha) \rangle \\
& + \langle (p_y)_4 | R(r)(-\sin\alpha\sin\beta)(-\cos\varphi_\perp \sin\alpha\cos\beta - \sin\varphi_\perp\cos\alpha) \rangle \Big] \\
= & \frac{1}{2} \langle (p_y) | R(r)\sin\alpha\sin\beta(-4\sin\varphi_\perp\cos\alpha) \rangle \\
= & \frac{1}{2} 4\sin\varphi_\perp \langle (p_y) | R(r)\sin\alpha\sin\beta\cos\alpha \rangle \\
= & \frac{1}{2} \sin\varphi_\perp \langle (p_y) | 3d_{yz} \rangle \\
= & 2\sin\varphi_\perp \langle 2p_\pi | 3d_\pi \rangle
\end{aligned}
\qquad (30)
$$

The $\langle 2p_\pi | 3d_\pi \rangle$ is a two-center overlap integral. Following this method and neglecting any ligand-ligand overlapping, the following

nonzero expressions for the group overlap integrals were obtained for each I.R.

A (N1g)

$$A14 = 2\left[\sin\delta'\langle 2s|4s\rangle + \cos\delta'\langle 2p_\sigma|4s\rangle\right]_i$$

$$A15 = \sqrt{2}\left[\sin\delta''\langle 2s|4s\rangle + \cos\delta''\langle 2p_\sigma|4s\rangle\right]_j$$

$$A24 = -\left[\sin\delta'\langle 2s|3d_\sigma\rangle + \cos\delta'\langle 2p_\sigma|3d_\sigma\rangle\right]_i \qquad (31)$$

$$A25 = \sqrt{2}\left[\sin\delta''\langle 2s|3d_\sigma\rangle + \cos\delta''\langle 2p_\sigma|3d_\sigma\rangle\right]_j$$

$$A34 = \sqrt{3}(\cos^2\varphi_\perp - \sin^2\varphi_\perp)\left[\sin\delta'\langle 2s|3d_\sigma\rangle + \cos\delta'\langle 2p_\sigma|3d_\sigma\rangle\right]_i$$

B (N3g)

$$B12 = 2\sqrt{3}\sin\varphi_\perp\cos\varphi_\perp\left[\sin\delta'\langle 2s|3d_\sigma\rangle + \cos\delta'\langle 2p_\sigma|3d_\sigma\rangle\right]_i \qquad (32)$$

C (N2g)

$$C12 = 2\cos\varphi_\perp\langle 2p_\pi|3d_\pi\rangle_i$$

$$C13 = \sqrt{2}\langle 2p_\pi|3d_\pi\rangle_j \qquad (33)$$

D (N4g)

$$D12 = 2\sin\varphi_\perp\langle 2p_\pi|3d_\pi\rangle_i \qquad (34)$$

E (N3u)

$$E12 = \sqrt{2}\left[\sin\delta''\langle 2s|4p_\sigma\rangle + \cos\delta''\langle 2p_\sigma|4p_\sigma\rangle\right]_j$$

$$E13 = 2\langle 2p_\pi|4p_\pi\rangle_i \qquad (35)$$

Z (N_{2u})

$$Z12 = 2\sin\varphi_1 \left[\sin\delta' \langle 2s \mid 4p_\sigma \rangle + \cos\delta' \langle 2p_\sigma \mid 4p_\sigma \rangle\right]_i \tag{36}$$

H (N_{4u})

$$H12 = 2\cos\varphi_1 \left[\sin\delta' \langle 2s \mid 4p_\sigma \rangle + \cos\delta' \langle 2p_\sigma \mid 4p_\sigma \rangle\right]_i$$

$$H13 = \sqrt{2} \langle 2p_\pi \mid 4p_\pi \rangle_j \tag{37}$$

where i stands for the shorter vanadium-oxygen distance and j for the longer one. A, B, C, D, E, Z, H stand for N_{1g}, N_{3g}, N_{2g}, N_{4g}, N_{3u}, N_{2u} and N_{4u}, and the numbers denote the orbitals in the corresponding I.R. as listed in Table 2. For example, C13 denotes the group overlap integral of the first (i.e., $3d_{yz}$) and third (i.e., χ_5) orbitals in the N_{2g} I.R.

2. Two-Center Overlap Integrals

It was seen that the group overlap integrals can be expressed in terms of two-center overlap integrals. In this paragraph the method of calculating the latter will be considered. For example, let the integral $\langle 2s \mid 4p_\sigma \rangle$ be calculated when the distances are in atomic units and the radial parts are given as

$$R(2s) = N_a r_a e^{-\mu_a r_a} \quad \text{and} \quad R(4p_\sigma) = N_b r_b^2 e^{-\mu_b r_b} \tag{38}$$

Note that the normalization constants N_a and N_b are given for the radial part only. Then

$$\langle 2s|4p_\sigma\rangle = N_a N_b \int r_a e^{-\mu_a r_a} \frac{1}{\sqrt{4\pi}} r_b^2 e^{-\mu_b r_b} \cos\theta_b \sqrt{\frac{3}{4\pi}}\, d\tau \tag{39}$$

Observing that in the spheroidal coordinate system of Figure 4

$$\begin{aligned} r_a &= \frac{R}{2}(\xi+\eta) & r_a\cos\theta_a &= \frac{R}{2}(1+\xi\eta) \\ r_b &= \frac{R}{2}(\xi-\eta) & r_b\cos\theta_b &= \frac{R}{2}(1-\xi\eta) \\ d\tau &= \left(\frac{R}{2}\right)^3 (\xi^2-\eta^2)\, d\xi\, d\eta\, d\varphi \end{aligned} \tag{40}$$

and defining

$$\begin{aligned} p &\equiv \frac{1}{2}(\mu_a+\mu_b)R \\ q &\equiv \frac{1}{2}(\mu_a-\mu_b)R \\ A_n(p) &= \int_1^\infty e^{-px} x^n\, dx \\ B_n(q) &= \int_{-1}^1 e^{-qx} x^n\, dx \end{aligned} \tag{41}$$

the integral $\langle 2s|4p_\sigma\rangle$ becomes

$$\langle 2s|4p_\sigma\rangle = \frac{N_a N_b \sqrt{3}}{4\pi} \int_{\xi=1}^{\infty} \int_{\eta=-1}^{1} \int_{\varphi=0}^{2\pi} e^{-\xi p-\eta q} \left(\frac{R}{2}\right)(\xi+\eta)\left(\frac{R}{2}\right)(\xi-\eta)\cdot$$

$$\cdot \left(\frac{R}{2}\right)(1-\xi\eta)\left(\frac{R}{2}\right)^3 (\xi^2-\eta^2)\, d\xi\, d\eta\, d\varphi$$

$$= N_a N_b \frac{\sqrt{3}}{2} \left(\frac{R}{2}\right)^6 \int_\xi e^{-\xi p} \left(-\xi^5 B_1 + 2\xi^3 B_3 - \xi B_5 + \xi^4 B_0 - 2\xi^2 B_2 + B_4\right) d\xi$$

$$= N_a N_b \frac{\sqrt{3}}{2} \left(\frac{R}{2}\right)^6 \left[-A_5 B_1 + 2A_3 B_3 - A_1 B_5 + A_4 B_0 - 2A_2 B_2 + B_4\right]$$

(42)

Similar expressions for the two-centered integrals needed in this work have been derived and are listed in Appendix D. The A and B integrals are tabulated in Refs. 32, 33, 34, and overall two-center integrals in Ref. 35. For the present problem the integrals A and B were calculated by a MAD program[43] using the following SCF radial functions.[23,27] For oxygen

$$\begin{aligned} R\ (2s) &= .5459\ \phi_2(1.80) + .4839\ \phi_2(2.80) \\ R\ (2p) &= .6804\ \phi_2(1.55) + .4038\ \phi_2(3.45) \end{aligned} \tag{43}$$

For vanadium

$$\begin{aligned} R\ (3d) &= .52430836\ \phi_3(1.8289) + .49893811\ \phi_3(3.6102) \\ &\quad + .11312810\ \phi_3(6.8020) + .00545223\ \phi_3(12.4322) \\ R\ (4s) = R\ (4p) &= -.02244797\ \phi_1(23.9091) - .01390591\ \phi_2(20.5950) \\ &\quad + .06962484\ \phi_2(10.16666) + .06773727\ \phi_3(9.3319) \\ &\quad - .09707771\ \phi_3(5.1562) - .024620956\ \phi_3(3.5078) \\ &\quad + .04411542\ \phi_4(3.8742) + .36068942\ \phi_4(1.8764) \\ &\quad + .608999600\ \phi_4(1.1462) + .14868524\ \phi_4(.7800) \end{aligned} \tag{44}$$

where

$$\Phi_\eta(\mu) = N r^{\eta-1} e^{-\mu r}$$

and

$$N = \sqrt{\frac{(2\mu)^{2\eta+1}}{(2\eta)!}} \tag{45}$$

The final results for the group overlap integrals (see Appendix D) are given in Table 5.

TABLE 5

GROUP OVERLAP INTEGRALS

	SnO_2	TiO_2	GeO_2
A14	.494	.495	.525
A15	.425	.445	.456
A24	-.148	-.162	-.180
A25	.217	.233	.255
A34	-.053	-.045	-.063
B12	.251	.278	.305
C12	.090	.112	.128
C13	.099	.113	.126
D12	.110	.131	.157
E12	.604	.627	.630
E13	.325	.359	.395
Z12	.504	.474	.502
H12	.409	.404	.408
H13	.227	.243	.259

3. Diagonal Energy Matrix Elements

The most subtle point in solving the secular Eq. (25) is the estimation of the energy matrix elements. Since these cannot be obtained from first principles, semiempirical methods to approximate them from known experimental spectroscopic data will be developed. Two types of energy matrix element are distinguished in the secular Eq. (25): (a) the diagonal elements H_{ii}'s, called Coulomb integrals, and (b) the off-diagonal ones H_{ij}'s, called resonance integrals.

The Coulomb integral H_{ii} gives the potential energy of an electron in the i-th orbital. It can be taken equal to the free atom (or ion) ionization energy of an electron on this orbital to the zero-th approximation. For a hybrid orbital, the weighted average is taken, and for an orbital consisting of linear combination of ligand orbitals again the ionization energy of one of the similar ligand orbitals is taken. However, a better estimate of the H_{ii}'s is obtained by means of the concept of the valence state ionization potential (VSIP). A discussion of the procedure is given by Moffitt[29] (see also Appendix H).

To use Moffitt's tables[29] for the oxygen VSIP, a binding scheme must be adopted. Here it will be shown that the adoption of the ionic states O^{+} and V^{2-} for the oxygen and vanadium respectively, can satisfy the symmetry requirements and the production of the ESR spectrum in a homopolar binding scheme with oxygen sp^2 hybridization. From Figure 1 the spatial arrangement of ions in the rutile structure suggests a valency of three (V_3) for the oxygen ions and a valency of six (V_6) for the metal ions. This implies that there are three and six

electrons with uncorrelated spins in the respective valence states (see Appendix H). The oxygen ion configuration giving valency of three is

$$O^{+}: [He]\, 2s\, 2p_z^2\, 2p_x\, 2p_y$$

According to Figure 2 and the discussion in Chapter II-3, the 2s, $2p_x$, and $2p_y$ form hybrid orbitals with three spin-uncorrelated electrons. The other two electrons will occupy the $2p_z$ orbital forming the so-called lone pair. Such an electron will be denoted as p_ℓ. For an overall crystal neutrality the metal ions must have a double negative charge. This implies that for vanadium there are seven valence electrons outside the argon core. This is expected if one considers the six bonds with the surrounding oxygen ions and the single unpaired electron which produces the ESR spectrum.

The bonding scheme fits the requirement of the symmetry and of the number of electrons except that oxygen has a much greater electronegativity than vanadium,[11] and Pauling's electroneutrality principle[11] asserts that the charge on each ion is in the range -1e to +1e. One can overcome these difficulties by assuming a partially ionic character of the bonds so that electronic charge is shifted towards the ligands, resulting in a small positive charge for vanadium and a correspondingly small negative charge for the oxygen ions. As it will be seen, the molecular orbital calculation will determine this ionicity of the bonds. In this sense the charges O^{+}, V^{2-} will be considered from now on as nominal charges.

Of course, none of the above problem arises if one considers a purely ionic bonding with V^{4+} and O^{2-}. The nearest noble gas

configuration is achieved for oxygen and metal ions except for V^{4+} which is left with one valence electron producing the ESR spectrum. However, it is believed that a purely ionic bonding is generally rare outside the I-VII compounds.

The VSIP's of O^+ calculated here are 416396 cm^{-1}, 277022 cm^{-1}, and 253122 cm^{-1} for an s-, p-, and p_ℓ - electron respectively. The oxygen atom in the rutile structures is assumed to have the configuration

$$O^+ : 1s^2\, 2s\, 2p_z^2\, 2p_x\, 2p_y$$

with three unpaired spins. The corresponding valence state, according to Moffitt, is designated as $s\, z^2\, xy\,(V_3)$ with promotion energy

$$\frac{1}{2}(^4P) + \frac{1}{4}(^2P) + \frac{1}{4}(^2D) = 154626.63\ cm^{-1}$$

The fact that 2s, $2p_x$, and $2p_y$ hybridize does not change this energy, as the configuration remains unchanged. This is called first-order hybridization. To estimate the ionization potential (I.P.) of an s- or p-electron, the valence state of the final configuration must also be considered. Thus, for an s-unpaired electron

$$sp^4(V_3) \longrightarrow p^4(V_2)$$

for a p-unpaired electron (46)

$$sp^4(V_3) \longrightarrow sp^3(V_2)$$

for a p_ℓ -electron of the lone pair

$$sp^4(V_3) \longrightarrow sp^3(V_4)$$

Therefore:

$$\text{VSIP of } \begin{pmatrix} s \\ p \\ p_\ell \end{pmatrix} = (\text{I.P. of } O^+ \text{ ground state}) - \text{promotion energy to } sp^4(V_3) + \text{promotion energy to } \begin{pmatrix} p^4(V_2) \\ sp^3(V_2) \\ sp^3(V_4) \end{pmatrix} \text{of } O^{++}$$

$$= (283550.9\ \text{cm}^{-1}) - (154626.63\ \text{cm}^{-1}) + \begin{pmatrix} 287472.15 \\ 148097.82 \\ 124197.90 \end{pmatrix} = \begin{pmatrix} 416396.42\text{cm}^{-1} \\ 277022.09\text{cm}^{-1} \\ 253122.20\text{cm}^{-1} \end{pmatrix} \quad (47)$$

as the promotion energies to $p^4(V_2)$, $sp^3(V_2)$ and $sp^3(V_4)$ of O^{++} are given by:

$$\frac{3}{4}(^3P) + \frac{1}{4}(^1D), \quad \frac{3}{8}(^3D^\circ) + \frac{1}{8}(^1D^\circ) + \frac{3}{8}(^3P^\circ) + \frac{1}{8}(^1P^\circ)$$

and

$$\frac{5}{16}(^5S^\circ) + \frac{3}{16}(^3S^\circ) + \frac{6}{16}(^3D^\circ) + \frac{2}{16}(^1D^\circ)$$

respectively.

The VSIP of O° and O^- are calculated next and found to be 222000 cm^{-1}, 115300 cm^{-1}, and 98968 cm^{-1} for an s-, p-, and p_ℓ - electron of O° respectively, and (80000 cm^{-1}?), 16200 cm^{-1}, and 3710 cm^{-1} for the corresponding electrons of O^-. The procedures are as follows: It was seen that the polarity of the bonds is expected to decrease the positive charge on the oxygen center and most likely to reverse it. In such a case the VSIP will be different, clearly smaller, so that it needs to be re-estimated. Since the tables give spectroscopic data of the elements with integral electronic charge, the VSIP of fractional charge is to be obtained by interpolation. Next we need to

see how to estimate the VSIP of an oxygen which is effectively neutral (or with -1 |e| charge) because of the polarity of the bonds. For this it is assumed that the VSIP of the isoelectronic ion will be a good approximation. For an effectively neutral oxygen or for O^-, the neutral nitrogen atom N° and the carbon negative ion C^- are considered instead. All VSIP for N° and C^-, except for the 2s electron of C^- are obtained from a table given by Skinner and Pritchard.[30] A value of about 10 eV is not unreasonable for the C^- 2s electron. The procedure of calculating the VSIP is the same as in the previous paragraph. The values taken from the tables of Skinner and Pritchard are:

(a) Valence state energies in eV.

$sp^4(V_3)$:	C^-	(9.38)	extrapolated
	N	14.23	
$sp^3(V_4)$:	C	8.14	
	N^+	11.64	
$sp^3(V_2)$:	C	9.69	
	N^+	14.03	
$p^4(V_2)$:	C	-	
	N^+	(27.2)	extrapolated

(b) Ionization potentials in eV.

$C^-(s^2p^3, {}^4S)$	$C(s^2p^2\ {}^3P)$	1.7
$N\ (s^2p^3, {}^4S)$	$N^+(s^2p^2\ {}^3P)$	14.54

Finally the VSIP of the vanadium d electrons are estimated. The results are summarized in the following table.

	$V^{++}(Co^{++})$	$V^{+}(Fe^{+})$	$V^{\circ}(Mn^{\circ})$
4p	165658 cm^{-1}	102308 cm^{-1}	38722 cm^{-1}
4s	219465	127369	54762
3d	295997	141178	62516

Moffitt does not give tables for 3d electrons, so the following procedure was adopted. The isoelectric series for vanadium in the rutile structure with nominally seven electrons, but with an effective charge of zero, +1e and +2e, is Mn°, Fe^{+}, Co^{++}. According to Moore's tables and notation,[28] the I.P. of Mn° ($a\,^6S$) to Mn^{+}($a\,^7S$) is 59960 cm^{-1}. The average of the two states of Mn°, $z\,^8P^{\circ}(a\,^7S + 4p\uparrow)$ and $z\,^6P^{\circ}(a\,^7S + 4p\downarrow)$, is 21257.74 cm^{-1}; therefore

$$\text{VSIP of 4p electron} \cong 59960-21237.74-0=38722.26\ cm^{-1} \tag{48}$$

The average, also, of the two states of Mn°, $a\,^6D(a\,^5D+4s\uparrow)$ and $a\,^4D(a\,^5D+4s\downarrow)$, is 19784.41 cm^{-1}; the average of $a\,^5D$ of Mn^{+} is 14586.16 cm^{-1}. Therefore

$$\text{VSIP of 4s electron} \cong 59960-19784.41+14586.16=54761.75\ cm^{-1} \tag{49}$$

The same procedure is applied for Fe^{+} and Co^{++}. The 3d VSIP for Mn°, Fe^{+}, and Co^{++} are estimated from the tables given by Slater[31] and Watson.[27]

In Table 6 the valence state ionization potentials for the vanadium charge range 0 to +.65e and the corresponding oxygen range 0 to -.325e are tabulated. Interpolation is used to obtain the VSIP's of the electrons on the vanadium orbitals 4p, 4s, 3d and on the oxygen orbital of the lone pair p_ℓ, for various fractional net charges of the vanadium and oxygen ions. For the electrons on the hybrid orbitals

$$\sigma_i = \sin\vartheta'(2s) + \cos\vartheta'(2p) \tag{50}$$

the VSIP's are the weighted averages:

$$(\text{VSIP}) = \sin^2\vartheta'(\text{VSIP of 2s}) + \cos^2\vartheta'(\text{VSIP of 2p}) \tag{51}$$

These are calculated for the integral values of the net ionic charge and then interpolated. The values of $\sin\vartheta'$ and $\cos\vartheta'$ are taken from Table 2.

These VSIP's present a weak point in all semiempirical calculations. However, there are two reassuring factors: (a) the use of isoelectronic-ion parameters does not affect the type and relative positions of molecular orbitals as the isoelectronic principle asserts,[32] and (b) since the VSIP's are used as parameters in solving the secular determinant even the numerical results will not be greatly different if the right parameters are chosen.

4. Off-Diagonal Energy Matrix Elements

The off-diagonal energy matrix elements, or resonant integrals, $H_{i,j}$ are even more difficult to estimate. Mulliken's[33] assertion

that H_{ij} is 1.5 to 2 times the quantity $S_{ij}(H_{ii} + H_{jj})/2$ is often followed. Wolfsberg and Helmholtz used both 1.67 and 2. More recently Gray and Ballhausen,[23] and Lipscomb[38] used 2. However, the geometric mean seems to give a better fit than the arithmetic mean, so throughout this work H_{ij} will be approximated by

$$H_{ij} = -2S_{ij}\sqrt{H_{ii}\,H_{jj}} \tag{52}$$

TABLE 6

VSIP OF VANADIUM AND OXYGEN IONS

		Vanadium Ionic Charge						
		+.000	+.050	+.100	+.150	+.200	+.250	+.300
	4p	038722	041968	045215	048461	051707	054954	058200
	4s	054839	057965	061092	064218	067344	070471	073600
	3d	062516	065680	068844	072008	075172	078336	081500
SnO_2	$2p_\ell$	098968	096240	093512	090784	088056	085328	082600
	σ_i	135335	132063	128790	125518	122245	118973	115700
	σ_δ	187962	184352	180741	177131	173521	169910	166300
TiO_2	$2p_\ell$	-	-	-	-	-	-	-
	σ_i	131835	128563	125290	122018	118745	115473	112200
	σ_δ	194962	191352	187741	184131	180521	176910	173300
GeO_2	$2p_\ell$	-	-	-	-	-	-	-
	σ_i	135195	131923	128650	125378	122105	118833	115560
	σ_δ	188242	184632	181021	177411	173801	170190	166580

TABLE 6--Continued

		Vanadium Ionic Charge						
		+.350	+.40	+.45	+.50	+.55	+.60	+.65
	4p	061546	064893	068239	071585	074932	078278	081624
	4s	076726	079853	083500	087000	091000	094500	097500
	3d	084664	087828	090992	095000	099100	103000	107000
SnO_2								
	$2p_\ell$	080000	077500	075000	072600	070000	067500	065500
	σ_i	112000	109100	106200	103200	100200	098000	095500
	σ_j	162700	159500	156200	153000	150000	146500	143500
TiO_2								
	$2p_\ell$	-	-	-	-	-	-	-
	σ_i	108500	105600	102700	099700	096700	094500	092000
	σ_j	169700	166500	163200	160000	157000	153500	150500
GeO_2								
	$2p_\ell$	-	-	-	-	-	-	-
	σ_i	111860	108960	106060	103060	101860	097860	095360
	σ_j	162980	159780	156480	153280	150280	146780	143780

CHAPTER V

SOLUTION OF SECULAR EQUATION

1. Energy Eigenvalues

Chapter III showed that the original secular Eq. (15) is reduced to other smaller Eqs. (25) by using LCAO transforming according to the I.R. of the D_{2h} group. To each I.R. corresponds a secular equation whose order depends on the number of functions belonging to it. For example, Table 3 shows that there is a secular equation of fifth order corresponding to the irreducible representation A. The group overlap integrals S_{ik} and the diagonal energy matrix elements H_{ii} were calculated in Chapter IV (see Tables 5 and 6). The latter is found to vary with the assumed ion charge. The former, however, does not seem to vary appreciably, according to the SCF calculations of Watson,[27] so that no correction is applied. The off-diagonal energy matrix elements are found by the approximation Eq. (52).

Secular Eqs. (25) are solved on the IBM 7090 computer, using a program written in MAD language (see Appendix J). The input consists of diagonal energy matrix elements H_{ii} and the group overlap integrals S_{ik}. The off-diagonal elements H_{ij} are calculated by the program following Eq. (52). The output consists of the one-electron eigenstates

and eigenvalues of the vanadium and oxygen valence electrons in the MO scheme. Also, the fraction of the orbital charge that can be assigned to vanadium is given (for more details on this see the next section, V-2).

Thus in Figure 5 the electron eigenvalues of SnO_2:V are shown. The VSIP of vanadium in the range 0 to +65e and of oxygen in the corresponding region 0 to -.325e are taken from Table 5 and used as parameters (see below). Only nineteen orbitals are shown: two others, A_5 and E_2, having energies around +90 Kcm^{-1}, are omitted. The central part of Figure 5 is drawn again in Figure 6. The levels are designated according to their symmetry. The subscripts are used to distinguish the various levels of the same symmetry. Similar curves for TiO_2:V and GeO_2:V are drawn in Figures 7 and 8 respectively. Energy eigenvalues are tabulated also in Appendix E.

The similarity of the three spectra for SnO_2, TiO_2, and GeO_2 is striking, as well as the fact that the relative positions and values of the energy levels are sensitive to small changes in the ionic charge. Figure 5 shows that the A_3 level crosses the four levels E_3, H_3, $|X_3>$, C_2. The levels A_2 and B_2 cross some levels also. Similar results apply for the TiO_2:V and GeO_2:V.

Now a justification is needed for treating the VSIP's as parameters. The difficulties in obtaining reliable values of the VSIP's were explained in Chapter IV. On the other hand, it is noticed that the energy eigenvalues depend rather critically on the VSIP's used. Therefore, any calculation based on a single set of VSIP's (i.e., on one

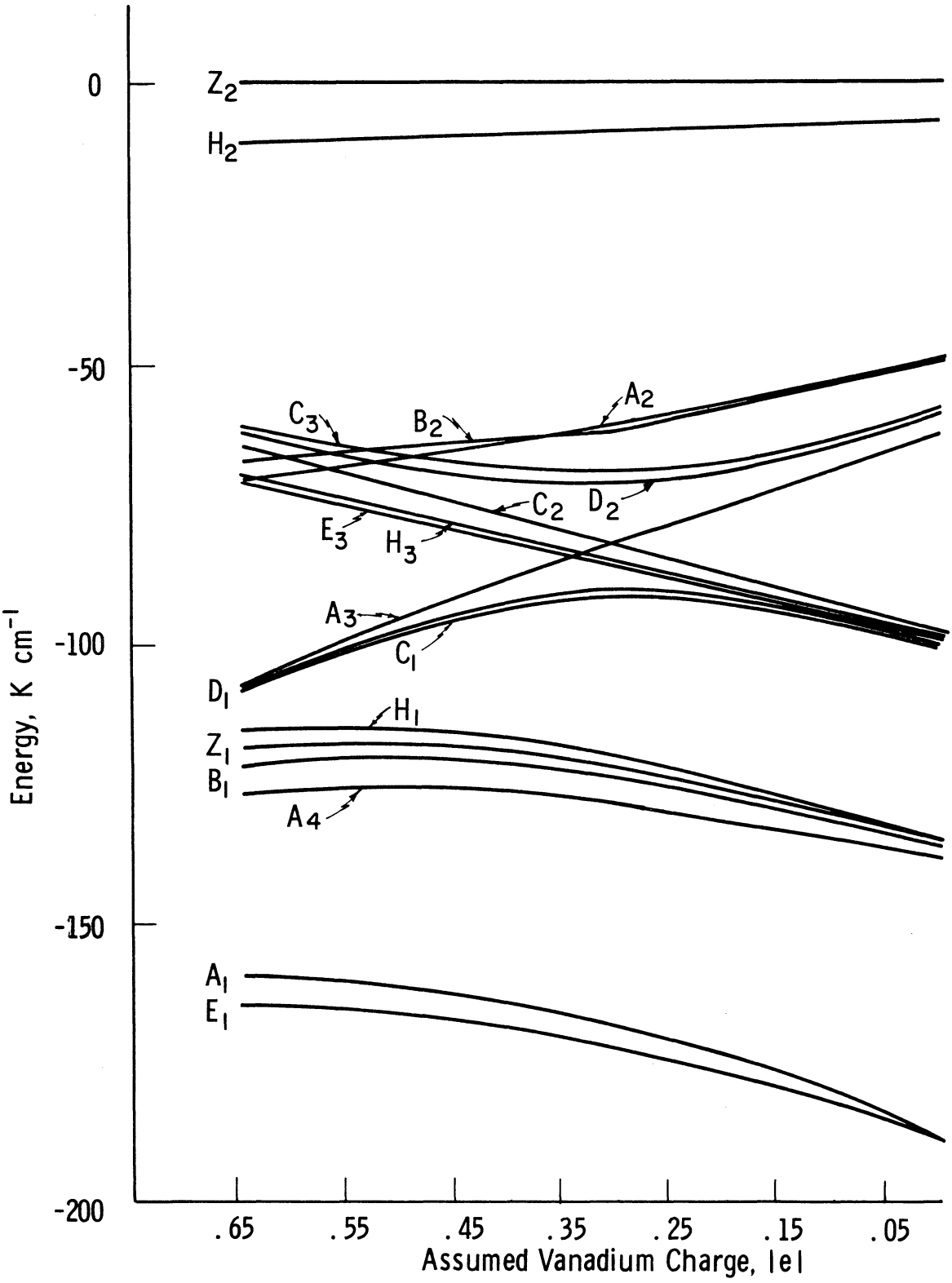

Fig. 5. MO Energy Levels of SnO_2:V

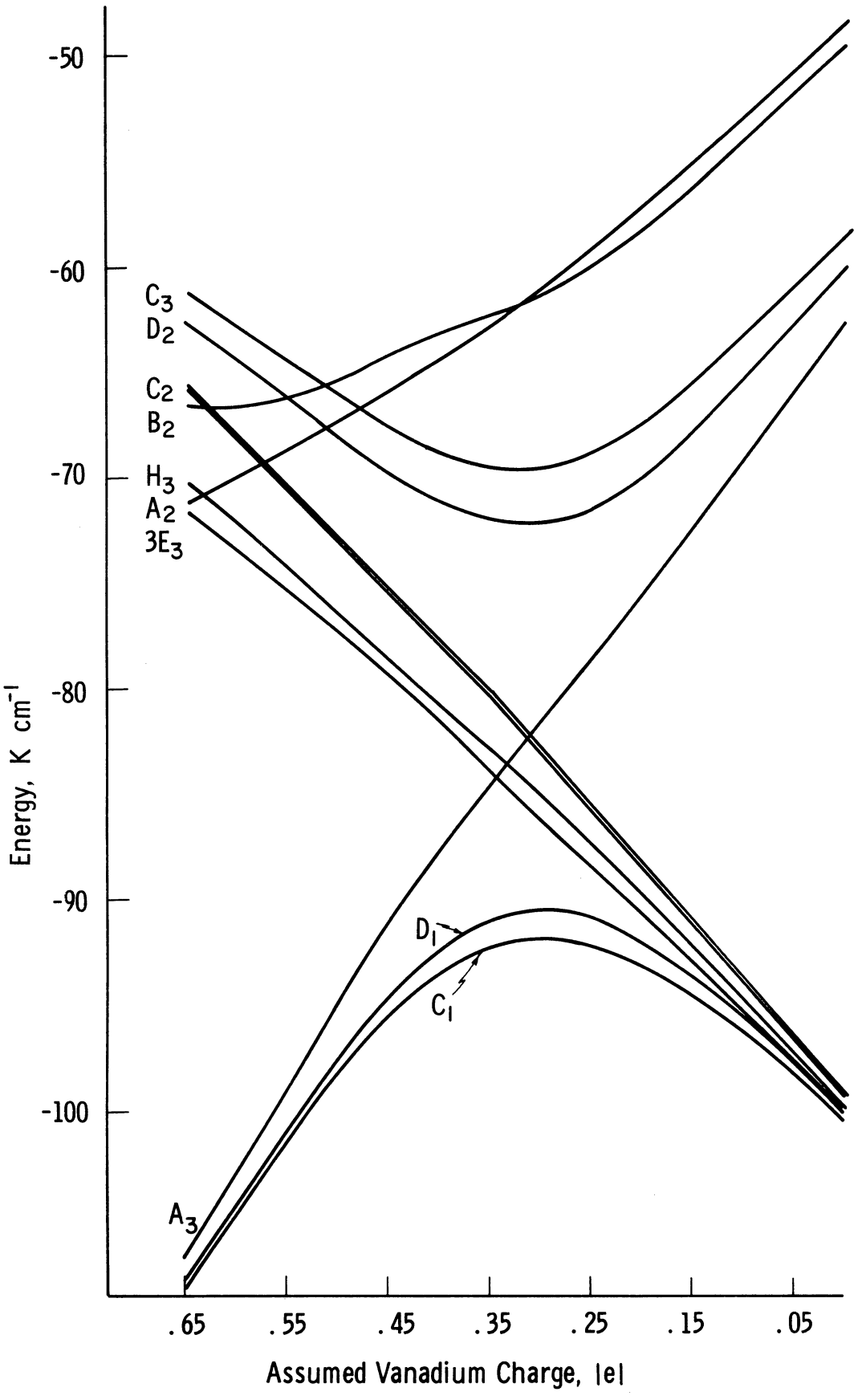

Fig. 6. Central MO Energy Levels of SnO_2:V

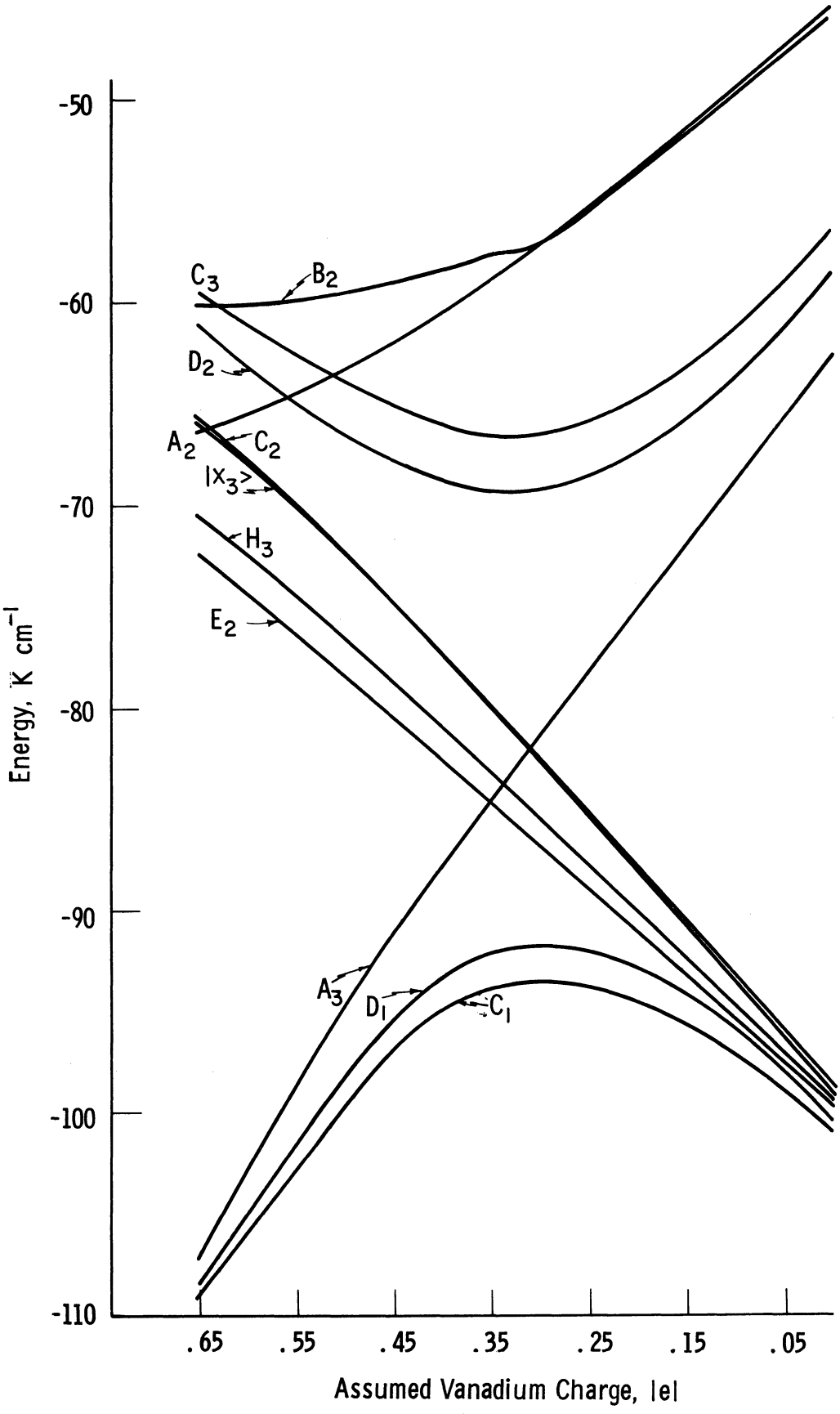

Fig. 7. Central MO Energy Levels of TiO_2:V

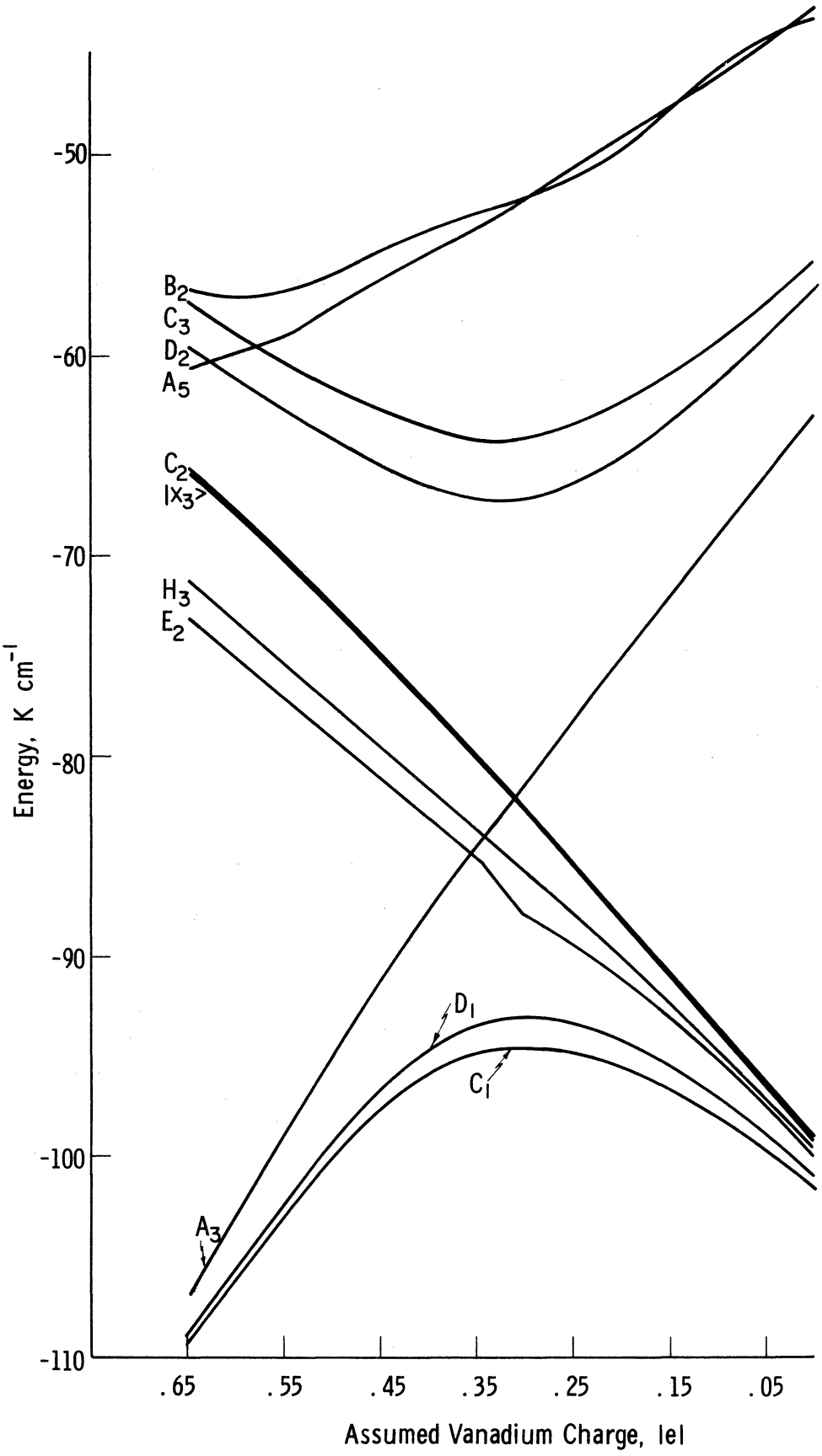

Fig. 8. Central MO Energy Levels of GeO_2:V

assumed vanadium charge) cannot be expected to give results in quantitative agreement with experiment. Thus it is clear that to find the best set of VSIP another physical quantity is needed to monitor the calculation. Usually the ionic charge is taken as the means of achieving self-consistency. This is explained below.

2. Charge Self-Consistency

To select the best set of VSIP's and thus the solution of the secular Eqs. (25), the vanadium charge is taken as a monitor.

A trial and error method is as follows: (a) A vanadium charge is assumed. (b) The corresponding VSIP's of vanadium and oxygen are selected from Table 6 and the secular equations are solved. (c) This solution is then used to calculate the vanadium charge which is compared to the assumed value. (d) The above procedures are repeated with different assumed vanadium charges until agreement is reached in step (c). When agreement is reached one says that charge self-consistency is fulfilled.

To carry out this program one must determine which MO's are occupied and then calculate the charge on the vanadium ion from the MO's. The charge is calculated (see Appendix J) as follows: The solution of the secular Eqs. (25) provide twenty-one eigenvalues and eigenfunctions. A typical set of eigenvalues and eigenfunctions is given in Table 7. The simplest normalized eigenfunctions, like the B_1, are of the form

$$\psi = c_1 \phi_{van} + c_2 \phi_{lig} \tag{53}$$

TABLE 7

EIGENFUNCTIONS OF VANADIUM IN SnO_2 FOR AN ASSUMED VANADIUM CHARGE OF +.25e

Energy in cm^{-1}		Eigenfunctions
86743	E_2	$-1.356\|4p_z\rangle+.894\|\Phi_6\rangle+.569\|\alpha_4\rangle$
80660	A_5	$-1.283\|4s\rangle-.076\|z^2\rangle+.075\|x^2-y^2\rangle+.827\|\Phi_1\rangle+.675\|\Phi_5\rangle$
-1182	Z_2	$-1.134\|4p_y\rangle+.775\|\Phi_3\rangle$
-8235	H_2	$-1.098\|4p_x\rangle+.623\|\Phi_4\rangle+.416\|\alpha_6\rangle$
-58941	A_2	$-.018\|4s\rangle+.999\|z^2\rangle+.133\|x^2-y^2\rangle+.365\|\Phi_1\rangle-.325\|\Phi_5\rangle$
-59396	B_2	$-.983\|xy\rangle+.554\|\Phi_2\rangle$
-68666	C_3	$-.852\|xz\rangle+.434\|\alpha_1\rangle+.483\|\alpha_5\rangle$
-71053	D_2	$-.860\|yz\rangle+.614\|\alpha_2\rangle$
-78298	A_3	$.067\|4s\rangle-.132\|z^2\rangle+.989\|x^2-y^2\rangle+.006\|\Phi_1\rangle+.003\|\Phi_5\rangle$
-85328	C_2	$-.0000001\|xz\rangle+.743\|\alpha_1\rangle-.669\|\alpha_5\rangle$
-85328	N_{1w}	$\|\alpha_3\rangle$
-87380	H_3	$.172\|4p_x\rangle-.166\|\Phi_4\rangle+.945\|\alpha_6\rangle$
-88314	E_3	$.178\|4p_z\rangle-.138\|\Phi_6\rangle+.934\|\alpha_4\rangle$
-90600	D_1	$.523\|yz\rangle+.797\|\alpha_2\rangle$
-92019	C_1	$.540\|xz\rangle+.517\|\alpha_1\rangle+.574\|\alpha_5\rangle$
-122743	H_1	$.211\|4p_x\rangle+.894\|\Phi_4\rangle+.018\|\alpha_6\rangle$
-124155	Z_1	$.235\|4p_y\rangle+.860\|\Phi_3\rangle$
-125185	B_1	$.317\|xy\rangle+.872\|\Phi_2\rangle$
-130140	A_4	$.261\|4s\rangle-.201\|z^2\rangle-.051\|x^2-y^2\rangle+.795\|\Phi_1\rangle-.138\|\Phi_5\rangle$
-171422	E_1	$.107\|4p_z\rangle+.932\|\Phi_6\rangle-.014\|\alpha_4\rangle$
-174822	A_1	$.161\|4s\rangle+.112\|z^2\rangle-.00006\|x^2-y^2\rangle+.006\|\Phi_1\rangle+.8921\|\Phi_5\rangle$

The orbital charge normalized to 1 is

$$\int \psi^2 d\tau = c_1^2 + 2c_1 c_2 \langle \phi_{vac} | \phi_{liq} \rangle + c_2^2 = 1 \qquad (54)$$

Following Mulliken's suggestion,[34] the fraction of MO charge on the vanadium is set equal to the charge c_1^2 found purely on vanadium, plus half of the overlap charge $2c_1 c_2 S_{v-l}$, i.e., the effective charge on vanadium due to orbital ψ is taken equal to

$$c_1^2 + c_1 c_2 S_{v-l} \qquad (55)$$

The generalization of this procedure to more complicated orbitals is obvious. In Figure 9 the fraction of the MO charge assigned to vanadium is plotted for the first thirteen molecular orbitals of SnO_2:V vs. the assumed vanadium charge. It is observed that this fraction does not change for some of the MO's such as A_3, E_3, H_3, C_2, and $|X_3>$. This is exemplified in Appendix F for the A_3 level. For the six MO's B_1, A_4, Z_1, H_1, A_1, E_1, there is a gradual decrease in the value of the orbital charge fraction assigned to vanadium from left to right, which corresponds to a gradual diminishing of the coefficients of the metal parts of the MO's. For the MO's D_1, C_1 this variation is larger.

Next we need to determine which of the above orbitals are occupied. A total of twenty-five electrons need to be accommodated in the MO's. There are three electrons from each oxygen ion--two electrons on 2p orbital and one a σ hybridized one--and seven electrons from the vanadium ion, as seen in Chapter VI-3. Following Pauli's principle, two

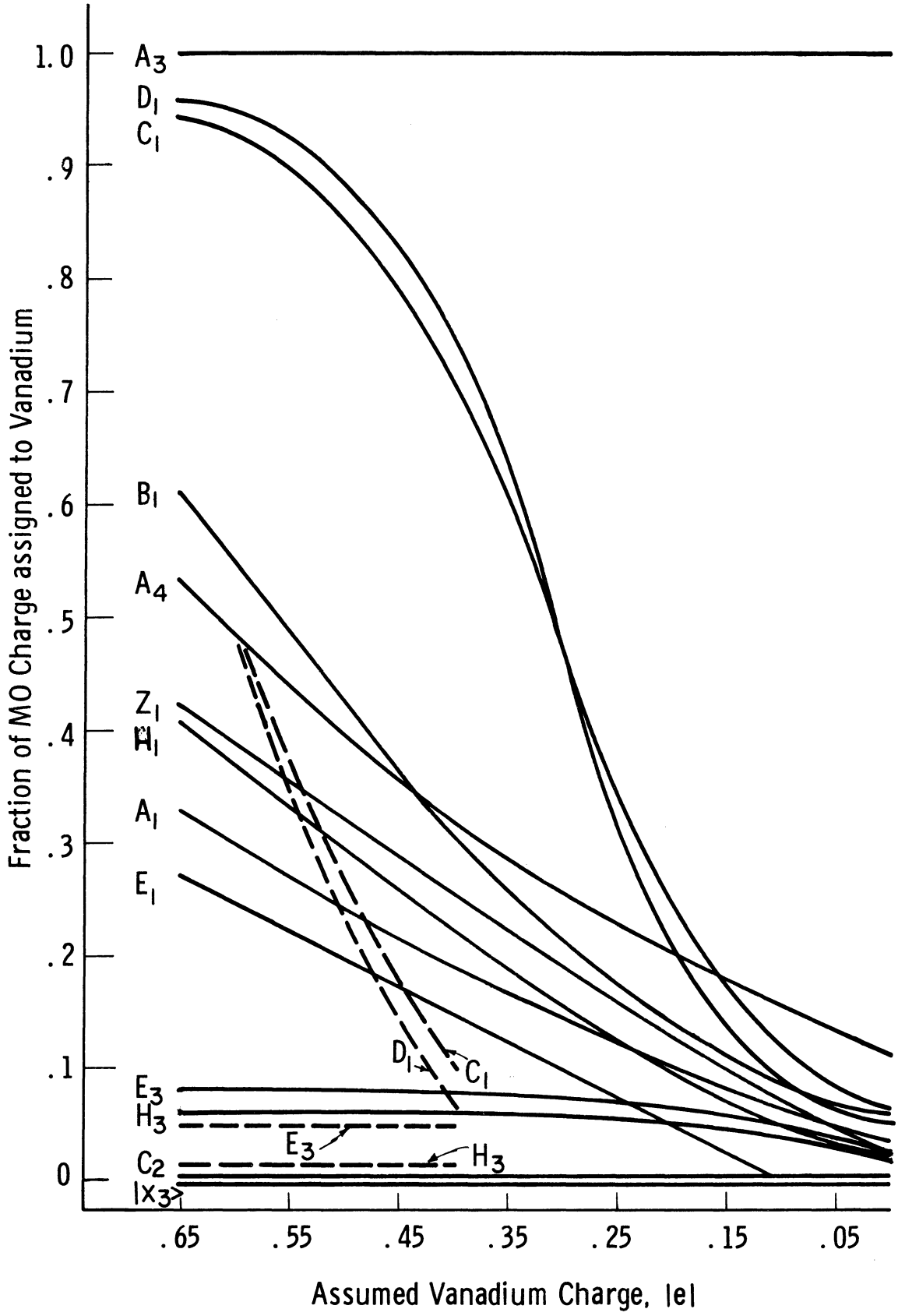

Fig. 9. Fraction of the Electronic Charge of the First Thirteen MO's Assign to Vanadium

electrons are accommodated in each MO starting from the energetically lower one until the number of electrons is exhausted.

The above twenty-five electrons are divided into two groups, twelve electrons on the oxygen 2p orbitals and thirteen electrons on the metal and σ oxygen orbitals. The nonhybridized oxygen 2p orbitals are distinguished from the rest because they have an almost symmetrical orientation with respect to the vanadium ion and two of the neighboring metal ions, so that their charge can be considered as belonging equally to any one of the crystal regions centered at the vanadium ion and the two neighboring metal ions. On the other hand, other orbitals assign their charge completely to the region centered at the vanadium ion.

The assumption of having twelve electrons in 2p ligand orbitals and thirteen in metal or σ orbitals is compatible with the situation that exists at the right-hand side of Figures 5 and 9 (i.e., for an assumed vanadium charge close to zero). In fact, the six orbitals C_1, D_1, E_3, H_3, $|\chi_3\rangle$, and C_2 accommodate twelve electrons on 2p oxygen orbitals. The rest are placed in metal and σ orbitals. When the twenty-five electrons are exhausted, it is seen that the ground state is the A_3 with one unpaired electron.

However, on the left-hand side of the figures (assumed vanadium charge close to +.60e) the situation is different since twelve electrons go into the first six orbitals, and the next four into C_1 and D_1 orbitals. The latter are of metal character and not of ligand 2p. The next orbital A_3 is also of metal character. This results from the fact that the metal orbitals are more stable than the oxygen 2p ones in this

region of the assumed charge. If all the twelve electrons of the ligand 2p orbitals migrate to metal orbitals only one-third of them would be attracted to vanadium orbitals and the other two-thirds into neighboring metal orbitals, provided no drastic energetic changes occur with respect to vanadium ones. Therefore in such a case only seventeen electrons (13+1/3•12) need be accommodated. It was seen that the left-hand part of the diagram can accommodate at least eighteen electrons before 2p ligand orbitals are used. This implies that only seventeen electrons have to be placed on the left, giving again, A_3 as the ground state. The situation at the center of the diagram is not clear. Fortunately the slopes of the C_1 and D_1 curves in Figure 9 are quite steep at the center, so that the ambiguity region is reduced appreciably.

In both cases, the wave function for the ground state A_3 can be written as a Slater's determinant

$$\left|A_1 \bar{A}_1 E_1 \bar{E}_1 \cdots C_1 \bar{C}_1 \cdots A_3\right| \qquad (56)$$

The unpaired molecular orbital A_3 determines the transformation properties of the determinant. The same results hold true for TiO_2:V and GeO_2:V. The net vanadium charge can now be calculated using Figures 5 and 9 and the fact that seventeen electrons are placed on the MO when the assumed vanadium charge is greater than +.35e and twenty-five when it is less than +.30e. Figure 10 plots the calculated vs. the assumed vanadium charge in the region 0 to +.65e for SnO_2:V. Charge self-consistency is shown to occur for an assumed value of about +.27e. Similarly, +.26e and +.25e are obtained for TiO_2:V and GeO_2:V. Table 7

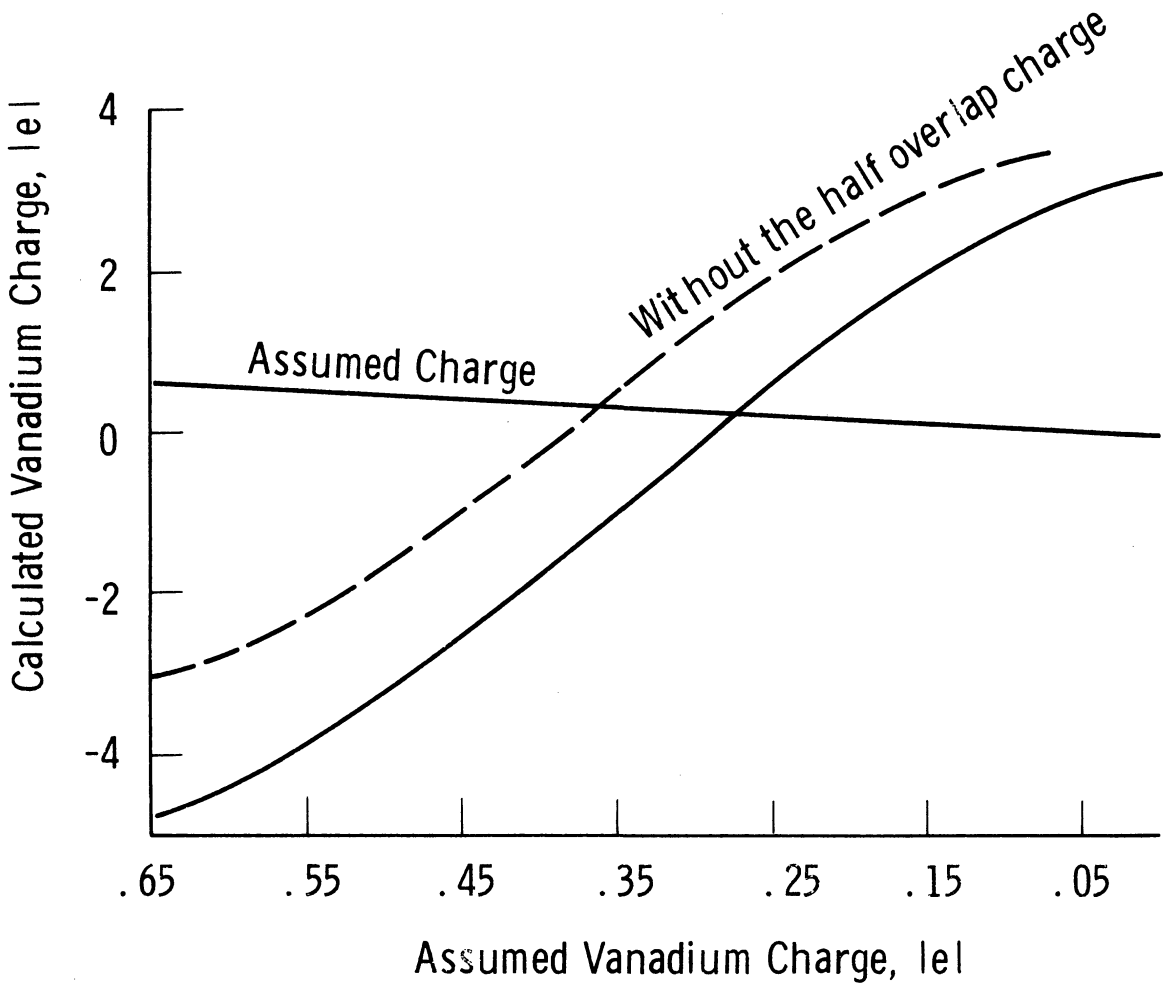

Fig. 10. Calculated Vanadium Charge vs. the Assumed Charge

gives the eigenfunctions and eigenvalues for SnO_2:V corresponding to +.25e.

3. Detailed Charge Self-Consistency

Usually a semiempirical calculation stops when charge self-consistency is achieved. However, for an overall consistency of the calculation the detailed electron distribution and the VSIP's should be compatible. That is, not only must the assumed and calculated net charges agree, but also there must be an agreement at the assumed and calculated orbital charge distribution which determines the VSIP.

As shown in Figure 9, at the assumed vanadium charge of +.25e the six σ -bonding orbitals give rise to the electronic charge distribution on the average as follows: 15% on the central metal ion and 85% on the six ligand oxygen ions, although it was assumed a 50% distribution when the VSIP's were calculated in Chapter IV-3. Similarly, for the π -orbitals C_1, C_2, D_1, E_3, H_3, and $|\chi_3\rangle$, a 100% distribution on the ligand ions was assumed in contrast to the calculated distribution which shifts roughly 35% of the electronic charge to the metal ion for the orbitals C_1 and D_1 and 7% for the orbitals E_3 and H_3. On the average, 14% of the π -orbital charge is shifted towards the metal ion. Therefore, relatively, the σ -orbital VSIP's should be increased and the π-orbital VSIP's decreased.

In order to see the effect of such a correction, the calculations were repeated in the region from +.60e to +.40e by reducing the VSIP's of the π -electrons only. The results for SnO_2:V with a

reduction of 35000 cm^{-1} and 45000 cm^{-1} are shown in Figures 11, 12, and 9. In Figure 9 the dotted lines represent changes produced by the π reduction of 35 Kcm^{-1}. Charge self-consistency occurs at about +.40e. It is observed that there is a change in the energy level position of the C , D , E , H , and $|\chi_3\rangle$ symmetries as well as in the electronic charge distribution.

Table 8 summarizes the assumed electronic charge occupancy of the σ and π oxygen orbitals in the bonding scheme of Chapter IV as well as in the calculated one.

TABLE 8

ASSUMED AND CALCULATED σ AND π ORBITAL OCCUPANCY

Orbital	Assumed	Calculated	
		no π VSIP reduction	35 Kcm^{-1} π VSIP red.
σ	50%	85%	76%
π	100%	86%	94%

It is observed that the calculated values in the second column of Table 8 imply a correction to the VSIP calculated in Chapter IV. The smaller charge of the π orbitals (86%) with respect to the assumed one (100%) indicates a reduction of the corresponding VSIP due to the decrease in the electron-electron repulsion energy. Similarly, the VSIP of the σ orbitals should be increased. In the last column the results are listed when the π electron VSIP is reduced by 35 Kcm^{-1}.

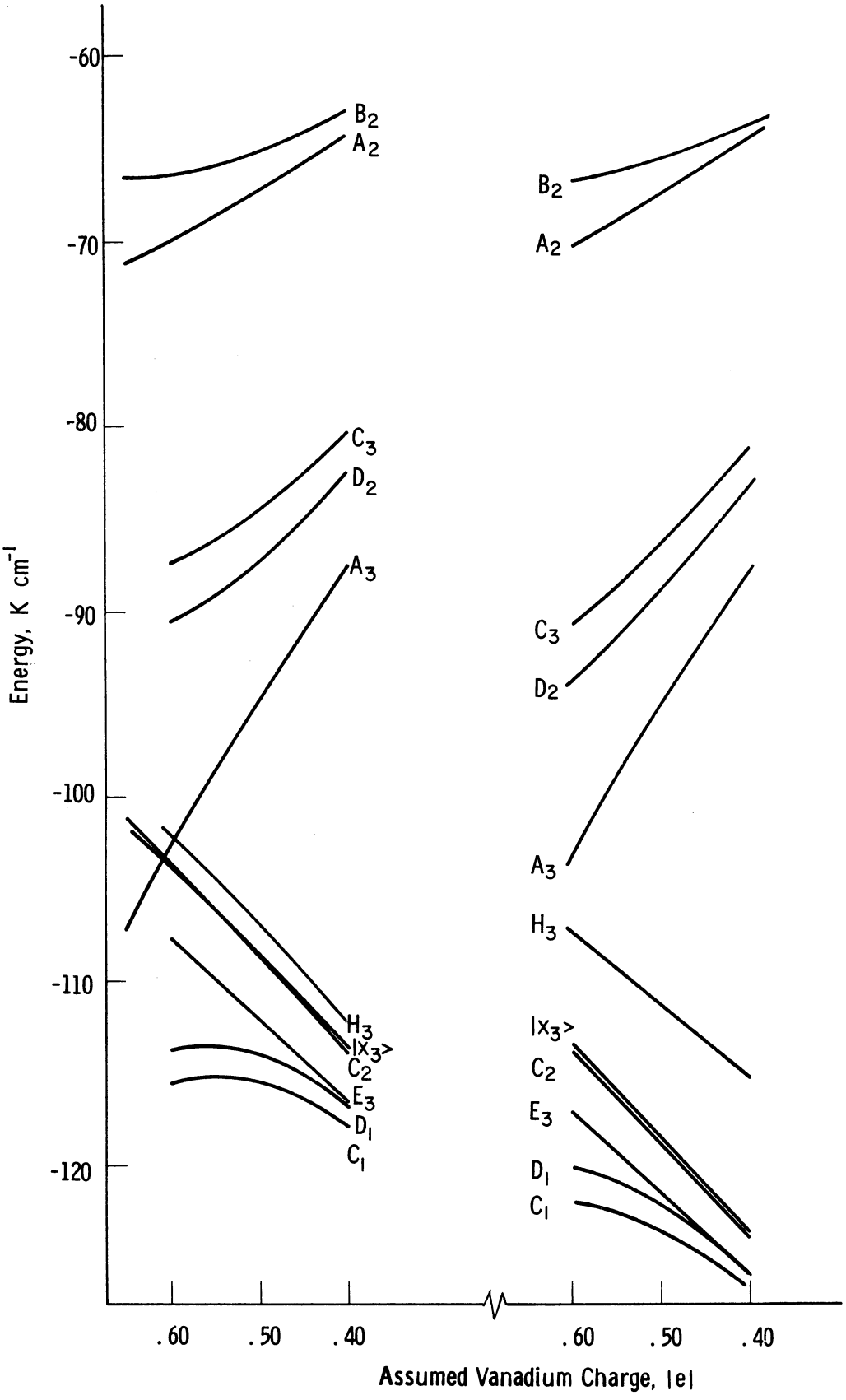

Fig. 11. MO Energy Levels of SnO_2:V for a π-electron VSIP Reduction of 35 Kcm^{-1} (left) and 45 Kcm^{-1} (right)

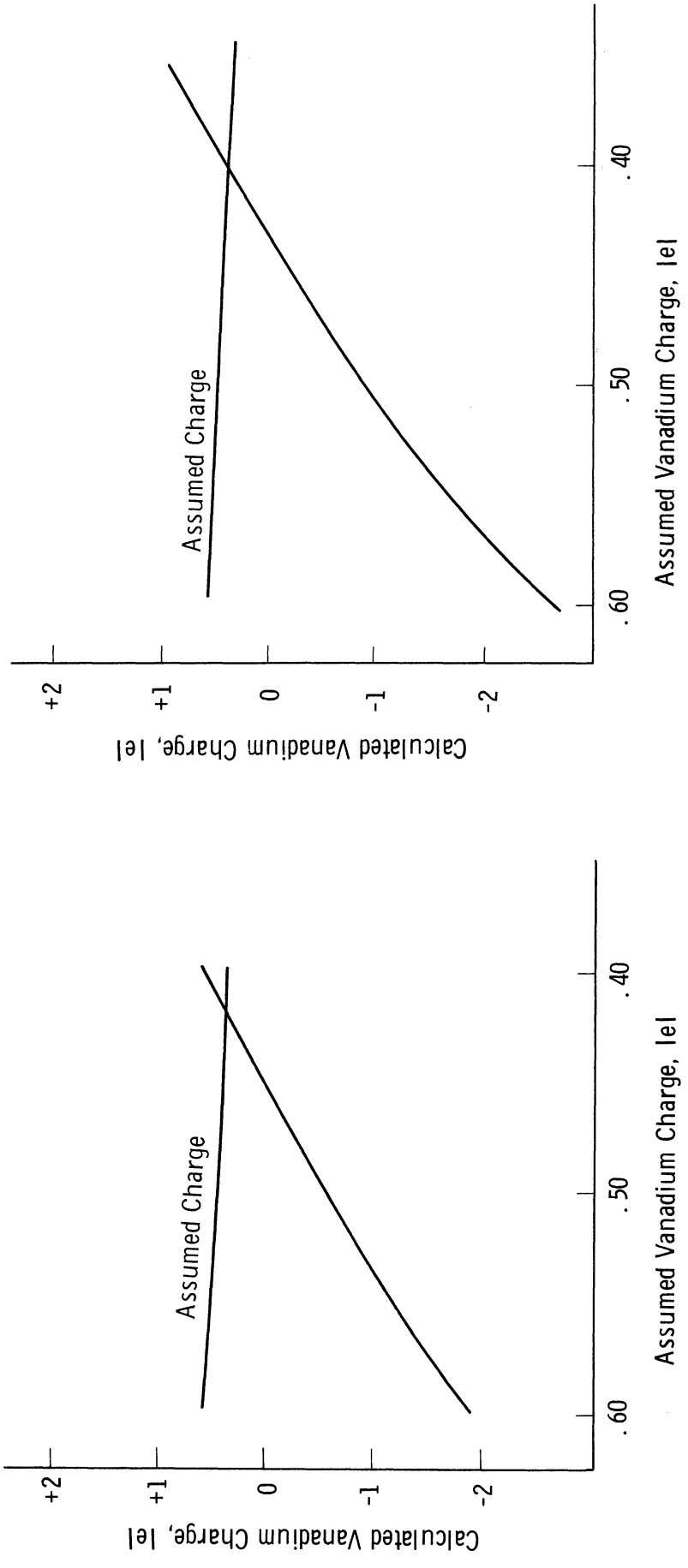

Fig. 12. Calculated Vanadium Charge vs. the Assumed Charge for a π-electron VSIP Reduction of 35 Kcm^{-1} (left) and 45 Kcm^{-1} (right)

The charge occupancy of the π orbitals increases to 94% while that of the σ orbitals decreases to 76%. These changes are in the direction that requires smaller reduction in the π electron VSIP. Therefore, in principle, consistent values of VSIP should exist with respect to the occupancy of the π and σ orbitals by the electronic charge. The determination of these consistent VSIP does not seem feasible without additional information (see also Chapters VI-1 and VII-2).

CHAPTER VI

THE ELECTRONIC g AND A TENSOR

In this chapter the electronic g tensor is used as a monitor instead of the ionic charge. The solutions that satisfy the g tensors are singled out and compared with those found in Chapter V. The hyperfine tensor A provides additional checking.

1. The Electronic g Tensor as a Monitor

As stated in the Introduction, the purpose of this work is to attempt an explanation of the observed ESR spectra in the rutile-type crystals having vanadium as an impurity. In Chapter V-2, the valence electronic levels were found using self-consistency. Since these solutions can be used to calculate the electronic tensors, the next step would be to compare the experimental results on the g tensors with the calculated ones. However, due to the approximate nature of the semi-empirical methods, the set of VSIP's which gives the best charge self-consistency is not necessarily expected to give the best fit for the g tensor. Furthermore, in Chapter V-3, the need of changing the VSIP's to obtain detailed charge self-consistency is pointed out. The need of π-orbital VSIP reduction was determined but not its amount. In view of these facts it is felt that the experimental tensors have to be used

as monitors in selecting the best solutions out of the many ones found in Chapter V. This procedure is followed in this section.

The experimentally found deviations of the g tensor from the free electron value are given in Table 9.

TABLE 9

EXPERIMENTAL DEVIATIONS OF g TENSORS COMPONENTS FROM THE FREE ELECTRON VALUES FOR VANADIUM IN SnO_2, TiO_2, GeO_2

	Δg_{xx}	Δg_{yy}	Δg_{zz}
SnO_2:V	-.061	-.097	-.057
TiO_2:V	-.085	-.087	-.044
GeO_2:V	-.079	-.079	-.037

The theory for the g tensor when the ground state is a singlet (orbital) has been worked out by Pryce.[35] The components of the most general g tensor are given by

$$g_{ij} = 2(\delta_{ij} - 2\lambda \Lambda_{ij}) \tag{57}$$

where

$$\Lambda_{ij} = \sum_{n \neq 0} \frac{\langle 0 | \hat{L}_i | n \rangle \langle n | \hat{L}_j | 0 \rangle}{E_n - E_0} \tag{58}$$

is a real, symmetric, positive, definite tensor and λ is the spin-orbit coupling constant. Excited states are denoted by $|n\rangle$. Using the

transformation properties of the eigenfunctions and the operators as shown in Appendix C and recalling that the ground state belongs to the identity I.R., one observes that:

(a) All off-diagonal elements Λ_{ij} $(i \neq j)$ in the relation Eq. (57) are identically zero. The reason is that in Eq. (58) the excited state $|m\rangle$ should belong to the same I.R. with the corresponding operator $\hat{L}_i$ or $\hat{L}_j$ for a nonzero matrix element and each one of the $\hat{L}_x$, $\hat{L}_y$, $\hat{L}_z$ transforms according to a different I.R., namely, D, C, and B respectively (see Appendix C).

(b) The only nonzero diagonal matrix elements Λ_{ii} occur with excited states belonging to the B, C, or D I.R. The ESR spectra of vanadium in SnO_2, TiO_2, and GeO_2, reveal an electronic spin of S = 1/2 Therefore, the excited states can occur in two ways: In the expression (56) of the ground states as a Slater determinant either the orbital A_3 is replaced by one of the higher lying orbitals of symmetry B, C, D or one of lower lying orbitals of symmetry B, C, D is replaced by the A_3 orbital (see Figure 13). The operators $\hat{L} = \sum_{j=1}^{17 \text{ or } 25} \hat{\ell}_{ji}$ are one-electron operators, so that

$$\langle \{A_1 \bar{A}_1 E_1 \bar{E}_1 \cdots D_1 \cdots A_3 \bar{A}_3\} | L_x | \{A_1 \bar{A}_1 \cdots D_1 \bar{D}_1 \cdots A_3\} \rangle = \pm \langle D_1 | \ell_x | A_3 \rangle \text{ etc.} \quad (59)$$

There are two eigenfunctions of type B, two of type D, and three of type C that must be considered (the B_1, B_2, D_1, D_2, C_1, C_2 and C_3 of Table 6). Using the following relations:

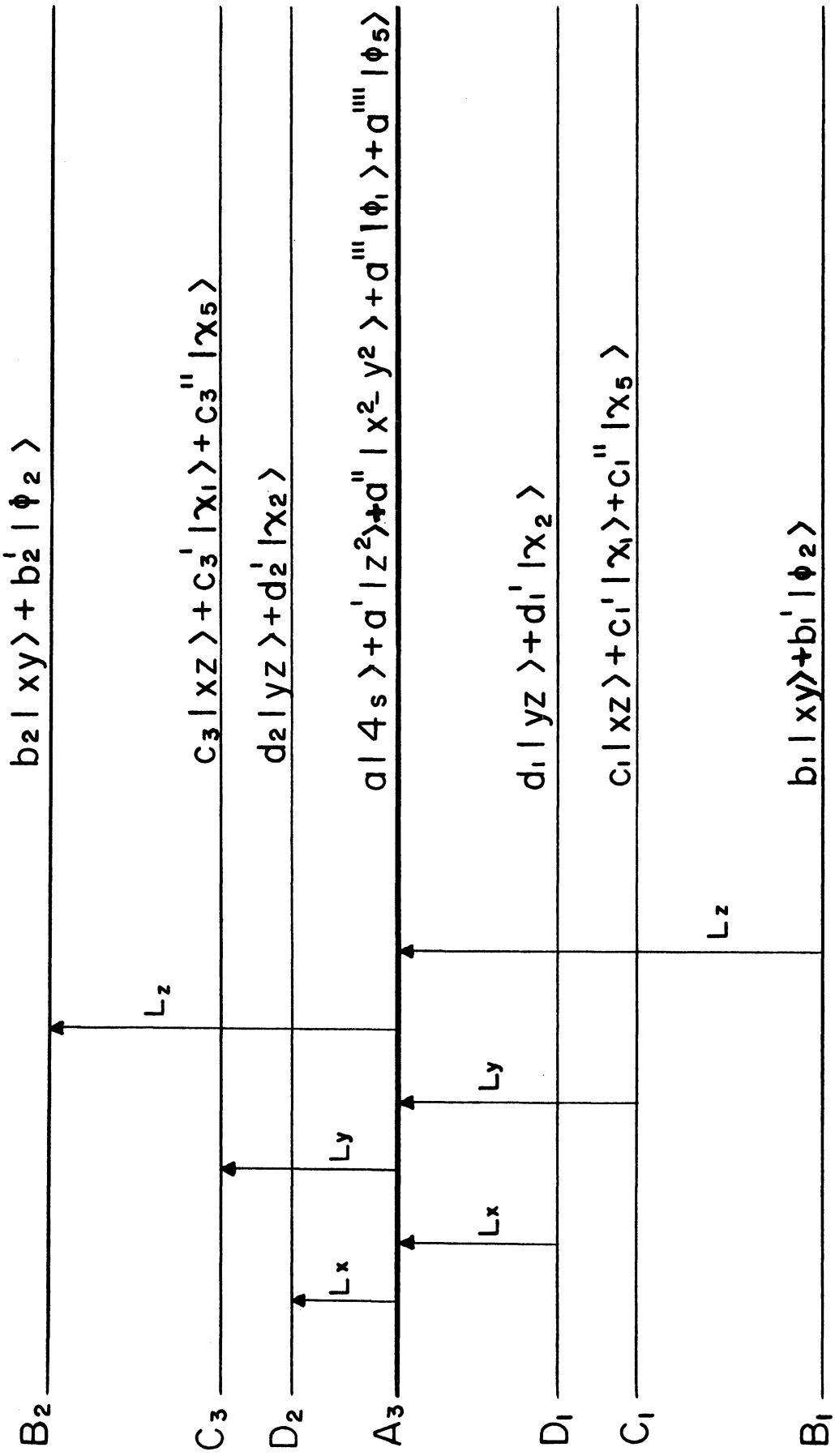

Fig. 13. Allowed Crystal Field and Charge Transfer Transitions

$$\hat{\ell}_x|x^2-y^2\rangle = -i|xz\rangle$$

$$\hat{\ell}_x|z^2\rangle = -i\sqrt{3}|yz\rangle$$

$$\hat{\ell}_y|x^2-y^2\rangle = -i|xz\rangle \qquad (60)$$

$$\hat{\ell}_y|z^2\rangle = i\sqrt{3}|xz\rangle$$

$$\hat{\ell}_z|x^2-y^2\rangle = 2i|xy\rangle$$

$$\hat{\ell}_z|z^2\rangle = 0$$

and neglecting contributions from the nonmetal parts of the orbitals (see Discussion) one gets:

$$\lambda\Lambda_{xx} = \zeta^2\left[\frac{\left|\langle d_2(yz)|-a_{z^2}i\sqrt{3}(yz)-a_{x^2-y^2}i(yz)\rangle\right|^2}{E_{D_2}-E_{A_3}}\right.$$

$$\left.-\frac{\left|\langle d_1(yz)|-a_{z^2}i\sqrt{3}(yz)-a_{x^2-y^2}i(yz)\rangle\right|^2}{E_{A_3}-E_{D_1}}\right]$$

$$=\zeta^2\left[\frac{d_2^2\left[a_{z^2}\sqrt{3}+a_{x^2-y^2}\right]^2}{E_{D_2}-E_{A_3}}-\frac{d_1^2\left[a_{z^2}\sqrt{3}+a_{x^2-y^2}\right]^2}{E_{A_3}-E_{D_1}}\right] \qquad (61)$$

$$\lambda\Lambda_{xx} = \zeta \left[\frac{d_2^2}{E_{D_2} - E_{A_3}} - \frac{d_1^2}{E_{A_3} - E_{D_1}} \right] \left[a_{x^2-y^2} + a_{z^2} \sqrt{3} \right]^2 \tag{62}$$

$$\lambda\Lambda_{yy} = \zeta \left[\frac{c_3^2}{E_{C_3} - E_{A_3}} - \frac{c_1^2}{E_{A_3} - E_{C_1}} \right] \left[a_{x^2-y^2} - a_{z^2} \sqrt{3} \right]^2 \tag{63}$$

$$\lambda\Lambda_{zz} = \zeta \left[\frac{b_2^2}{E_{B_2} - E_{A_3}} - \frac{b_1^2}{E_{A_3} - E_{B_1}} \right] \left[2 a_{x^2-y^2} \right]^2 \tag{64}$$

where a_i, b_i, c_i, d_i are the coefficients of the corresponding metal parts in the molecular orbitals A, B, C, and D respectively, and ζ is the one-electron spin orbit coupling constant. The minus sign before the second term in the first brackets is due to the fact that the charge transfer transitions affect electrons with opposite spin.[36] The coefficients a_i, b_i ... and the energy terms E_{A_3}, E_{B_1} . . . were obtained in Chapter V for the range of the assumed vanadium charge +.65e to 0. This range is extended to -.40e in this chapter. The needed energy matrix elements in the interval 0 to -.40e are taken from Chapter IV-3 with the necessary interpolations.

The calculated values of Λ_{ii} are plotted in Figures 14, 15, and 16 for SnO_2:V, TiO_2:V, and GeO_2:V respectively. A significant point to note is that Λ_{zz} is always larger than Λ_{xx}. From the Eq. (57) one gets

$$\Delta g_{ii} = -2\lambda \Lambda_{ii} \qquad i = x, y, z \qquad (65)$$

Therefore, the calculated Δg_{zz} is always absolutely larger than Δg_{xx} although the experimental results (see Table 9) show the opposite. The spin-orbit parameter λ is taken as constant in the range 140 cm^{-1} to 250 cm^{-1} according to Moore's spectroscopic tables.

The results so far indicate that none of the sets of the VSIP derived in Chapter IV can be compatible with the observed g tensors. In Chapter V-3, the first need for a change of the VSIP's used was seen. Now an additional factor is added. It is interesting to see what changes in the values of the VSIP's are needed to account for the observed g tensor and how these changes compare with the results found in Chapter V-3.

Consider first g_x and g_y. The calculated and experimental values are tabulated in Table 10. The calculated values were obtained by selecting the points (see arrows in Figures 14, 15, and 16) giving the best agreement between experimental and calculated values of Δg_{ii} $(i = x, y)$. The spin-orbit coupling parameter λ was taken to be 250 cm^{-1}.

So far g_z was not considered. For this problem one notes that the calculation of Λ_{zz} involves the energy levels A_3, B_1, and

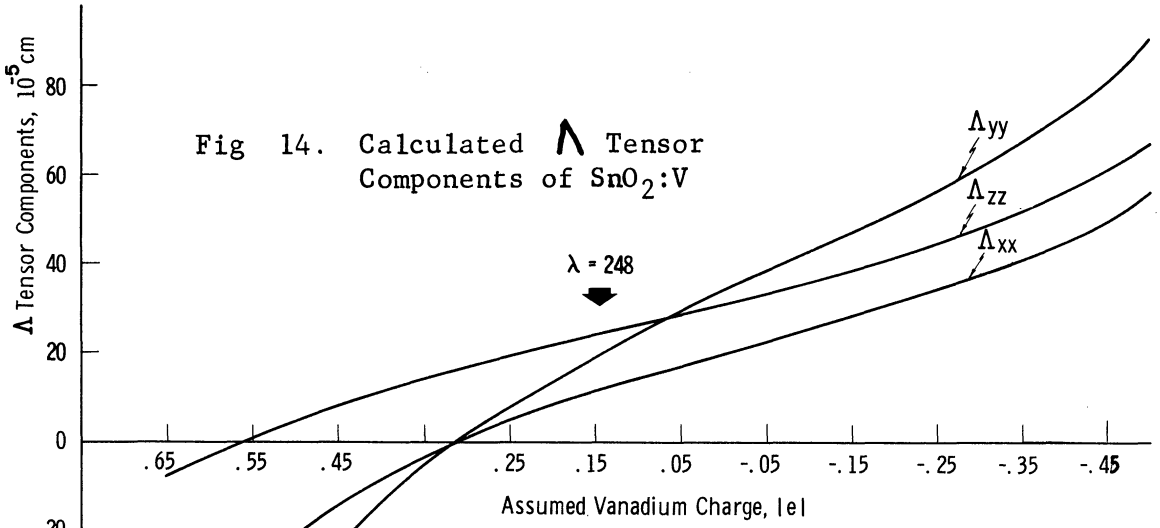

Fig 14. Calculated Λ Tensor Components of SnO_2:V

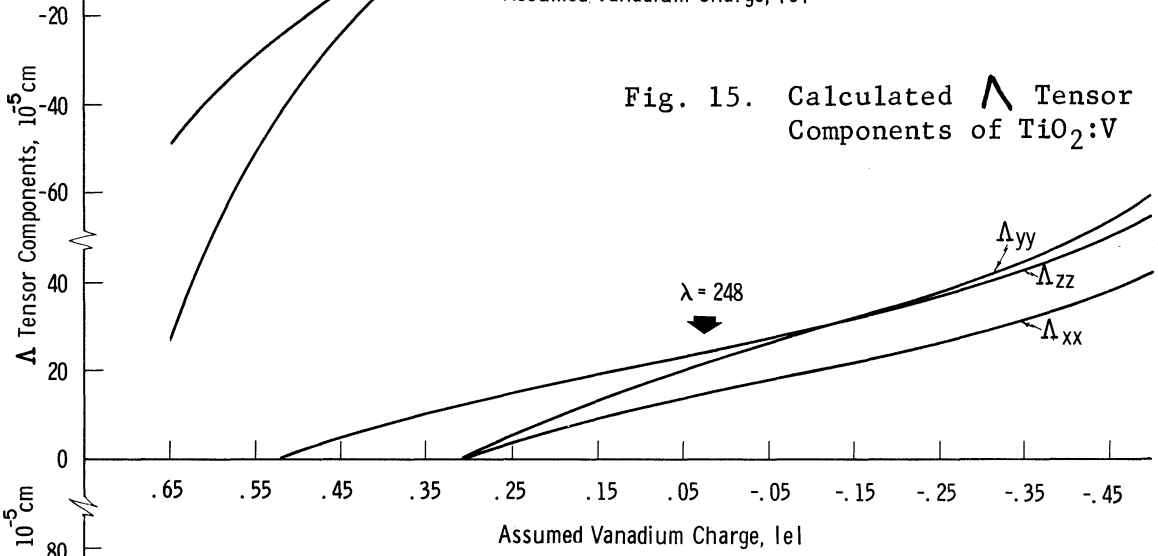

Fig. 15. Calculated Λ Tensor Components of TiO_2:V

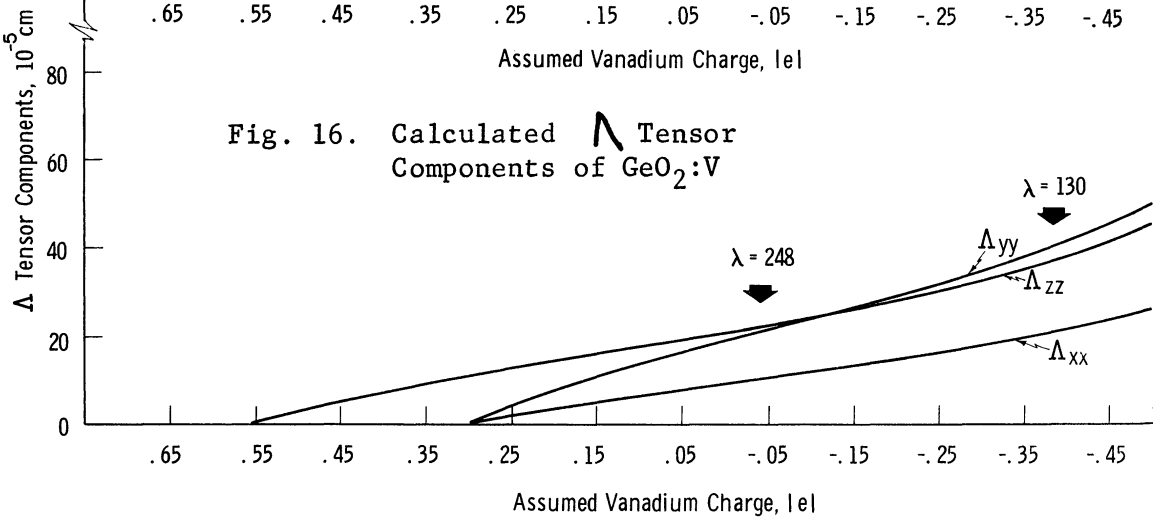

Fig. 16. Calculated Λ Tensor Components of GeO_2:V

B_2 (see Figure 13). These levels remain unchanged by the π electron VSIP reduction mentioned in Chapter V-3, in contrast to Λ_{xx} and Λ_{yy} which involve the levels D_i and C_i. The last two sets of levels are both affected by the π-electron VSIP reduction.

TABLE 10

OBSERVED AND CALCULATED g TENSOR COMPONENTS OF VANADIUM IN SnO_2, TiO_2, AND GeO_2

	g_x	g_y	g_z
obs.	1.939	1.903	1.943
SnO_2:V cal.	1.943	1.903	
obs.	1.915	1.913	1.955
TiO_2:V cal.	1.928	1.898	
obs.	1.921	1.921	1.963
GeO_2:V cal.	1.949	1.819	

The components of Λ tensors were calculated with a π-electron VSIP reduction of 35 Kcm^{-1} and 45 Kcm^{-1} in the interval +.60e to +.40e of the assumed vanadium charge. The results are plotted in Figures 17, 18, and 19 for SnO_2:V, TiO_2:V, and GeO_2:V respectively. The upper part of each figure corresponds to the 45 Kcm^{-1} reduction. In the case of SnO_2:V agreement is achieved at +.40e with 45 Kcm^{-1} reduction. A charge self-consistency calculation requires a vanadium charge of +.41e (see Figure 12). Therefore, an almost exact coincidence of the two methods is reached. Similar results can be found with TiO_2:V and GeO_2:V, although a greater π-electron VSIP reduction is needed (10 Kcm^{-1} to 20 Kcm^{-1} more).

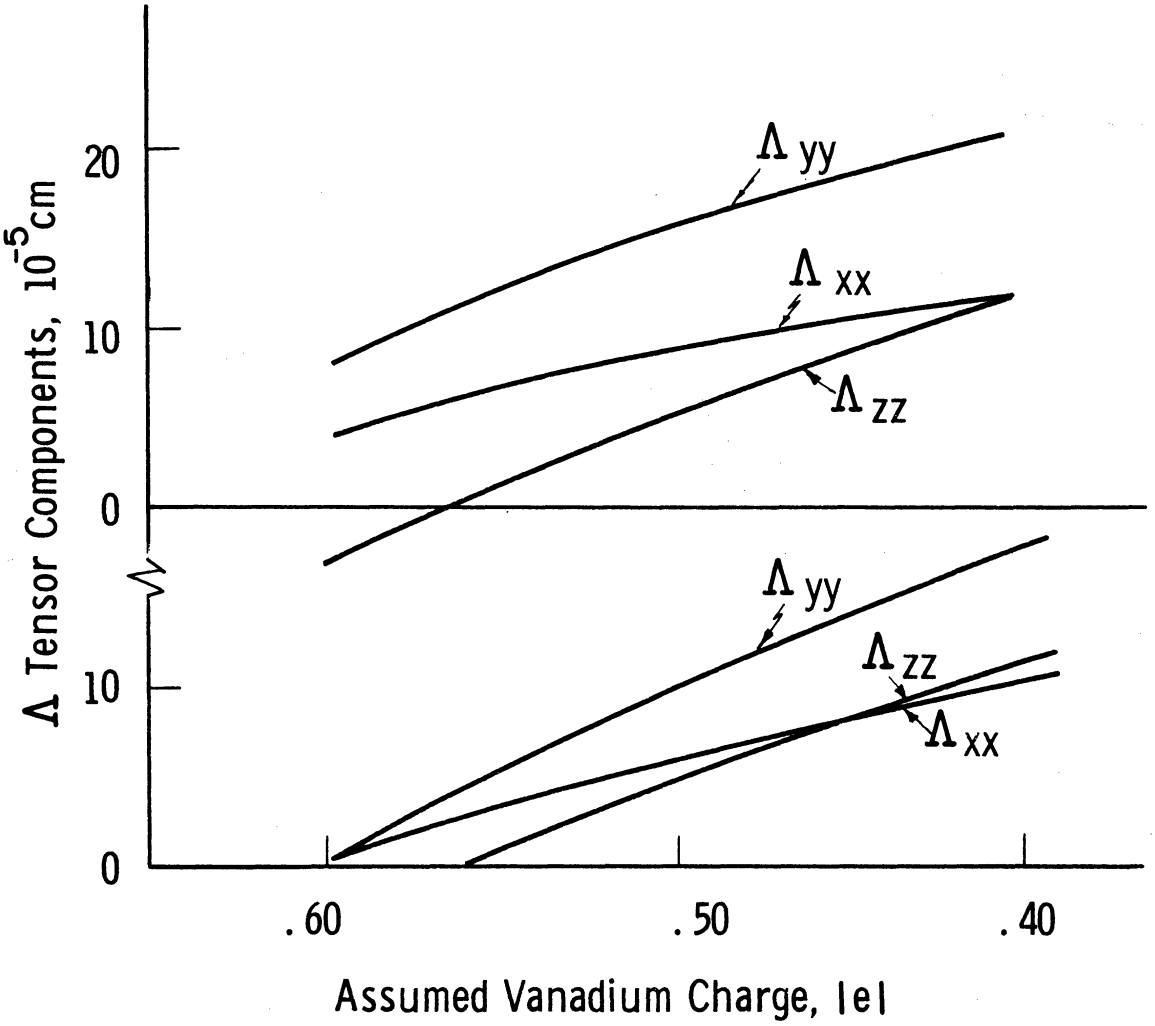

Fig. 17. Calculated Λ Tensor Components of SnO_2:V for a π-electron VSIP Reduction of 35 Kcm^{-1} (lower) and 45 Kcm^{-1} (upper)

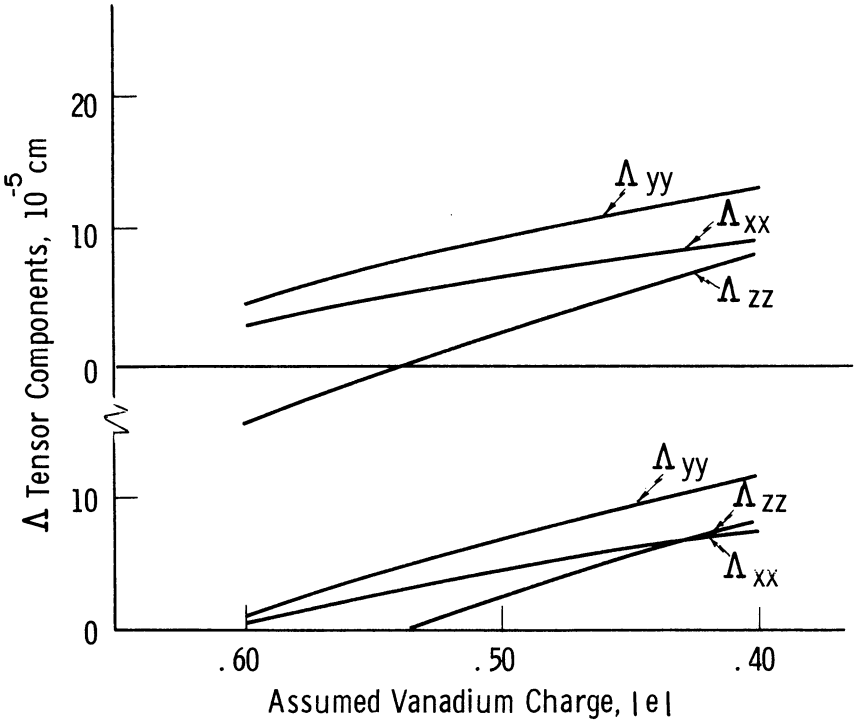

Fig. 18. Calculated Λ Tensor Components of TiO_2:V for a π-electron VSIP Reduction of 35 Kcm^{-1} (lower) and 45 Kcm^{-1} (upper)

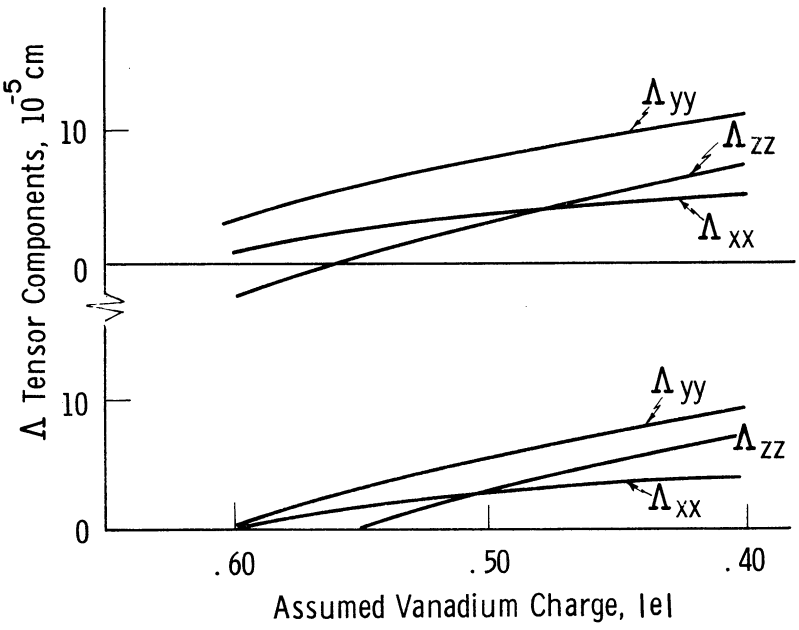

Fig. 19. Calculated Λ Tensor Components of GeO_2:V for a π-electron VSIP Reduction of 35 Kcm^{-1} (lower) and 45 Kcm^{-1} (upper)

The result of the previous paragraph is that a choice of the π-electron VSIP can be made so that the calculated value of g_{zz} is the same as the experimental value. Thus Table 10 is completed. Whether this choice of the VSIP represents also the crystal reality and not just a mathematical device is not known. It is observed, though, that the change needed by the g tensor in the VSIP of π-electrons coincides with the similar need of the detailed charge self-consistency (see also Chapter VII-2).

2. The Hyperfine Interaction Tensor A

The hyperfine tensor A can also be used to check the results found in Chapter V. The anisotropic part of the hyperfine tensor A depends on the form of the ground state wave function, and the discussion that follows is limited to this state.

The ESR spectra of vanadium in SnO_2, TiO_2, and GeO_2 reveal a strong hyperfine interaction of the unpaired electron with the vanadium nucleus. Experimental values of the hyperfine tensor in units of 10^{-4} cm^{-1} are given in Table 11. Since the relative sign of the hyperfine tensor components cannot be determined, they are assumed to be all of the same sign so that the isotropic part becomes maximum. Subtraction of the isotropic part leads to the following components of the anisotropic part listed in Table 12.

TABLE 11

EXPERIMENTAL HYPERFINE TENSOR COMPONENTS OF VANADIUM IN SnO_2, TiO_2, AND GeO_2

	A_x	A_y	A_z
SnO_2:V	21	44	144
TiO_2:V	31	43	142
GeO_2:V	37	38	134

TABLE 12

ANISTROPIC PART OF THE HYPERFINE TENSOR COMPONENTS DEDUCED FROM EXPERIMENT

	A_x^{anis}	A_y^{anis}	A_z^{anis}
SnO_2:V	-49	-26	75
TiO_2:V	-41	-29	70
GeO_2:V	-33	-32	65

In Chapter V-2, it was found that the A_3 level was the ground state Its form is given in Table 7 of Chapter V. In Appendix F the coefficients of the metal parts of the A_3 level are listed for the interval +.65e to -.50e of the assumed vanadium charge. The variation of these coefficients is negligible. Therefore any result based on these coefficients does not depend critically on the assumed vanadium charge. For the discussion of the anisotropic part of the hyperfine tensors only the parts of the ground state wave functions that contain the metal $|x^2-y^2\rangle$ and $|z^2\rangle$ states are needed. These are taken from Appendix F. The vanadium charge is taken as +.40e because of the results found in Chapter VI-1. Using the relation

$$|x^2-y^2\rangle - \sqrt{3}\,|z^2\rangle = 2\,|x^2-z^2\rangle \tag{66}$$

and the coefficients in Appendix F, one gets

$$\begin{aligned} &SnO_2{:}V && .912\ |x^2-y^2\rangle + .154\ |x^2-z^2\rangle \\ &TiO_2{:}V && .929\ |x^2-y^2\rangle + .126\ |x^2-z^2\rangle \\ &GeO_2{:}V && .907\ |x^2-y^2\rangle + .160\ |x^2-z^2\rangle \end{aligned} \tag{67}$$

The field produced at the center by an electron in the orbital $|x^2-y^2\rangle$ has a relative strength of 1, 1, and -2 when an external magnetic field is applied along the x, y, and z axes respectively, while for the orbital $|x^2-z^2\rangle$ it is 1, -2, and 1. When the occupational probability for an orbital is less than one, the relative strengths have to be multiplied by that probability. For example, the coefficient of the $|x^2-y^2\rangle$ state of SnO_2:V is .912 in Eq. (67), the occupational

probability is $(.912)^2 \approx .82$ and the field produced at the nucleus will be proportional to .82, .82, and -1.64. In this way, one gets from Eqs. (67) the following relative strengths of the magnetic field and therefore of the hyperfine interaction.

TABLE 13

CALCULATED RELATIVE STRENGTH OF THE MAGNETIC FIELD AT THE VANADIUM NUCLEUS DUE TO THE GROUND STATE ELECTRONIC CHARGE

		x	y	z
SnO_2:V	from $\|x^2-y^2\rangle$	.820	.820	-1.640
	$\|x^2-z^2\rangle$	.026	-.052	.026
	Total	.846	.768	-1.636
TiO_2:V		.881	.833	-1.714
GeO_2:V		.854	.782	-1.636

Normalizing them to the A_z^{anis} of Table 11 one gets the results in Table 14.

TABLE 14

CALCULATED ANISOTROPIC PART OF THE HYPERFINE TENSORS NORMALIZED TO A_z^{anis}

	A_x^{anis}	A_y^{anis}	A_z^{anis}
SnO_2:V	-39	-36	75
TiO_2:V	-36	-34	70
GeO_2:V	-34	-31	65

The agreement with the experimental data of Table 11 is good. For SnO_2:V and TiO_2:V, it is noted that a greater contribution of the $|z^2\rangle$ state is required than indicated by the coefficients in Appendix F.

CHAPTER VII

DISCUSSION AND CONCLUSIONS

In conclusion, a summary of the obtained results is presented with some additional discussion.

1. Summary of Results

The main results found in this work are:

(a) The ground state is found to be A_3, which is mainly x^2-y^2 as Kasai[4] and From, Kikuchi, and Dorain[5] indicated earlier, but with a small admixture of z^2 and an even smaller admixture of 4s orbital. These admixtures are caused by the rhombic component of the crystalline field. In a tetragonal or axial field this admixture would be symmetry forbidden. As evident from Appendix F, the admixture coefficients are relatively constant over a wide region of the assumed vanadium charge from +.65 to -.50. The relatively lower admixture of the z^2 state in TiO_2 can be attributed to the smaller rhombicity that this crystal presents with respect to the other two.

(b) The ordering of the levels involved in the g tensor is found invariably to be $B_1(xy)$, $C_1(xz)$, $D_1(yz)$, $A_3(x^2-y^2)$, $D^2(yz)$, $C_3(xz)$, $B_2(xy)$ in increasing energy[42] (see Figures 5, 6, 7, 8, and 11). The levels D_2, C_3, and B_2 above the ground level $A_3(x^2-y^2)$ correspond to

the levels of the crystal field theory. It is observed that $D_2(yz)$ is below $C_3(xz)$ whereas the simple crystal field theory predicts the reverse order. The formulas (62), (63), and (64) derived in Chapter VI-1 show the importance of the z^2 admixture in calculating the Δg_{ii} values. For example, in SnO_2:V the relative importance of admixture is given by the fraction

$$\frac{\left[a_{x^2-y^2} - a_{z^2}\sqrt{3}\right]^2}{\left[a_{x^2-y^2} + a_{z^2}\sqrt{3}\right]^2} = \frac{\left[.989 + .133\sqrt{3}\right]^2}{\left[.989 - .133\sqrt{3}\right]^2} \simeq 2.5 \tag{68}$$

This fraction shows that the admixture of $-.133|z^2\rangle$ in the ground state introduces a factor of 2.5 in the value of Δg_{yy} with respect to Δg_{xx}. The numerical values of the coefficients are taken from Appendix F. (Note that this admixture gives an occupational probability of the state $|z^2\rangle$ of less than 2%.)

(c) The small admixture of z^2 function is important also in explaining the features of the anisotropic part of the hyperfine tensor components.

(d) Although a tetragonal symmetry implies a g tensor of axial symmetry, the converse is not always true. The same ordering of levels can be compatible with very different g tensors, as found in SnO_2:V and TiO_2:V.

(e) In a heuristic way, assuming a ground state of the form $-\alpha|z^2\rangle + \beta|x^2-y^2\rangle$, the coefficients α and β that satisfy the anisotropic parts of the hyperfine tensor are found to be:

$-.293\,|\,z^2\rangle + .958\,|x^2-y^2\rangle$ for SnO_2:V

$-.232\,|\,z^2\rangle + .972\,|x^2-y^2\rangle$ for TiO_2:V

$-.083\,|\,z^2\rangle + .996\,|x^2-y^2\rangle$ for GeO_2:V

(f) Using the above ground states and neglecting the effects of any charge transfer transition and of any admixture of ligand functions in the excited states $D_2(yz)$, $C_3(xz)$, and $B_2(xy)$, the following sequences of levels satisfy the observed g tensors.

	SnO_2:V	TiO_2:V	GeO_2:V
$B_2(xy)$	$31900cm^{-1}$	$42400cm^{-1}$	$53200cm^{-1}$
$C_3(xz)$	$11000cm^{-1}$	$10700cm^{-1}$	$8160cm^{-1}$
$D_2(yz)$	$1650cm^{-1}$	$1895cm^{-1}$	$4550cm^{-1}$
A_3	0	0	0

For the sake of comparison, the calculated levels of SnO_2:V are given below when a reduction of the π-electron VSIP of 35 Kcm^{-1} and 45 Kcm^{-1} are used (see Chapter VI-1)

Reduction in π-Electron VSIP

	35 Kcm^{-1}	45 Kcm^{-1}
$B_2(xy)$	24202	24202
$C_3(xz)$	7599	6767
$D_2(yz)$	5315	4662
A_3	0	0

(g) Finally, the discussion in the next section shows that the ligand parts of the MO, which were neglected in the calculation of the Δg_{ii} in Chapter VI-1, may have absolute contributions of from 5% up to 25%.

2. Discussion

The freedom in choosing the VSIP of the π-electrons independently from the σ-electrons is enough to bring the values in the right region although the necessary reduction in the above VSIP is found to be somewhat large. Further study of this matter is desirable. For the moment one can observe that even within the framework of this calculation a smaller reduction of the π-electron VSIP is really needed. The Δg_{ii} values are due to the interplay of the spin-orbit coupling and the orbital Zeeman perturbations.

In formula (58) one of the matrix elements is due to $\lambda \underline{L} \cdot \underline{S}$ and the other to $\underline{H} \cdot \underline{L}$. Due to $1/r^3$ dependence of the S - O coupling parameter, only metal-metal and ligand-ligand terms need be kept in the first matrix element. In the second matrix element, though, the metal-ligand terms may become appreciable depending on the overlapping of metal and ligand functions.[37] Since the A_3 level consists almost exclusively of metal functions, no correction is needed in the S - O matrix elements.

The correction due to the orbital Zeeman term amounts in substituting

$$d_i\left[d_i + d_i'\langle \chi_2 | yz\rangle\right] \qquad \text{for } d_i^2$$

$$c_i\left[c_i + c_i'\langle \chi_1 | xz\rangle + c_i''\langle \chi_5 | xz\rangle\right] \qquad \text{for } c_i^2$$

$$b_i\left[b_i + b_i'\langle \Phi_2 | xy\rangle\right] \qquad \text{for } b_i^2$$

(69)

in formulas (62), (63), and (64) respectively, where the orbitals $B_i\,(i=1,2)$, $C_i\,(i=1,3)$, and $D_i\,(i=1,2)$ are written as follows:

$$B_i: \quad b_i|xy\rangle + b_i'|\Phi_2\rangle$$

$$C_i: \quad c_i|xz\rangle + c_i'|\chi_1\rangle + c_i''|\chi_5\rangle$$

$$D_i: \quad d_i|yz\rangle + d_i'|\chi_2\rangle \qquad (70)$$

(see Appendix I).

Since the coefficients b_2, c_3, and d_2 of the corresponding anti-bonding orbitals are negative, a reduction is implied in the calculated values of Λ_{ii} by using the Eqs. (62), (63), and (64). Similarly, the positive coefficients b_1, c_1, and d_1 of the bonding orbitals imply also a reduction in the values of Λ_{ii}. A numerical calculation gives the

reductions of Λ_{ii}'s listed in Table 15, when the assumed vanadium charge of +.40e and the π-electron VSIP reduction of 35 Kcm^{-1} are used.

TABLE 15

REDUCTION IN Λ_{ii} VALUES DUE TO LIGAND ORBITAL PARTS AT +.40e ASSUMED VANADIUM CHARGE AND 35 Kcm^{-1} π-ELECTRON VSIP REDUCTION

SnO_2:V	TiO_2:V	GeO_2:V
4.5%	6.0%	8.5%
5.5%	8.5%	10.5%
25.0%	45.0%	47.5%

From Table 15 one observes that the inclusion of the ligand part has the greatest effect on Λ_{zz}. In Chapter VI-1 the reduction of the π-electron VSIP was used for the purpose of reducing Λ_{zz}. Now a more careful calculation of the orbital Zeeman matrix elements with the inclusion of the ligand part shows that the required π-electron VSIP reduction is less by about 10 Kcm^{-1} to 20 Kcm^{-1} than the original estimate. However, Table 15 is somewhat misleading for the following reason. The much greater percentage in the reduction of the Λ_{zz} with respect to the Λ_{xx} and Λ_{yy} is partly due to the greater contribution of the charge transfer process. The latter point is made clear in Table 16 where the contributions from crystal field and charge transfer transitions are shown. If one decides to consider the reductions in the

Λ_{ii}'s due to the ligand orbital part, then the calculated values of the Λ_{ii}'s become too small to fit the observed Δg_{ii}'s. Thus a point corresponding to a smaller vanadium charge than the .40e is needed, according to Figures 14, 15, and 16, for such a point the charge transfer contribution to Λ_{zz} becomes much smaller than the value listed in Table 16. A rough estimate gives 18%, 22%, and 25% for the last row of Table 15.

TABLE 16

CRYSTAL FIELD AND CHARGE TRANSFER CONTRIBUTIONS TO THE Λ TENSOR COMPONENTS IN SnO_2:V IN UNITS OF 10^{-5}cm (.40e METAL CHARGE AND 35 Kcm^{-1} REDUCTION IN π-ELECTRON VSIP)

	Λ_{xx}	Λ_{yy}	Λ_{zz}
Crystal field	10.014	17.797	13.853
Charge transfer	-.170	-.538	-2.529
Total	9.844	17.529	11.325

This thesis has been concerned with the properties of vanadium in SnO_2, TiO_2, and GeO_2. Recent ESR spectra of Mo^{5+} and W^{5+} in TiO_2 have been reported.[44] Comments on these experimental results are given in Appendix K.

APPENDIX A

GENERAL THEORY

The Hamiltonian for a system of k nuclei and N electrons is

$$H=\sum_{j}^{k}\left(-\frac{\hbar^2}{2M_j}\nabla_j^2\right)-\frac{\hbar^2}{2m}\sum_{i}^{N}\nabla_i^2+\sum_{j<j'}^{k}\frac{Z_j Z_{j'} e^2}{r_{jj'}}-$$
$$-\sum_{i}^{N}\sum_{j}^{k}\frac{Z_j e^2}{r_{ij}}+\sum_{i<i'}^{N}\frac{e^2}{r_{ii'}} \qquad \text{(A-1)}$$

To this Hamiltonian one should have added terms depending on the electron spin, the nuclear spin, quadrupole moments, etc., but due to their smallness in comparison with H they are neglected. Thus the Hamiltonian H in Eq. (A-1) is spin independent.

The Schrödinger equation for a stationary state is

$$H\Psi = E_{\text{total}}\Psi \qquad \text{(A-2)}$$

The Born-Oppenheimer[7] approximation simplifies Eq. (A-2) to

$$\left\{-\frac{\hbar^2}{2m}\sum_{i}^{N}\nabla_i^2+\sum_{j<j'}\frac{Z_j Z_{j'} e^2}{r_{jj'}}-\sum_{i}^{N}\sum_{j}^{k}\frac{Z_j e^2}{r_{ij}}+\right.$$
$$\left.+\sum_{i<i'}^{N}\frac{e^2}{r_{ii'}}\right\}\Psi_{el}=E\Psi_{el} \qquad \text{(A-3)}$$

Equation (A-3) is simplified to

$$\left\{\sum_{i}^{N}\left(-\frac{\hbar^2}{2m}\nabla_i^2-\sum_{j}^{k}\frac{Z_j e^2}{r_{ij}}\right)+\sum_{i<i'}^{N}\frac{e^2}{r_{ii'}}\right\}\Psi_{el}=E_{el}\Psi_{el} \tag{A-4}$$

by using the definition

$$E_{el}\equiv E-\sum_{j<j'}^{k}\frac{Z_j Z_{j'} e^2}{r_{jj'}} \tag{A-5}$$

Unfortunately, only approximate numerical solutions of Eq. (A-4) can be obtained by the use of high speed computers in the very simple cases of small molecules. The difficulty comes from the last term giving the electron-electron interactions

The Electron-Independent Model.

The simplest (and crudest) approximation in solving Eq (A-4) is to neglect completely the electron-electron interaction, i.e., to solve the equation:

$$\sum_{i}^{N}\left(-\frac{\hbar^2}{2m}\nabla_i^2-\sum_{j}^{k}\frac{Z_j e^2}{r_{ij}}\right)\Psi_{el}(1,2\ldots N)=E_{el}\Psi(1,2\ldots N) \tag{A-6}$$

As the Hamiltonian is a sum of one-electron operators, the solutions of Eq. (A-6) are of the form of product functions:

$$\Psi_{el}(1,2\ldots N)=\Phi_{K_1}(1)\,\Phi_{K_2}(2)\ldots\Phi_{K_N}(N) \tag{A-7}$$

where the Φ's are solutions of the equation

$$\left(-\frac{\hbar^2}{2m}\nabla_i^2 - \sum_j^k \frac{Z_j e^2}{r_{ij}}\right)\Phi_K(i) = \varepsilon_K \Phi_K(i) \qquad \text{(A-8)}$$

A wave function $\Phi_K(i)$ which depends on the spatial coordinates of one electron only is generally called an orbital. If the one-electron wave function depends on the spatial and spin coordinates it is called a spin-orbital. When the Hamiltonian is independent of spin, a spin-orbital is a product of an orbital and a spin function like

$$\Phi_K(i)\,\alpha(i) \qquad \text{or} \qquad \Phi_K(i)\,\beta(i)$$

Thus, every product function of the form (A-7) can produce 2^N product functions, if spin is included. However, not all of them are necessarily possible, on account of the Pauli's principle and the indistinguishability of the electrons, which are both satisfied if a product function like

$$\Phi_{K_1}(1)\,\alpha(1)\,\Phi_{K_2}(2)\,\beta(2)\,\cdots\,\Phi_{K_N}(N)\,\alpha(N) \qquad \text{(A-9)}$$

is replaced by the normalized Slater determinant, which will be abbreviated usually as

$$\left|\Phi_{K_1}(1)\,\alpha(1)\,\Phi_{K_2}(2)\,\beta(2)\,\cdots\,\Phi_{K_N}(N)\,\alpha(N)\right| \qquad \text{(A-10)}$$

Self-Consistent (SCF).

The previous approximation, in neglecting the electron-electron interaction term, brought a great simplification of the problem, but one does not expect to get anything like the true energy eigenfunctions and eigenvalues.

In the SCF approximation, each electron is considered to move in a fixed effective electric field which is obtained by averaging over the positions of all the other electrons, in addition to the field produced by the nuclei. Therefore, each electron is expected to be described by an orbital (or a spin-orbital) and the Hamiltonian becomes again a sum of one-electron operators with product functions as solutions of the Schrodinger's equation. Using a trial function of the form:

$$\Psi_{el} = \Phi_1(1)\,\Phi_2(2)\,\cdots\cdots\,\Phi_N(N) \tag{A-11}$$

and applying the variational principle to minimize

$$E = \frac{\langle \Psi | H | \Psi \rangle}{\langle \Psi | \Psi \rangle} \tag{A-12}$$

where H is the Hamiltonian in Eq. (A-4) one gets[8] the following N Hartree equations:

$$\left\{ -\frac{\hbar^2}{2m}\nabla_i^2 - \sum_{\delta}^{k}\frac{Z_\delta e^2}{r_{i\delta}} + \sum_{\substack{i'=1 \\ i'\neq i}}^{N} \left\langle \Phi_{i'}(2)\left|\frac{e^2}{r_{ii'}}\right|\Phi_{i'}(2)\right\rangle \right\}\Phi_i(1) = E_i\,\Phi_i(1) \tag{A-13}$$

If, instead of a product function, a Slater determinant like Eq. (A-10) is used one gets[9] the following N Hartree-Fock equations:

$$\left\{-\frac{\hbar^2}{2m}\nabla_i^2-\sum_j^k\frac{Z_j e^2}{r_{ij}}+\sum_{i'=1}^{N}\left\langle\Phi_{i'}(2)\left|\frac{e^2}{r_{12}}\right|\Phi_{i'}(2)\right\rangle\right\}\Phi_i(1)-$$

$$-\sum_{\substack{i'=1\\ i'\neq i}}^{N}\left\{\left\langle\Phi_{i'}(2)\left|\frac{e^2}{r_{12}}\right|\Phi_i(2)\right\rangle\right\}\Phi_{i'}(1)=E_i\Phi_i(1) \qquad \text{(A-14)}$$

The term self-consistent field is appropriate since each Φ_i depends on every $\Phi_{i'}$ and whichever orbital Φ_i one chooses, it must come as a solution of the Schrodinger equation in which the potential energy due to all the other orbitals has been calculated by means of the Φ_i's.

The self-consistent orbitals are obtained by iterations. In general, the results of SCF calculations are good but the calculations are quite complicated and lengthy, and the wave functions are expressed in a numerical table or at best as sums of many analytical functions.

Atoms.

If there is only one nucleus, i.e., $k = 1$, and the potential

$$\sum_{\substack{i'=1\\ i'\neq i}}^{N}\left\langle\Phi_{i'}(2)\left|\frac{e^2}{r_{ii'}}\right|\Phi_{i'}(2)\right\rangle$$

is, if necessary, averaged (approximation) over all directions so as to be always spherically symmetric, then the Hamiltonian of the Hartree

equations (A-13) becomes spherically symmetric and the solutions can be expressed[8] as hydrogen-like orbitals.

$$\Phi_{n,l,m} = j_{n,l}(r)\ \Theta_{l,m}(\vartheta)\ \Phi(\varphi) \qquad \text{(A-15)}$$

This is in agreement with an empirical method that Slater[10] had suggested earlier.

Molecules (Complexes, Solids).

The presence of many nuclei does not allow spherical symmetry (even approximately), and the problem of solving Eq. (A-13) or Eq. (A-14) becomes extremely difficult. Only for the hydrogen molecule have SCF-molecular orbitals (SCF-MO) been obtained.[12] An approximation that is widely used in "small molecules" like HF, H_2, CH, CH_2 . . . is to consider a linear combination of atomic orbitals centered on the nuclei of the molecule (the term "molecule" will be used collectively for molecules, complexes, and solids), i.e.,

$$\Phi_i = \sum_{\alpha} c_{i\alpha}\ \Psi_{\alpha} \qquad \text{(A-16)}$$

See Refs. 13 to 19.

Semiempirical Methods.

The result of the Hartree SCF method was to change the Hamiltonian of Eq. (A-4) into a sum of one-electron operators of the form:

$$H_i = \frac{-\hbar^2}{2m}\nabla_i^2 - \sum_{j}^{k}\frac{Z_j e^2}{r_{ij}} + \sum_{\substack{i'=1 \\ i'\neq i}}^{N}\int \Phi_{i'}^{*}(2)\frac{e^2}{r_{ii'}}\Phi_{i'}(2)\,d\tau_2 \qquad \text{(A-17)}$$

The last sum of integrals is the operator whose expected value expresses the Coulombs potential energy of the i-th electron (strictly speaking of an electron in the i-th orbital) due to the average field of the rest of the electrons, and it is different for different orbitals. However, if two orbitals are approximately in the same relative position with respect to the others, one anticipates almost the same expectation values. This idea is reflected, also, in the Slater's rules which give the same screening constant σ for all the orbitals of the same group. The case of complex molecules is certainly more involved as there is no spherical symmetry in the Hamiltonian. As a more complex situation needs more drastic measures, the following assumptions are made:

(a) Electrons are divided into core and valence electrons.

(b) Core electrons form closed shells that affect the motion of the valence electrons only through the screening of the corresponding nuclei.

(c) Each of the valence electrons moves on an orbital Φ_v satisfying the Schrodinger equation:

$$H_{eff}(\mu)\,\Phi_v(\mu) \equiv \left\{ -\frac{\hbar^2}{2m}\nabla_\mu^2 - \sum_j^k \frac{Z_j^* e^2}{r_{\mu j}} + V(\underline{r}_\mu) \right\} \Phi_v(\mu)$$

$$= E_v\,\Phi_v(\mu) \qquad \text{(A-18)}$$

where Z_j^* is the effective charge of the j-th nucleus and $V(\underline{r}_\mu)$ is the average potential energy of the valence electron due to the rest of the electrons.

(d) The function $V(\underline{r})$ is the same for all valence electrons even if they occupy orbitals corresponding to an excited state of the group of valence electrons.

(e) ζ_j^{*}'s and $V(\underline{r})$ are not to be used explicitly.

Suppose that one knows the H_{eff} and let $\{\varphi_i\}$ be a complete, but not necessarily orthogonal, set of one-electron functions that obey the same mathematical restrictions as the valence orbitals. Then one can always expand Φ_v in an infinite series:

$$\Phi_v = \sum_i^{\infty} c_i \varphi_i \tag{A-19}$$

Substituting in Eq. (A-18)

$$H_{eff} \sum_{i=1}^{\infty} c_i \varphi_i = E \sum_{i=1}^{\infty} c_i \varphi_i \tag{A-20}$$

and multiplying on the left by φ_j^{*} $(j = 1, 2 \ldots \infty)$ and integrating one gets an infinite number of equations:

$$\sum_{i=1}^{\infty} c_i \left[\int \varphi_j^{*} H_{eff} \varphi_i \, d\tau - E \int \varphi_j^{*} \varphi_i \, d\tau \right] = 0 \qquad j = 1, 2 \ldots \infty \tag{A-21}$$

Since there are mathematical and practical difficulties in dealing with an infinite number of equations, one generally restricts the expansion (A-19) to a small number n of functions φ_i hoping that with the proper selection of φ_i's and the best coefficients c_i's the approximation

$$\Phi_v \sim \sum_{i=1}^{n} c_i \varphi_i \tag{A-22}$$

will be adequate. The selection of the proper φ_i's rests on intuition and experience, but the best coefficients c_i's are determined

rigorously by the variational method, i.e., one minimizes

$$E = \frac{\int \Phi_v^* H_{eff} \Phi_v \, d\tau}{\int \Phi_v^* \Phi_v \, d\tau} \qquad \text{(A-23)}$$

Thus (see Appendix B), the following secular equations and secular determinants are obtained:

$$\sum_{i=1}^{n} c_i (H_{ik} - E S_{ik}) = 0 \qquad k = 1, 2 \ldots n \qquad \text{(A-24)}$$

$$\det | H_{ik} - E S_{ik} | = 0 \qquad i, k = 1, 2 \ldots n \qquad \text{(A-25)}$$

where by definition

$$H_{ik} \equiv \int \varphi_i^* H_{eff} \varphi_k \, d\tau \quad \text{and} \quad S_{ik} \equiv \int \varphi_i^* \varphi_k \, d\tau \qquad \text{(A-26)}$$

Since the Hamiltonian operator is hermitian $H_{ii} = H_{ii}^*$ and $H_{ij} = H_{ji}^*$; if the functions φ_i's are real, as is almost always the case, then $H_{ij} = H_{ji}$. As for the set of orbitals φ_i to be used, generally, atomic orbitals centered at the different nuclei are selected so that $\Phi_v = \sum_i^n c_i \varphi_i$ is a linear combination of atomic orbitals (LCAO). The selected atomic orbitals are the energetically lower valence orbitals as the atoms-in-molecules[14] method implies. At an infinite separation of the nuclei, the valence electrons are rigorously on atomic orbitals. However, at a smaller separation of the nuclei the LCAO is only an approximation.

APPENDIX B

APPLICATION OF THE VARIATION METHOD TO LINEAR FUNCTIONS

Substituting relation (A-22) into (A-23) and using definitions

(A-26)

$$E = \frac{\sum_{i,j}^{n} c_i c_j H_{ij}}{\sum_{i,j}^{n} c_i c_j S_{ij}} \tag{B-1}$$

Normalization of Φ_v requires that

$$\sum_{i,j}^{n} c_i c_j S_{ij} = 1 \tag{B-2}$$

Bringing the denominator on the left side and differentiating with respect to c_k, one gets

$$\frac{\partial E}{\partial c_k} \sum_{i,j}^{n} c_i c_j S_{ij} + E \frac{\partial}{\partial c_k} \sum_{i,j}^{n} c_i c_j S_{ij} = \frac{\partial}{\partial c_k} \sum_{i,j}^{n} c_i c_j H_{ij} \tag{B-3}$$

For a minimum in energy, necessarily

$$\frac{\partial E}{\partial c_k} = 0 \qquad k = 1, 2 \ldots n \tag{B-4}$$

Therefore

$$E \frac{\partial}{\partial c_k} \sum_{i,j}^{n} c_i c_j S_{ij} = \frac{\partial}{\partial c_k} \sum_{i,j}^{n} c_i c_j H_{ij} \tag{B-5}$$

or

$$E \, 2 \sum_{i}^{n} c_i S_{ik} = 2 \sum_{i} c_i H_{ik} \tag{B-6}$$

or

$$\sum_{i=1}^{n} c_i \left(H_{ik} - E S_{ik} \right) = 0 \qquad k = 1, 2 \ldots n \tag{B-7}$$

For a nontrivial solution, necessarily

$$\left| H_{ik} - E S_{ik} \right| = 0 \tag{B-8}$$

The coefficients c_i's are determined by solving the equations:

$$\sum_{i \neq 1}^{n} \frac{c_i}{c_1} \left[H_{ji} - E S_{ji} \right] = - H_{j1} + E S_{j1} \tag{B-9}$$

for the ratios $\frac{c_i}{c_1}$ and then using the normalization condition (A-2).

APPENDIX C

GROUP CHARACTER TABLE FOR THE SINGLE-VALUED

IRREDUCIBLE REPRESENTATIONS

			E	C_2^z	C_2^y	C_2^x	I	σ_h^z	σ_v^y	σ_v^x	
A	Γ_{1g}	N_{1g}	1	1	1	1	1	1	1	1	$3z^2-r^2; x^2-y^2; S$
B	Γ_{2g}	N_{3g}	1	1	-1	-1	1	1	-1	-1	xy ; $\hat{L}_z$
C	Γ_{3g}	N_{2g}	1	-1	1	-1	1	-1	1	-1	zx ; $\hat{L}_y$
D	Γ_{4g}	N_{4g}	1	-1	-1	1	1	-1	-1	1	yz ; $\hat{L}_x$
	Γ_{1u}	N_{1u}	1	1	1	1	-1	-1	-1	-1	
E	Γ_{2u}	N_{3u}	1	1	-1	-1	-1	-1	1	1	z
Z	Γ_{3u}	N_{2u}	1	-1	1	-1	-1	1	-1	1	y
H	Γ_{4u}	N_{4u}	1	-1	-1	1	-1	1	1	-1	x
$N_{2g} \otimes N_{3g}$			1	-1	-1	1	1	-1	-1	1	N_{4g}
$N_{2g} \otimes N_{4g}$			1	1	-1	-1	1	1	-1	-1	N_{3g}
$N_{3g} \otimes N_{4g}$			1	-1	1	-1	1	-1	1	-1	N_{2g}
$N_{4u} \otimes N_{4u}$			1	1	1	1	1	1	1	1	N_{1g}

APPENDIX D

TWO-CENTER OVERLAP INTEGRALS

The two-center overlap integrals are calculated using the following formulas:

$$K=\langle 2s|3d_\sigma\rangle=N_a N_b\frac{\sqrt{5}}{4}\left(\frac{R}{2}\right)^6\left[A_0(-3B_3+B_5)+A_1(-3B_2+5B_4)+\right.$$
$$+A_2(3B_1+4B_3-3B_5)+A_3(3B_0-4B_2-3B_4)+A_4(-5B_1+3B_3)+$$
$$\left.+A_5(-B_0+3B_2)\right]$$

$$L1=\langle 2s|3p_\sigma\rangle=N_a N_b\frac{\sqrt{3}}{2}\left(\frac{R}{2}\right)^6\left[A_0B_4-A_1B_5-2A_2B_2+2A_3B_3+A_4B_0-A_5B_1\right]$$

$$L2=\langle 2s|4p_\sigma\rangle=N_a N_b\frac{\sqrt{3}}{2}\left(\frac{R}{2}\right)^7\left[-A_0B_5+A_1(B_4+B_6)+A_2(2B_3-B_5)\right.$$
$$\left.-2A_3(B_2+B_4)+A_4(-B_1+2B_3)+A_5(B_0+B_2)-A_6B_1\right]$$

$$M1=\langle 2s|3s\rangle=N_a N_b\frac{1}{2}\left(\frac{R}{2}\right)^6\left[-A_0B_5+A_1B_4+2A_2B_3-2A_3B_2-A_4B_1+A_5B_0\right]$$

$$M2=\langle 2s|4s\rangle=N_a N_b\frac{1}{2}\left(\frac{R}{2}\right)^7\left[A_0B_6-2A_1B_5-A_2B_4+4A_3B_3-A_4B_2-2A_5B_1+A_6B_0\right]$$

$$N=\langle 2p_\sigma|3d_\sigma\rangle=N_a N_b\frac{\sqrt{15}}{4}\left(\frac{R}{2}\right)^6\left[A_0(-3B_2+B_4)+A_1(B_3+B_5)+\right.$$
$$\left.+A_2(3B_0+B_4)-A_3(B_1+3B_5)-A_4(B_0+B_2)+A_5(-B_1+3B_3)\right]$$

$$O=\langle 2p_\pi|3d_\pi\rangle=N_a N_b\frac{3\sqrt{5}}{4}\left(\frac{R}{2}\right)^6\left[A_0(B_2-B_4)+A_1(-B_3+B_5)+\right.$$
$$\left.+A_2(-B_0+B_4)+A_3(B_1-B_5)+A_4(B_0-B_2)+A_5(-B_1+B_3)\right]$$

$$P1=\langle 2p_\sigma|3p_\sigma\rangle=N_a N_b\frac{3}{2}\left(\frac{R}{2}\right)^6\left[A_0B_3-A_1B_2-A_2(B_1+B_5)+A_3(B_0+B_4)\right.$$
$$\left.+A_4B_3-A_5B_2\right]$$

$$P2=\langle 2p_\sigma|4p_\sigma\rangle=N_a N_b\frac{3}{2}\left(\frac{R}{2}\right)^7\left[-A_6B_1+2A_5B_3+A_4B_0-2A_3(B_1+B_5)+\right.$$

$$+ A_2 B_6 + 2A_1 B_3 - A_0 B_4]$$

$$Q1 = \langle 2p_\sigma | 3s \rangle = N_a N_b \frac{\sqrt{3}}{2} \left(\frac{R}{2}\right)^6 [-A_0 B_4 + A_1(2B_3 - B_5) + 2A_2 B_4 - 2A_3 B_1 +$$
$$+ A_4(B_0 - 2B_2) + A_5 B_1]$$

$$Q2 = \langle 2p_\sigma | 4s \rangle = N_a N_b \frac{\sqrt{3}}{2} \left(\frac{R}{2}\right)^7 [A_0 B_5 + A_1(B_6 - 3B_4) + A_2(-3B_5 + 2B_3)$$
$$+ A_3(2B_4 + 2B_2) + A_4(2B_3 - 3B_1) + A_5(-3B_2 + B_0) + A_6 B_1]$$

$$R1 = \langle 2p_\pi | 3p_\pi \rangle = N_a N_b \frac{3}{4} \left(\frac{R}{2}\right)^6 [A_0(-B_3 + B_5) + A_1(B_2 - B_4) + A_2(B_1 - B_5)$$
$$+ A_3(-B_0 + B_4) + A_4(-B_1 + B_3) + A_5(B_0 - B_2)]$$

$$R2 = \langle 2p_\pi | 4p_\pi \rangle = N_a N_b \frac{3}{4} \left(\frac{R}{2}\right)^7 [A_0(-B_6 + B_4) + A_1(2B_5 - 2B_3) + A_2 B_6$$
$$- A_2 B_4 + A_3(-2B_5 + 2B_1) + A_4(B_2 - B_0) + A_5(2B_3 - 2B_1) + A_6(-B_2 + B_0)]$$

The radial parts are given by $R(\mu) = N_\mu r^{n-1} e^{-\mu r}$. However, many times the radial part of an ns, np or nd function is given with a smaller exponent as in (38) or as a sum of functions of different exponents as in (44). In such a case one should be careful to look for the proper principal quantum number. For example, the computed expression of $\langle 2s | 4p_\sigma \rangle$ in the text will appear as $\langle 2s | 3p_{\sigma'} \rangle$ in the tables since the radial part of $4p_\sigma$ is given as $R(4p_\sigma) = N r^2 e^{-\mu r}$ and not as $R(4p_\sigma) = N' r^3 e^{-\mu r}$. Values of the two-center integrals are given below.

	SnO_2:V	TiO_2:V	GeO_2:V
$K_{\perp}$	.109	.128	.146
K_{γ}	.108	.120	.132
$L1_{\perp}$	-.002	-.002	-.003

	SnO_2:V	TiO_2:V	GeO_2:V
$L1_{\perp}$	-.002	-.002	-.002
$L2_{\perp}$	.403	.429	.450
$L2_{\parallel}$	.402	.419	.434
$M1_{\perp}$	-.002	-.002	-.003
$M1_{\parallel}$	-.002	-.002	-.002
$M2_{\perp}$	.265	.286	.304
$M2_{\parallel}$	.264	.277	.290
$n_{\perp}$	.113	.124	.131
$N_{\parallel}$	.113	.120	.125
$O_{\perp}$	.071	.086	.101
$O_{\parallel}$	.070	.080	.089
$P1_{\perp}$	-.004	-.005	-.006
$P1_{\parallel}$	-.004	-.004	-.005
$P2_{\perp}$	.178	.170	.159
$P2_{\parallel}$	.179	.174	.168
$Q1_{\perp}$	-.005	-.006	-.007
$Q1_{\parallel}$	-.005	-.005	-.006
$Q2_{\perp}$	.156	.157	.159
$Q2_{\parallel}$	.156	.158	.159
$R1_{\perp}$	-.001	-.001	-.001
$R1_{\parallel}$	-.001	-.001	-.001
$R2_{\perp}$	.162	.181	.198
$R2_{\parallel}$	.161	.173	.184

APPENDIX E

ENERGY EIGENVALUES IN Kcm^{-1} FOR SnO_2:V

.65	.55	.45	.35	.30	.20	.10	.00
111. E_2	106.5E_2	101. E_2	94.5E_2	90.5E_2	82.5E_2	73.5E_2	67. A_5
93.5A_5	91.5A_5	88. A_5	84.5A_5	83. A_5	78.5A_5	73. A_5	63. E_2
1.5Z_2	1.5Z_2	1.5Z_2	1.5Z_2	1. Z_2	1. Z_2	1. Z_2	1. Z_2
-10. H_2	-10. H_2	-9.5H_2	-9. H_2	-8.5H_2	-8. H_2	-7. H_2	-6. H_2
-61. C_3	-64.5C_3	-64.5B_2	-62.5B_2	-61. A_2	-57. A_2	-52.5A_2	-48. A_2
-62.5D_2	-66. B_2	-65.5A_2	-62.5A_2	-61. B_2	-57.5B_2	-53.5B_2	-49. B_2
-65.5C_2	-66. D_2	-67.5C_3	-69.5C_3	-69.5C_3	-67.5C_3	-63.5C_3	-58. C_3
-65.5	-69. A_2	-70. D_2	-72. D_2	-72. D_2	-69.5D_2	-65. D_2	-59.5D_2
-66.5B_2	-70. C_2	-75. C_2	-80. C_2	-81.5A_3	-75. A_3	-69. A_3	-62.5A_3
-70. H_3	-70.	-75.	-80.	-82.5C_2	-88. C_2	-93.5C_2	-99. C_2
-71. A_2	-74. H_3	-78.5H_3	-83. H_3	-82.5	-88.	-93.5	-99.
-71.5E_3	-75.5E_3	-79.5E_3	-84. E_3	-85. H_3	-89.5H_3	-94.5H_3	-99.5H_3
-107. A_3	-99. A_3	-91. A_3	-84.5A_3	-86. E_3	-90.5E_3	-95. E_3	-99.5E_3
-108. D_1	-101. D_1	-94. D_1	-91. D_1	-90. D_1	-92. D_1	-95.5D_1	-100. D_1
-108.5C_1	-101.5C_1	-95. C_1	-92.5C_1	-91.5C_1	-93. C_1	-96. C_1	-100.5C_1
-115. H_1	-115. H_1	-116.5H_1	-118.5H_1	-121.5H_1	-125. H_1	-130. H_1	-135.5H_1
-118.5Z_1	-118. Z_1	-119. E_1	-121. Z_1	-122.5Z_1	-126. Z_1	-130. Z_1	-135.5Z_1
-122. B_1	-119.5B_1	-119.5B_1	-121.5B_1	-123.5B_1	-127.5B_1	-132. B_1	-137. B_1
-127. A_4	-125.5A_4	-126. A_4	-127. A_4	-128.5A_4	-131.5A_4	-135. A_4	-139. A_4
-159. E_1	-161. E_1	-163.5E_1	-166.5E_1	-169. E_1	-174. E_1	-180.5E_1	-188.5A_1
-164. A_1	-165.5A_1	-167.5A_1	-170. A_1	-172.5A_1	-177. A_1	-182.5A_1	-189. E_1

ENERGY EIGENVALUES IN Kcm^{-1} FOR TiO_2:V

.65	.55	.45	.35	.30	.20	.10	.00
$153.5E_3$	$147. E_3$	$139.5E_3$	$130.5E_3$	$125. E_3$	$114. E_3$	$101. E_3$	$87. E_3$
$105. A_5$	$103. A_3$	$99.5A_3$	$95. A_5$	$93. A_5$	$88. A_5$	$82. A_5$	$75.5A_5$
$-8.5Z_2$	$-8. Z_2$	$-8. Z_2$	$-7.5Z_2$	$-7. Z_2$	$-6.5Z_2$	$-6. Z_2$	$-5. Z_2$
$-9. H_2$	$-8.5H_2$	$-8.5H_2$	$-8. H_2$	$-7.5H_2$	$-7. H_2$	$-6.5H_2$	$-5.5H_2$
$-59.5C_3$	$-60. B_2$	$-59. B_2$	$-57.5B_2$	$-56. B_2$	$-53.5B_2$	$-50. B_2$	$-45.5A_2$
$-60. B_2$	$-62.5C_3$	$-61.5A_2$	$-59. A_2$	$-57.5A_2$	$-54. A_2$	$-50. A_2$	$-46. B_2$
$-61. D_2$	$-64.5A_2$	$-65. C_3$	$-66.5C_3$	$-66.5C_3$	$-65. C_3$	$-61. C_3$	$-56.5C_3$
$-65.5C_2$	$-65. D_2$	$-68. D_2$	$-69.5D_2$	$-69.5D_2$	$-67.5D_2$	$-63.5D_2$	$-58.5D_2$
-65.5	$-70. C_2$	$-75. C_2$	$-80. C_2$	$-81.5A_3$	$-75. A_3$	$-69. A_3$	$-62.5A_3$
$-66.5A_2$	-70.	-75.	-80.	$-82.5C_2$	$-88. C_2$	$-93.5C_2$	$-99. C_2$
$-70.5H_3$	$-74.5H_3$	$-79. H_3$	$-83. H_3$	-82.5	-88.	-93.5	-99.
$-72.5E_2$	$-76. E_2$	$-80.5E_2$	$-84.5E_2$	$-85.5H_3$	$-90. H_3$	$-94.5H_3$	$-99.5H_3$
$-107. A_3$	$-99. A_3$	$-91. A_3$	$-84.5A_3$	$-86.5E_2$	$-91. E_2$	$-95.5E_2$	$-100. E_2$
$-108.5D_1$	$-101.5D_1$	$-95. D_1$	$-92. D_1$	$-91.5D_1$	$-93. D_1$	$-96. D_1$	$-100.5D_1$
$-109. C_1$	$-102.5C_1$	$-96.5C_1$	$-94. C_1$	$-93.5C_1$	$-94.5C_1$	$-97. C_1$	$-101. C_1$
$-112.5H_1$	$-112. H_1$	$-113.5H_1$	$-115.5H_1$	$-117.5H_1$	$-121.5H_1$	$-126.5H_1$	$-132. H_1$
$-115. Z_1$	$-114.5Z_1$	$-115.5Z_1$	$-117. Z_1$	$-119. Z_1$	$-122.5Z_1$	$-127. Z_1$	$-132. Z_1$
$-122. B_1$	$-119.5B_1$	$-118.5B_1$	$-120. B_1$	$-121.5B_1$	$-125. B_1$	$-129.5B_1$	$-134.5B_1$
$-126. A_4$	$-124. A_4$	$-124. A_4$	$-125. A_4$	$-126.5A_4$	$-129. A_4$	$-132. A_4$	$-136. A_4$
$-165.5E_1$	$-167.5E_1$	$-170. E_1$	$-173. E_1$	$-175.5E_1$	$-181. E_1$	$-188. E_1$	$-195.5A_1$
$-170.5A_1$	$-172.5A_1$	$-174. A_1$	$-177. A_1$	$-179.5A_1$	$-184. A_1$	$-189.5A_1$	$-196.5E_1$

ENERGY EIGENVALUES IN Kcm^{-1} FOR GeO_2:V

.65	.55	.45	.35	.30	.20	.10	.00
176. E_3	170. E_3	161.5E_3	151.5E_3	145.5E_3	133. E_3	118.5E_3	102.5E_3
137.5A_4	135.5A_4	130.5A_4	125. A_4	122.5A_4	116. A_4	108.5A_4	99.5A_4
.5Z_2	.5Z_2	.5Z_2	.5Z_2	.5Z_2	.5Z_2	.5Z_2	.5Z_2
5.5H_2	-4. H_2	-5. H_2	-4.5H_2	-4.5H_2	-4. H_2	-4. H_2	-3.5H_2
-56.5B_2	-56.5B_2	-54.5B_2	-53. B_2	-52. B_2	-49.5B_2	-45.5A_5	-41.5A_5
-60.5A_5	-59. A_5	-56. A_5	-53.5A_5	-52. A_5	-49. A_5	-46. B_2	-42.5B_2
-57.5C_3	-60.5C_3	-63. C_3	-64. C_3	-64. C_3	-62.5C_3	-59. C_3	-55. C_3
-59.5D_2	-62.5D_2	-65.5D_2	-67. D_2	-67. D_2	-65. D_2	-61. D_2	-56.5D_2
-65.5C_2	-70. C_2	-75. C_2	-80. C_2	-81.5A_3	-75. A_3	-69. A_3	-62.5A_3
-65.5	-70.	-75.	-80.	-82.5C_2	-88. C_2	-93.5C_2	-99. C_2
-71. H_3	-77. E_2	-79.5H_3	-83.5H_3	-82.5	-88.	-93.5	-99.
-73. E_2	-90. H_3	-81. E_2	-84.5A_3	-85.5H_3	-90. H_3	-95. H_3	-99.5H_3
-107. A_3	-99. A_3	-91. A_3	-85. E_2	-87. E_2	-91.5E_2	-95.5E_2	-100. E_2
-109. D_1	-102.5D_1	-96.5D_1	-93.5D_1	-93. D_1	-94. D_1	-97. D_1	-101. D_1
-109.5C_1	-103. C_1	-97.5C_1	-95. C_1	-94.5C_1	-95.5C_1	-98. C_1	-101.5C_1
-115. H_1	-119.5Z_1	-116.5H_1	-118.5H_1	-120.5H_1	-125. H_1	-129.5H_1	-135.5H_1
-118.5Z_1	-125. H_1	-119. Z_1	-120.5Z_1	-122.5Z_1	-126. Z_1	-130. Z_1	-135.5Z_1
-125.5B_1	-124. B_1	-122. B_1	-124. B_1	-125.5B_1	-129. B_1	-133. B_1	-138. B_1
-129.5A_2	-129.5A_2	-128. A_2	-129. A_2	-130.5A_2	-133. A_2	-136. A_2	-139.5A_2
-160. E_1	-162. E_1	-164. E_1	-167. E_1	-169.5E_1	-174.5E_1	-181. E_1	-189. A_1
-166.5A_1	-168. A_1	-169. A_1	-172. A_1	-174. A_1	-178. A_1	-183. A_1	-189. E_1

APPENDIX F

VARIATION OF THE z^2 AND 4S ADMIXTURE IN THE GROUND STATE A_3

	SnO_2:V			TiO_2:V			GeO_2:V		
Assumed Vanadium Charge	4s	z^2	x^2-y^2	4s	z^2	x^2-y^2	4s	z^2	x^2-y^2
.65	.073	-.139	.986	.068	-.114	.992	.082	-.140	.987
.55	.071	-.135	.988	.059	-.110	.992	.078	-.136	.987
.45	.069	-.133	.989	.058	-.108	.992	.077	-.135	.988
.35	.068	-.132	.989	.057	-.108	.992	.076	-.134	.988
.30	.068	-.132	.989	.057	-.107	.993	.076	-.134	.988
.20	.067	-.131	.989	.056	-.106	.993	.075	-.133	.988
.10	.067	-.130	.989	.056	-.106	.993	.749	-.133	.988
.00	.066	-.130	.989	.055	-.105	.993	.074	-.132	.988
-.10	.065	-.130	.989	.055	-.105	.993	.074	-.132	.988
-.20	.065	-.129	.989	.054	-.105	.993	.073	-.132	.989
-.30	.064	-.129	.990	.054	-.104	.993	.073	-.131	.989
-.40	.064	-.128	.990	.053	-.104	.993	.072	-.131	.989
-.50	.063	-.128	.990	.053	-.103	.993	.072	-.130	.989

APPENDIX G

POINT CHARGE CRYSTALLINE FIELD CALCULATION OF THE ELECTRONIC LEVELS OF SnO_2:V

Using Watson's radial functions the following splitting of the nearest 3d vanadium electronic levels is obtained. The number of the nearest ions, which have been considered in each case, is written in parentheses. The cases with 8 and 32 nearest ions are considered closest to reality because the corresponding total charge of the complex is zero.

Appendix G Table

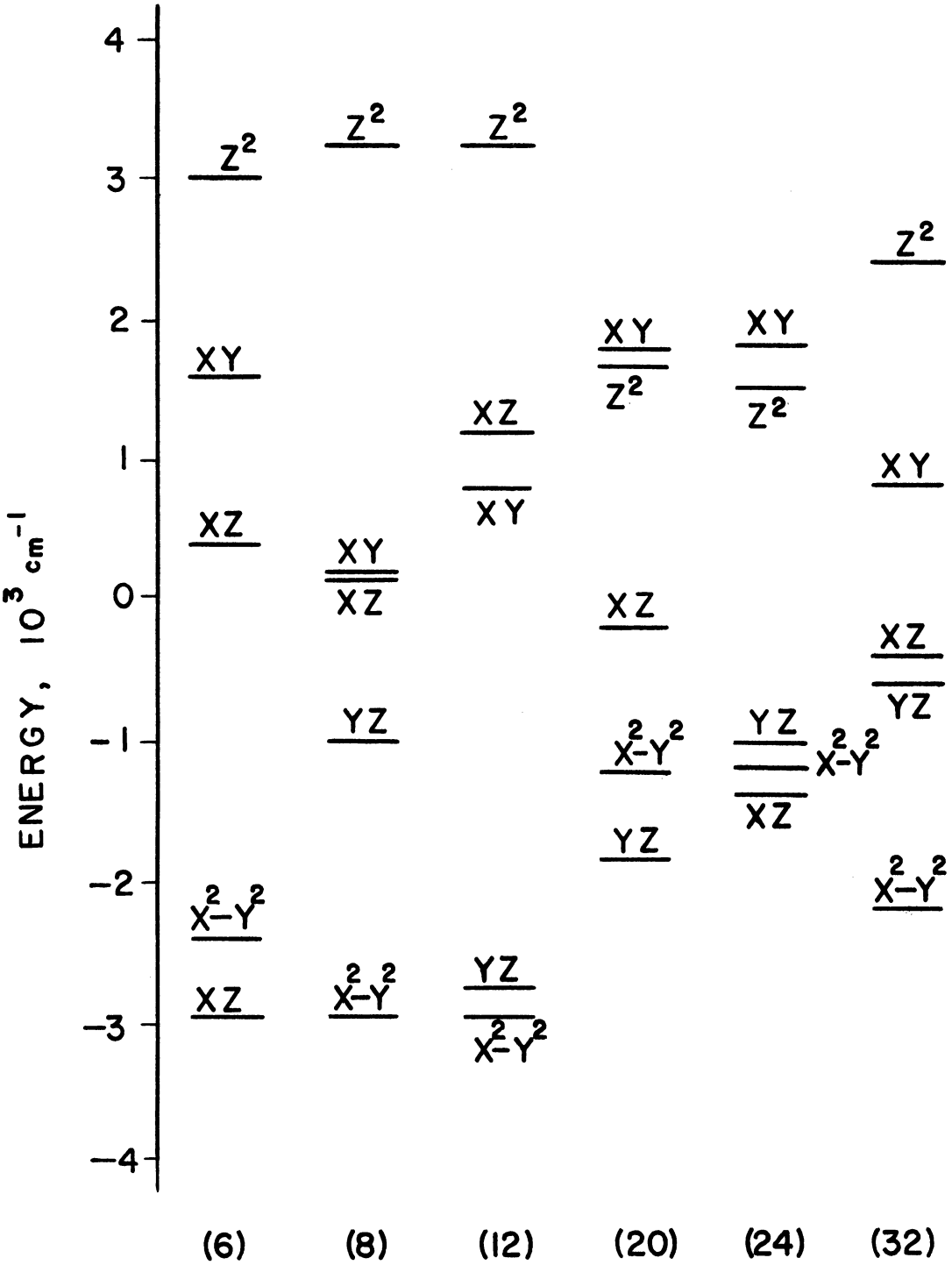

APPENDIX H

VALENCE STATE, VALENCE STATE IONIZATION POTENTIAL (VSIP), VALENCY AND PROMOTION ENERGY

A simplified discussion of the water molecule is given to clarify the above ideas.

The ground configuration of oxygen is $1s^2 2s^2 2p_z^2 2p_x 2p_y$ and it is a ^3P with the two unpaired electrons having parallel spins. The ionization energy[28] is 109836.7 cm^{-1}(13.614 eV). The water molecule is formed by pairing each of these two electrons with the electrons of the two hydrogen atoms (neglect hybridization). The two oxygen electrons are randomly oriented with respect to each other. If by some imaginary process one could remove the hydrogen atoms and still keep the spins of the two oxygen electrons uncorrelated, the state of the oxygen atom would be a <u>valence state</u>. The number of the spin-uncorrelated electrons determines the <u>valency</u> of the state. In this example, the oxygen is divalent. The ionization energy of one of the valence electrons is less than in the case of the single oxygen atom by the amount that is needed to uncouple the two electrons from the triplet state. Since the singlet state ^1D is 15867.7 cm^{-1} higher than the ground state ^3P the <u>valence state ionization potential</u> (VSIP) is

less than in the free atom by the amount $\frac{3}{4}(0)+\frac{1}{4}(15867.7)$, where the factors $\frac{3}{4}$ and $\frac{1}{4}$ take into account the spin multiplicity. From this example, it is obvious that the valence state is <u>not</u> a spectroscopic state and excitation to it is not physically possible. It is a non-stationary state. The amount $\frac{3}{4}(0)+\frac{1}{4}(15867.7)$ is usually referred to as the <u>promotion energy</u>.

In general, the orbital part of the valence state of an ion can be a linear combination of the form $\alpha|2s\rangle+\beta|2p\rangle$, for example, which is referred to as a hybrid orbital. In this case, the promotion energy might have, also, a contribution from the hybridization.

APPENDIX I

EFFECTS OF THE LIGAND ORBITAL PART IN THE CALCULATION OF THE ZEEMAN MATRIX ELEMENTS

Using the notation in Eq. (70) for the calculation of Λ_{xx} one has the matrix elements:

$$\left\langle a_{z^2}|z^2\rangle + a_{x^2-y^2}|x^2-y^2\rangle \middle| \hat{L}_x \middle| d_i|yz\rangle \right\rangle \otimes$$

$$\otimes \left\langle d_i|yz\rangle + d_i'|x_2\rangle \middle| \hat{L}_x \middle| a_{z^2}|z^2\rangle + a_{x^2-y^2}|x^2-y^2\rangle \right\rangle$$

$$= \left\langle a_{z^2}|z^2\rangle + a_{x^2-y^2}|x^2-y^2\rangle \middle| d_i\left[i|x^2-y^2\rangle + i\sqrt{3}|z^2\rangle\right] \right\rangle$$

$$\otimes \left\langle d_i|yz\rangle + d_i'|x_2\rangle \middle| a_{z^2}(-i\sqrt{3})|yz\rangle + a_{x^2-y^2}(-i)|yz\rangle \right\rangle$$

$$= d_i(a_{z^2} i\sqrt{3} + a_{x^2-y^2} i)\left[d_i(-a_{z^2} i\sqrt{3} - i a_{x^2-y^2}) + \right.$$

$$\left. + d_i(-a_{z^2} i\sqrt{3} - i a_{x^2-y^2})\langle x_2|yz\rangle\right]$$

$$= (a_{x^2-y^2} + a_{z^2}\sqrt{3})^2 d_i\left[d_i + d_i'\langle x_2|yz\rangle\right]$$

$$\left\langle a_{z^2}|z^2\rangle + a_{x^2-y^2}|x^2-y^2\rangle \middle| \hat{L}_y \middle| c_i\,|xz\rangle \right\rangle$$

$$\otimes \left\langle c_i\,|xz\rangle + c_i'\,|\alpha_1\rangle + c_i''\,|\alpha_5\rangle \middle| \hat{L}_y \middle| a_{z^2}|z^2\rangle + a_{x^2-y^2}|x^2-y^2\rangle \right\rangle$$

$$= (a_{x^2-y^2} - a_{z^2}\sqrt{3})^2 c_i \left[c_i + c_i' \langle \alpha_1 | xz\rangle + c_i'' \langle \alpha_5 | yz\rangle\right]$$

$$\left\langle a_{z^2}|z^2\rangle + a_{x^2-y^2}|x^2-y^2\rangle \middle| \hat{L}_z \middle| b_i\,|xy\rangle \right\rangle \otimes$$

$$\left\langle b_i\,|xy\rangle + b_i'\,|\Phi_2\rangle \middle| \hat{L}_z \middle| a_{z^2}|z^2\rangle + a_{x^2-y^2}|x^2-y^2\rangle \right\rangle$$

$$= 4 a^2_{x^2-y^2}\, b_i \left[b_i + b_i' \langle \Phi_2 | xy\rangle\right]$$

APPENDIX J

COMPUTER PROGRAM IN MAD LANGUAGE FOR SOLVING THE SECULAR EQUATIONS (25)

```
$COMPILE MAD, EXECUTE, PUNCH OBJECT
          PRINT COMMENT $1 SOLUTION OF THE CHARACTERISTIC VALUE PROBLEM
         1 (A-LB)X=0 $
          PRINT COMMENT $0 WHERE A AND B ARE SYMMETRIC MATRICES, AND B
         1 IS POSITIVE DEFINITE $
          DIMENSION A(400,V), B(400,V),X(400,V), APRIME(400,V),E(400,V)
          DIMENSION D(400,V), UT(400,V), R(400,V), ST(400,V),
         1S(400,V), LAMBDA(400,V), YT(400,V)
          EQUIVALENCE(D,R,ST,E),(UT,S,YT,X),(APRIME,LAMBDA),
         1(V(2),N)
          VECTOR VALUES V=2,1,0
          INTEGER N,I,J,K,CH
START     READ AND PRINT DATA
          EXECUTE ZERO.(A(1,1)...A(N,N),B(1,1)...B(N,N))
          READ AND PRINT DATA
          THROUGH  LOOP1, FOR I= 2,1,I.G.N
          THROUGH  LOOP1, FOR J = 1,1,J.E.I
          A(I,J)=-2.*B(I,J)*SQRT.(A(I,I)*A(J,J))
          A(J,I) = A(I,J)
LOOP1     B(J,I) = B(I,J)
          IND1=5.
          IND2=5.
          IND3=5.
          IND4=5.
          IND5=5.
          IND6=5.
          THROUGH LOOP1A, FOR I=1,1, I.G.N*N
LOOP1A    D(I)=B(I)
          SCFACT = 1.
          IND1=EIGN.(D(1),N,1,UT(1),SCFACT)
          WHENEVER IND1.E.3.
          CONTINUE
          OR WHENEVER IND1.E.1.
          PRINT COMMENT $0 B MATRIX NOT ACCEPTED BY SUBROUTINE $
          TRANSFER TO END
          OR WHENEVER IND1.E.2.
          PRINT COMMENT $0 CHARACTERISTIC VALUES OF B MATRIX SCALED BY$
          PRINT RESULTS SCFACT
          TRANSFER TO END
          END OF CONDITIONAL
          THROUGH LOOP2, FOR I=1,1,I.G.N
          WHENEVER D(I,I).LE.0.
          PRINT COMMENT $0 B MATRIX IS NOT POSITIVE DEFINITE $
          TRANSFER TO END
          OTHERWISE
          R(I,I)=D(I,I).P.-.5
LOOP2     END OF CONDITIONAL
          THROUGH LOOP3, FOR I=1,1,I.G.N
          THROUGH LOOP3, FOR J=1,1, J.G.N
          WHENEVER I.E.J
          CONTINUE
          OTHERWISE
          R(I,J)=0.
LOOP3     END OF CONDITIONAL
          IND2=DPMAT.(N,ST(1),UT(1))
          WHENEVER IND2.E.0., TRANSFER TO END
          THROUGH LOOP 5, FOR I=1,1,I.G.N
          THROUGH LOOP 5, FOR J=1,1,J.G.N
          S(I,J)=ST(J,I)
```

```
LOOP5     APRIME(I,J)=ST(I,J)
          IND3=DPMAT.(N,APRIME(1),A(1))
          WHENEVER IND3.E.0., TRANSFER TO END
          IND4=DPMAT.(N,APRIME(1),S(1))
          WHENEVER IND4.E.0., TRANSFER TO END
          THROUGH LOOP6, FOR I=2,1, I.G.N
          THROUGH LOOP6, FOR J=1,1, J.E.I
LOOP6     APRIME(I,J) = APRIME(J,I)
          SCFACT =1.
          IND5=EIGN.(LAMBDA(1),N,1,YT(1),SCFACT)
          WHENEVER IND5.E.3.
          CONTINUE
          OR WHENEVER IND5.E.1.
          PRINT COMMENT $0 APRIME MATRIX NOT ACCEPTED BY SUBROUTINE $
          TRANSFER TO END
          OR WHENEVER IND5.E.2.
          PRINT COMMENT $0 CHARACTERISTIC VALUES SCALED BY $
          PRINT RESULTS SCFACT
          END OF CONDITIONAL
          IND6=DPMAT.(N,YT(1),ST(1))
          THROUGH LOOP7, FOR I=1,1,I.G.N
          XSUMSQ = 0.
          THROUGH LOOP8, FOR  J=1,1, J.G.N
          THROUGH LOOP8, FOR K=1,1,K.G.N
LOOP8     XSUMSQ=XSUMSQ+X(I,J)*X(I,K)*B(J,K)
          ROOT = XSUMSQ.P..5
          THROUGH LOOP7, FOR J =1,1, J.G.N
LOOP7     X(I,J)=X(I,J)/ROOT
          PRINT COMMENT $0 CHARACTERISTIC VALUES $
          THROUGH LOOP8A, FORI=1,1,I.G.N
LOOP8A    PRINT RESULTS LAMBDA(I,I)
          PRINT COMMENT $0 THE ROWS OF THE FOLLOWING MATRIX ARE THE NOR
         1MALIZED CHARACTERISTIC VECTORS $
          PRINT RESULTS  X(1,1)...X(N,N)
          DIMENSION MA(5),MB(2),MC(3),MD(2),ME(3),MZ(2),MH(3),
         1HOVA(5),HOVB(2),HOVC(3),HOVD(2),HOVE(3),HOVZ(2),HOVH(3),
         2CHA(5),CHB(2),CHC(3),CHD(2),CHE(3),CHZ(2),CHH(3)
          WHENEVER  CH.E.1
          THROUGH LOA , FOR J=1,1,J.G.5
          MA(J)=S(J,1)*S(J,1)+S(J,2)*S(J,2)+S(J,3)*S(J,3)
          HOVA(J)=S(J,1)*S(J,4)*B(1,4)+S(J,1)*S(J,5)*B(1,5)+S(J,2)*S(
         1J,4)*B(2,4)+S(J,2)*S(J,5)*B(2,5)+S(J,3)*S(J,4)*B(3,4)
          CHA(J)=MA(J)+HOVA(J)
LOA       PRINT RESULTS MA(J),HOVA(J),CHA(J)
          OR WHENEVER CH.E.2
          THROUGH LOB ,  FOR J=1,1,J.G.2
          MB(J)=S(J,1)*S(J,1)
          HOVB(J)=S(J,1)*S(J,2)*B(1,2)
          CHB(J)=MB(J)+HOVB(J)
LOB       PRINT RESULTS  MB(J),HOVB(J),CHB(J)
          OR WHENEVER  CH.E.3
          THROUGH LOC ,FOR J=1,1,J.G.3
          MC(J)=S(J,1)*S(J,1)
          HOVC(J)=S(J,1)*S(J,2)*B(1,2)+S(J,1)*S(J,3)*B(1,3)
          CHC(J)=MC(J)+HOVC(J)
LOC       PRINT RESULTS MC(J),HOVC(J),CHC(J)
          OR WHENEVER  CH.E.4
          THROUGH LOD ,  FOR J=1,1,J.G.2
          MD(J)=S(J,1)*S(J,1)
```

```
            HOVD(J)=S(J,1)*S(J,2)*B(1,2)
            CHD(J)=MD(J)+HOVD(J)
 LOD        PRINT RESULTS  MD(J),HOVD(J),CHD(J)
            OR WHENEVER  CH.E.5
            THROUGH LOE ,FOR J=1,1,J.G.3
            ME(J)=S(J,1)*S(J,1)
            HOVE(J)=S(J,1)*S(J,2)*B(1,2)+S(J,1)*S(J,3)*B(1,3)
            CHE(J)=ME(J)+HOVE(J)
 LOE        PRINT RESULTS ME(J),HOVE(J),CHE(J)
            OR WHENEVER CH.E.6
            THROUGH LOZ ,  FOR J=1,1,J.G.2
            MZ(J)=S(J,1)*S(J,1)
            HOVZ(J)=S(J,1)*S(J,2)*B(1,2)
            CHZ(J)=MZ(J)+HOVZ(J)
 LOZ        PRINT RESULTS  MZ(J),HOVZ(J),CHZ(J)
            OR WHENEVER  CH.E.7
            THROUGH LOH ,FOR J=1,1,J.G.3
            MH(J)=S(J,1)*S(J,1)
            HOVH(J)=S(J,1)*S(J,2)*B(1,2)+S(J,1)*S(J,3)*B(1,3)
            CHH(J)=MH(J)+HOVH(J)
 LOH        PRINT RESULTS MH(J),HOVH(J),CHH(J)
            END OF CONDITIONAL
            WHENEVER SCFACT.E.1.
            CONTINUE
            OTHERWISE
            PRINT COMMENT $0 ERROR MATRIX NOT COMPUTED$
            TRANSFER TO END
            END OF CONDITIONAL
 END        PRINT COMMENT $0 INDICATOR VALUES $
            PRINT RESULTS IND1, IND2, IND3, IND4, IND5,IND6
            TRANSFER TO START
            END OF PROGRAM
$DATA
N=5,CH=1  *
A(1,1)=-81080.,A(2,2)=-096700.,A(3,3)=-096700.,A(4,4)=-105200.,
A(5,5)=-154800.,
B(1,1)=1.,B(2,2)=1.,B(3,3)=1.,B(4,1)=.493677,-.148237,-.052744,1.,
B(5,1)=.416020,.190671,B(5,5)=1.,  *
N=2,CH=2  *
A(1,1)=-96700.,A(2,2)=-105200.,
B(1,1)=1.,B(2,1)=.251278,1.,  *
N=3,CH=3  *
A(1,1)=-086000.,A(2,2)=-79400.,A(3,3)=-79400.,
B(1,1)=1.,B(2,1)=.089535,1.,B(3,1)=.099466,0.,1.,  *
N=2,CH=4  *
A(1,1)=-086000.,A(2,2)=-79400.,
B(1,1)=1.,B(2,1)=.110280,1.,  *
N=3,CH=5  *
A(1,1)=-55800.,A(2,2)=-163230.,A(3,3)=-79400.,
B(1,1)=1.,B(2,1)=.612076,1.,B(3,1)=.322816,0.,1.,  *
N=2,CH=6  *
A(1,1)=-62520.,A(2,2)=-105200.,
B(1,1)=1.,B(2,1)=.504168,1.,  *
N=3,CH=7  *
A(1,1)=-55800.,A(2,2)=-112800.,A(3,3)=-79400.,
B(1,1)=1.,B(2,1)=.409328,1.,B(3,1)=.227028,0.,1.,  *
```

APPENDIX K

Mo^{5+} AND W^{5+} IN TiO_2

Recently the ESR spectra of Mo^{5+} and W^{5+} in TiO_2 were observed. The following values for the g and A tensor components were found experimentally

	g_x	g_y	g_z	A_x	A_y	A_z
				(in $10^{-4}cm^{-1}$)		
$TiO_2:Mo^{5+}$	1.8155	1.7923	1.9167	24.66	30.80	65.73
$TiO_2:W^{5+}$	1.4731	1.4463	1.5945	40.51	63.34	92.01

Following the calculation in Chapter VII-1, the ground state wave functions and the crystal field energy levels listed below were found:

	Ground State w.f.	Energy Levels
$TiO_2:Mo^{5+}$	$-.324\|z^2\rangle + .945\|x^2-y^2\rangle$	$\Delta E(xy) = (2\lambda)(43.000)$ $(xz) = (2\lambda)(12.800)$ $(yz) = (2\lambda)(.368)$ $(x^2-y^2) = 0$
$TiO_2:W^{5+}$	$-.397\|z^2\rangle + .920\|x^2-y^2\rangle$	$\Delta E(xy) = (2\lambda)(83.500)$ $(xz) = (2\lambda)(3.930)$ $(yz) = (2\lambda)(.247)$ $(x^2-y^2) = 0$

20. V. Heine, Group Theory in Quantum Mechanics, Pergamon Press (1960), p. 102.

21. V. Heine, Group Theory in Quantum Mechanics, Pergamon Press (1960), p. 119.

22. M. Wolfsberg and L. Helmheltz, J. Chem. Phys. 20, 837 (1952).

23. C. J. Ballhausen and H. B. Gray, Inorg. Chem. 1, 111 (1962).

24. C. J. Ballhausen, Ligand Field Theory, McGraw-Hill, New York (1962), 162.

25. L. Pauling, J. Am. Chem. Soc. 53, 1367 (1931).

26. R. S. Mulliken, J. Am. Chem. Soc. 72, 4493 (1950).

27. R. E. Watson, Iron Series Hartree-Fock Calculations Solid State and Molecular Theory Group, MIT Press (1959).

28. C. E. Moore, Atomic Energy Levels, NBS Circ. 467 (1949, 1952, 1958).

29. W. Moffitt, Repts. Prog. Phys. 17, 173 (1954).

30. H. A. Skinner and H. O. Pritchard, Trans. Faraday Soc. 49, 1254 (1953).

31. J. C. Slater, Phys. Rev. 98, 1039 (1955).

32. C. A. Coulson, Valence, Oxford University Press (1961).

33. R. S. Mulliken, J. Chimie Physique 46, 497 (1949).

34. R. S. Mulliken, J. Chem. Phys. 23, 1833 (1955).

35. M. H. L. Pryce, Proc. Phys. Soc. (London) A63, 25 (1950).

36. C. P. Slichter, Principles of Magnetic Resonance, Harper and Row, New York (1963).

37. R. Lacroix et G. Emch, Covalence et resonance paramagnetique, Helvetica Physica Acta 35, 592 (1962).

38. L. L. Lohr, Jr. and W. N. Lipscomb, J. Chem. Phys. 38, 1607 (1963).

39. J. D. Roberts, Notes on Molecular Orbital Calculations, W. A. Benjamin, New York (1961).

40. D. K. Rei, Sov. Phys. Solid State 3, 1845 (1962).

41. K. W. H. Stevens, Proc. Roy. Soc. (London) A219, 542 (1953).

42. S. Karavelas, C. Kikuchi, and H. Watanabe, Bull. Am. Phys. Soc. 9, 403 (1964).

43. I. Chen, On the Theory of Superhyperfine Interaction in Iron Group Ion Complexes, PhD Thesis, University of Michigan, 1964.

44. T. Chang, Bull. Am. Phys. Soc. 9, 568 (1964).